UNIVERSITÀ DEGLI STUDI DELLA Tuscia

Dipartimento Di Produzioni Animali

DOTTORATO DI RICERCA IN

GENETICA E BIOLOGIA CELLULARE

XXIII CICLO

Analysis of the Genetic Expression in Livestock Breeds Through Proteomic Methods

AGR/17

Coordinatore:
Prof. Giorgio Prantera

Tutor:
Dr. Lorraine Pariset

Dottorando:
Leonardo Murgiano

Part I

Part II

AIM OF THE STUDY

During the last decade, the application of genetics to livestock production increased and the improvement of relevant traits is at present an essential element to support meat and milk consumption and to satisfy the consumer's demands regarding eating, health and nutritional quality. The increasing consumer's awareness of food quality and the development of the field of genomics have driven breeding companies to consider with more attention meat and milk quality, and to include quality traits as an integral part of selection programmes, where genomic markers can be incorporated. Meat quality is influenced by a large number of factors including muscle characteristics, but genetic effects play a crucial role in 'designing' livestock animals carcass composition and quality, although the heritability of quality traits is quite low[1]. Generally, between 10% and 30% of the variation in meat products quality, such as ultimate pH, colour, water-holding capacity, drip loss, tenderness, marbling, etc. is determined by the genetic background of the animal[1,2]. As for dairy products, Milk fat globule membrane (MFGM) represents an important milk fraction, which is rich in bioactive proteins. In order to better understand functionality of milk fractions and, thereby, enhance the benefits of milk products, detailed qualitative and quantitative protein knowledge of fractions such as MFGM is required.

Proteomics is a powerful tool to identify relevant proteins in milk, liver and muscle. Identification of proteins associated with the various aspects of milk production and of liver can provide a baseline for new research relative to the biology of lactation and of musclular tissue.

In agricultural sciences as in all other areas of life science, the implementation of proteomics and other post-genomic tools is an important step towards more detailed understanding of the complex biological systems that control physiology and pathology of living beings. Farm animals are raised in large-scale operations, with the aim to obtain animal products for human consumption. Hence, understanding the biological traits that impact yield and quality of these products is the specific aim of much biological experimentation. However, most of the data gathered from experiments on swine and cattle are relevant not only to farm animal sciences, but also to our understanding of complex biological mechanisms of human health and diseases. In a recent review, Bendixen et al [3] point out the progress in understanding the Proteome markers for meat and milk quality in the context of individuation of these important traits. Authors intriguingly go further this

concept, suggesting farm animals as new generation Proteome markers for meat and milk quality, especially regarding obesity and metabolism.

Liver is considered a very interesting subject because it displays functions of synthesis, homeostasis, excretion, and defense. Two dimensional electrophoresis analyses indicated that the differentially expressed proteins correspond to liver-specific enzymes[4], with a major role in the metabolism of fatty acids, carbohydrates, AA, and the urea cycle.

Proteomics has been shown an useful tool in the investigation of human liver, and examples exist especially in the pathology field[5,6]. On a similar route, Xu and Wang published a Comparative proteomics analysis of livers from ketotic cows. More recently, Miarelli and Signorelli investigated into the Differential expression of liver proteins in Chianina and Friesian young bulls. The latter study was more oriented on an actual characterization of the differences between the two breeds and more related on production traits.

Proteomics has been used extensively as a tool for the investigation of skeletal muscle differentiation, neuromuscular disorders and fiber aging[7]. Knowledge in these fields (especially the former) is undoubtley essential in the study of genomic traits in livestock.

Proteomics has been, and still are, used in numerous studies on skeletal muscle of livestock. Recent articles we focused on its use in the study of livestock muscle development and meat quality. Changes in protein profiles during myogenesis are described in cattle, pigs and fowl using comparative analyses across different ontogenetic stages[8]. This approach allows a better understanding of the key stages of myogenesis and helps identifying processes that are similar or divergent between species. Genetic variability of muscle properties analysed by the study of hypertrophied cattle and sheep[9], and even chicken[10] has been discussed. Regarding pigs, Bendixen et al again pointed out interesting implications[11].

Studies of low birth weight offspring have a long history in pig science. These pigs have reduced growth potential and poor carcass quality compared to their higher birth weight littermates. In contemporary commercial sows with between 10 and 15 total pigs born/litter, between-litter differences in average birth weight appear to make the largest contribution to variation in postnatal growth performance, independent of numbers born[12].

Complementary to the raw muscle studies**,** intramuscular fat content studies is important for many meat quality parameters. Identifying functional categories of genes associated with natural variation among individuals in intramuscular fat content to help the design of genetic schemes for high marbling potential[13].

Moreover, more commons are studies related to a comparison between two or more breeds with the purpose of identifying relevant markers[14-16]. Comparison at the level of both age and race has been performed as well[17.]

Proteomics is a valid strategy for the identification of proteins in complex mixtures, has gained popularity as a means to characterize proteins in various bovine milk fractions, both under normal physiological conditions and during clinical mastitis[18]. The biological complexity of bovine milk has, however, precluded the complete annotation of the bovine milk proteome. Conventional approaches to reducing sample complexity, including fractionation and the removal of high abundance proteins, has improved proteome coverage, but the dynamic range of proteins present, and abundance of a relatively small number of proteins, continues to hinder comparative proteomic analyses of bovine milk.

Milk fat globule membrane Fraction, in particular, has been subject of interest both as a whole-analysis subject and in comparative analysis related to mammary gland development[19,20].

It should be pointed out that cattle milk is not the only one been analysed – as an example, sow milk in different zone of the mammary gland has been successfully studied[21].

Ths PhD thesis is aimed to investigate through proteomics methods protein expression in livestock products (pig muscle, cattle milk and cattle liver, organ strictly related with milk production).

Samples provided for each esperiment belong to breeds significantly different in the specific production trait examined (Chianina has been selected for meat while Friesian has been selected for milk; Casertana has a different lean/fat mass ratio than Large White).

Data obtained can be useful for the understanding of physiological mechanisms behind livestock products, for breed selection and comparison of genetic traits in livestock.

It should be pointed out that interesting results accomplished are of interest in systems biology research in terms of integration and analysis of high-throughput expression data from mammalian tissues. These studies confirm the reliability of high output expression data in genomics study[22]. In a recent study, Davoli et al pointed out that among the new fields of genomics recently developed, functional genomics and proteomics that allow considering many genes and proteins at the same time are very useful tools for a better understanding of the function and regulation of genes, and reported how these participate in complex networks controlling the phenotypic characteristics of a trait[1]. In particular, global gene expression profiling at the mRNA and protein level can provide a better understanding of gene regulation that underlies biological functions and physiology related

to the delivery of a better pig meat quality. Moreover, the possibility to realize an integrated approach of genomics and proteomics with bioinformatics tools is essential to obtain a complete exploitation of the available molecular genetics information. The development of this knowledge will benefit scientists, industry and breeders considering that the efficiency and accuracy of the traditional pig selection schemes will be improved by the implementation of molecular data into breeding programs[1].

This PhD thesis integrated proteomics data with data from post translactional analysis experiments and from transcriptomics experiments. Informatic tools are used extensively to assure a proper handling of the huge data output.

Part I

2D IEF SDS PAGE ANALYSIS – A BREAKDOWN

2D gel electrophoresis is generally used as a component of proteomics and is the step used for the isolation of proteins for further characterization by mass spectroscopy. In this work of Thesis the use of this technique is differential expression the comparison of two or more samples to find differences in their protein expression. The procedure shown is a comparison the tissues of *Longissimus lumborum* pig muscle samples.

A preliminary analysis with the purpose of optimize extraction method is shown along with principles of 1-Dimensional Sodium Dodecyl Sulphate Polyacrilamide Gel Electrophoresis. After the selection of the best extraction technique, treatment of the sample and first dimension Isoelectrofocusing separation is shown, as well as successive second dimension separation through SDS PAGE.

Procedures reported in Part I are part of the personal laboratory experience of this PhD thesis. Source literature is wide but a breakdown can be provided[23-42].

1. SETTING EXTRACTION METHODS.

First and foremost, sample extraction must be optimized for the experiment. Sample preparation is a key factor in successful 2DE, with complete solubilisation and denaturation of sample proteins being the ultimate aim.

Comparison of the 1D SDS PAGE gel protein lanes of 10 samples of the same *Longissimus lumborum* muscle follows, each result of five extraction methods per two protein precipitation methods.

1.1. Reagents

1.1.1. Samples

Longissimus lumborum samples gathered as described in methods (see pag 64).

1.1.2. Extraction Buffers

Extraction Buffer (1): PBS; 0.9% (w/v), NaCl, 50 mMsodium phosphate, (pH 7.4) and 2ml of 10% (v/v) Triton X-100 in Double Deionized H_2O.

Extraction Buffer (2): 8 mol urea, 4% w/v CHAPS, 40 mmol Tris base in Double Deionized H_2O.

Extraction Buffer (3): 40 mMTris (pH 8), 2 mMEDTA in Double Deionized H_2O.

Extraction Buffer (4): 10 mM Tris, pH 7.6, 1 mM EDTA, and 0.25 M sucrose in Double Deionized H_2O.

Extraction Buffer (5): 0.175 M tris/HCl pH 8.8, 5% (w/v) SDS, 15% (v/v) glycerol, 0.3 M dithiothreitol in Double Deionized H_2O.

1.1.3. Precipitation

Precipitation solution 1: Precipitation solution is composed by100% Acetone.

Precipitation solution 2: Precipitation solution is composed by 12 volumes of Acetone (85,71 % of total solution), 1 Volume of Methanol (7,14 %) and 1 volume of Tributhylphosphate (7,14 %).

Resuspention Buffer: 7M Urea 2M Thiourea 4% CHAPS. In Double Deionized H_2O.

1.1.4. Electrophoresis.

Acrylammide: 30% T 3% C.

Stacking Gel Buffe(SGB)r: 25_mM Tris, 192 mM glycine, 0.1% SDS, pH 6.8 in Deionized H_2O.

Stacking gel: for 20 ml: 5 ml SGB, 2,66 ml Acrylamide, 12,33 Deionized Water.

Storage Buffer: SGB 5 ml, Deionized Water 15 ml.

Running Gel Buffer (RGB): 25 mM Tris, 192 mM glycine, 0.1% SDS, pH 8.8 in Deionized H_2O.

5% Running Gel: per 40 ml: RGB 10 ml, 6,66 ml Acrylamide, 23,33 Deionized Water.

17% Stacking Gel: 10 ml RGB 22,6 ml Acrylamide, 7,33 Deionizzed Water.

Sample Buffer: 4M Urea, 200 mM Dithiothreithol, 12% Sucrose, 50 mM HCl, 4% SDS, 0.01% Bromophenol Blue in Deionized H_2O.

Cathode Buffer: 0.025 M Tris, 0.192 Glycine, 0.1% SDS in Deionized H_2O

Anode Buffer: 0.025 M Tris, 0.192 Glycine in Deionized H_2O

Fixing Solution 50% H_2O, 40% Methanol, 10% Acetic Acid

Mother Staining Solution :10% (w/v) Ammonium Sulphate, 11.8 % Phosphoric Acid, 0.1% Coomassie G250 in Deionized H_2O

Staining Solution: 80% Mother, 20% Methanol

Caveat: Roles of Chemical Ingredients:

- **Tris (tris (hydroxy methyl) aminomethane)** It has been used as a buffer because it is an innocuous substance to most proteins. Its pKa is 8.3 at 20°C, making it a very satisfactory buffer in the pH range from roughly 7 to 9.
- **Glycine (Amino Acetic Acid)** Glycine has been used as the source of trailing ion or slow ion because its pKa is 9.69 and mobility of glycinate are such that the effective mobility can be set at a value below that of the slowest known proteins of net negative charge in the pH range. The minimum pH of this range is approximately 8.0.
- **Acrylamide** It is a white crystalline powder. While dissolving in water, autopolymerization of acrylamide takes place. It is a slow spontaneous process by which acrylamide molecules join together by head on tail fashion. But in presence of free radicals generating system, acrylamide monomers are activated into a free-radical state. These activated monomers polymerise quickly and form long chain polymers. This kind of reaction is known as Vinyl addition polymerisation. A solution of these polymer chains becomes viscous but does not form a gel, because the chains simply slide over one another. Gel formation requires hooking various chains together. Acrylamide is a neurotoxin. It is also essential to store acrylamide in a cool dark and dry place to reduce autopolymerisation and hydrolysis.

- **Bisacrylamide (N,N'-Methylenebisacrylamide)** Bisacrylamide is the most frequently used cross linking agent for poly acrylamide gels. Chemically it is thought of having two-acrylamide molecules coupled head to head at their non-reactive ends.
- **Sodium Dodecyl Sulfate (SDS)** SDS is the most common dissociating agent used to denature native proteins to individual polypeptides. When a protein mixture is heated to 100°C in presence of SDS, the detergent wraps around the polypeptide backbone. It binds to polypeptides in a constant weight ratio of 1.4 g/g of polypeptide. In this process, the intrinsic charges of polypeptides becomes negligible when compared to the negative charges contributed by SDS. Thus polypeptides after treatment becomes a rod like structure possessing a uniform charge density, that is same net negative charge per unit length. Mobilities of these proteins will be a linear function of the logarithms of their molecular weights.
- **Ammonium persulfate** must be made fresh as it decomposes in water. The other solutions can be pre-made and stored at 4°C. Fixing solution and staining solution are stored at room temperature.
- **Urea**-containing buffers should not be heat > 37°C; otherwise protein carbamylation may occur.

1.1.5. Protein Quantification

2D Quanti-Kit Amersham Biosciences

1.1.6. Image Analysis

QuantityOne, Biorad.

1.2. Methods

1.2.1. Extractions

Extraction one (1): Frozen sample of cattle *Longissimus lumborum* from, approximately 20 mg, were crushed in a mortar containing liquid nitrogen.

A particular care has been used to be sure that the fragmentation of the tissue could be as fine as possible.

After the crushing, the material has been gathered and inserted in a 2 ml eppendorf for approximately 500 ul of volume. The remnant volume has been filled with the extraction buffer 1, added at ice-cold temperature.

After 5 minutes of violent vortexing, the sample has been left overnight (16 h) at 4°C on a rotary shaker.

The suspended samples were centrifuged at 20,000 g for 60 min at 4°C to remove tissue debris.

The supernatant has been centrifuged a second time at 20,000 for 60 min room temperature (25°). Lasting supernatant has been quantified and then frozen at -20°.

Extraction two (2): Frozen sample of cattle *Longissimus lumborum* from, approximately 20 mg, were crushed in a mortar containing liquid nitrogen.
A particular care has been used to be sure that the fragmentation of the tissue could be as fine as possible.
After the crushing, the material has been gathered and inserted in a 2 ml eppendorf for approximately 500 ul of volume. The remnant volume has been filled with the extraction buffer 2, added at ice-cold temperature.
After 5 minutes of violent vortexing, the sample have been left on a rotary shaker at room temperature for 2 hour. Samples were taken and violently vortexed once every 15 minutes.
The suspended samples were centrifuged at 20,000 g for 60 min at 4°C to remove tissue debris.
The supernatant has been centrifuged a second time at 20,000 for 60 min at 4°C.
Lasting supernatant has been quantified and then frozen at -20°.

Extraction three (3): Muscle was homogenized, using a potter on ice, adding progressively extraction buffer 3 up to a volume of approximatively 2 ml. Proteins has been potted in ice for approximatively 15 minutes, paying attention to finely crush the muscle as much as possible.
The volume has been gathered into a 2 ml eppendorf. Eventually, the eppendorf has been re-filled if the volume did not reach 2 ml.
After 5 minutes of violent vortexing, the sample has been left on a rotary shaker at room temperature for 2 hour. Samples were taken and violently vortexed once every 15 minutes.
After that period, samples have been centrifuged at 20,000 g for 60 min at 4°C to remove tissue debris.
The supernatant has been centrifuged a second time at 20,000 for 60 min at 25°C.
Lasting supernatant has been quantified and then frozen at -20°.

Extraction four (4): Muscle was homogenized, using a potter on ice, adding progressively extraction buffer 4 up to a volume of approximatively 2 ml. Proteins has been potted in

ice for approximatively 15 minutes, paying attention to finely crush the muscle as much as possible.
10 minutes of violent vortexing has been performed 6 times, the sample was cooled in ice after each session for approximately 5 minutes. Vortex and support were cooled at 4°C as well.
Samples were leftt on a rotary shaker at room temperature for 1 hour. Samples were taken and violently vortexed once every 15 minutes.
After that period, samples have been centrifugued 20,000 g for 60 min at 4°C to remove tissue debris.
The supernatant has been centrifuged a second time at 10,000 RPM for 60 min at 4°C.
Lasting supernatant has been quantified and then frozen at -20°.

Extraction five (5): Frozen sample of cattle *Longissimus lumborum* from, approximately 20 mg, were crushed in a mortar containing liquid nitrogen.
A particular care has been used to be sure that the fragmentation of the tissue could be as fine as possible.
After the crushing, the material has been gathered and inserted in a 2 ml eppendorf for approximately 500 ul of volume. The remnant volume has been filled with the extraction buffer 1, added at ice-cold temperature.
After 5 minutes of violent vortexing, the sample has been left for 2 hours at 25°C on a rotary shaker.
The suspended samples were centrifuged at 20,000 g for 60 min at 4°C to remove tissue debris.
The supernatant has been centrifuged a second time at 20,000 for 60 min at 4°C.
Lasting supernatant has been quantified and then frozen at -20°C.
NOTE: Hot SDS can be used to increase initial protein solubilisation. However, before electrophoresis it must be removed by competitive displacement in SD buffer. Post solubilisation TCA/acetone extraction may be required to remove problematic components and this can be combined with SDS solubilisation.
Urea solutions, , on the other hand, CANNOT raise in temperatureif proteins are present to avoid risk of carbamylations.

1.2.2. Precipitations

Addition of miscible solvents such as ethanol or methanol to a solution may cause proteins in the solution to precipitate. The solvation layer around the protein will decrease as the organic solvent progressively displaces water from the protein surface and binds it in hydration layers around the organic solvent molecules. With smaller hydration layers, the proteins can aggregate by attractive electrostatic and dipole forces. Important parameters to consider are temperature, which should be less than 0°C to avoid denaturation, pH and protein concentration in solution. Miscible organic solvents decrease the dielectric constant of water, which in effect allows two proteins to come close together.

Precipitation method 1: Precipitation solution 1 has been added to an amount (300 ul) of the extracted protein solution. Precipitation solution 1 has been added in a 4:1 ration respect to the protein solution (1,200 ul, for 1,500 ul in total). Samples were kept overnight (16 h) at a temperature of -20°C. After this period, samples were centrifugued at 20,000 g for 20 minutes, 4°C. Surnatant has been decanted and dryed in vacuum at room temperature for 15 minutes.

Precipitation method 2: Precipitation solution 2 has been added to an amount (300 ul) of the extracted protein solution. Precipitation solution 2 has been added in a 4:1 ratio respect to the protein solution (1200 ul, for 1500 ul in total). Samples were kept on a rotary shaker for 1.5 h at a temperature of 4°C. After this period, samples were centrifugued at 20,000 g for 20 minutes, 4°C. Surnatant has been decanted and dryed in vacuum at room temperature for 15 minutes.

Resuspention: Samples have been resuspended in a volume of 500 ul of Resuspention Buffer through strong agitation. In some case, overnight agitation on rotary shaker was needed.

1.2.2. Quantification

Resuspended samples have been quantified by 2D Quanti-Kit Amersham Biosciences following strictly the protocol suggested by the producers.

1.2.3. Gel Casting

Electrophoresis gel has been cast using 20x20 (front) and 20x22 cm (rear) glasses. Plastic tight spacer 1.5 thick has been used (Biorad). Glasses has been cleaned with ethanol (70% ethanol at least) and placed on support. Cleaning of and completely drying the glass

plates, combs, and any other pertinent materials is very important to avoid contaminations, especially of keratin.

Deionized water (followed by drying though absorbent paper) has been used to check the tight of the structure.

To insure proper alignment and casting, the glass plates, spacers, combs and casting stand gaskets must be clean and dry. Glass plates are whashed with detergent and then submerged in deionized water. Periodical wash with nitric acid assures removal of residues. The glass plates should be cleaned with 70% ethanol.

Glass plates must be assembled on a clean surface. The longest glass plate is layed down asv first, and then two spacers are placed. Spacers vary from 0.5 to 1.5 mm in thickness. One dimensional gel was 1 mm thick and 2D gels (see later) were 1.5 mm. Next, the shorter glass plate is placed on top of the spacers so that the bottom ends of the spacers and glass plates are aligned (see Fig 1).

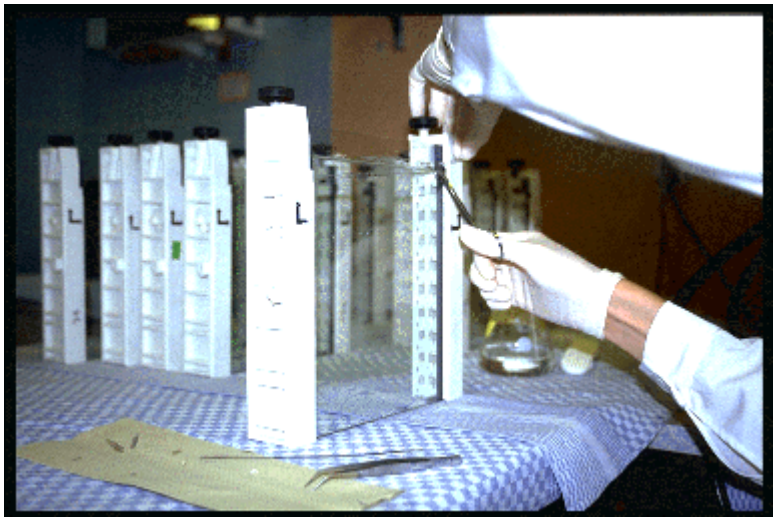
Fig. 1.

The structure is put vertical and is slightly tighten. Then with a firm grasp the glass plate sandwich with the longer plate facing away from the operator, and gently slide into into the clamp assembly, to check alignment. If a spacer is not aligned, an extra one can be used to move it toward the border of the structure. The whole structure is tighten and then a perfect and constant pressure of support is assured to avoid dangerous, glass-breaking imbalances.

Structure hold must be tested before adding gel solution – in fact, a preemptive test with wather can avoid the chance of material loss. It should be noted that for extra safety, the bottom line of the glasses can be anointed with siliconic grease.

Structure could be also sealed with a 5% agarose solution, but this method has been avoided because less pratical of the siliconic grease. It is very important, after water removal, cleaning residues with laboratory absorbing paper because water residuals can alter the gel solution composition.

Running Gel has been cast using a Hoefer 15 ml gradient maker, connected to a MasterFlex C/L aspiration pump by a rubber tube. Gradient maker has been placed on a so that the bottom of the chambers are higher than the top of the gel cassette, and a stir has been placed on each chamber. Tube has been clamped into position so that the outflow is directed into the cassette from the top center. The opposite side of the rubber tube (tipped by a syringe needle) has been inserted into the glasses.

The stopcock between the gradient maker chambers and the outlet from the gradient maker has been closed. The low percentage gel solution is poured into the non-outlet (reservoir) side of the gradient maker. Opening stopcock between the two chambers and allows 0.1 - 0.3 ml of solution to flow through to clear any bubbles. Sometimes it is necessary to remove excess of gel solution with a pipette and replace it in the original chamber. Then the high percentage gel solution into the outlet side (mixing chamber) of the gradient chamber and mixing Start mixing in the gradient maker is initiated activating the mixer. A 10% Ammonium Persulfate in water (w/v) is prepared and temporarily stored in ice. Following steps need rapidity and preparation because must be carried out quickly to avoid premature polymerization.

9,5 ml of 5% (light) and 9.5 ml of 17% (heavy) gel buffer has been put into the cylinders (heavy near the pump aspiration).

When ready to pour the gel, per 100 ml of solution, 1.0 ml of 10% APS and 0.1 ml TEMED are added. Particular care should be taken to be sure to have both APS and TEMED wholly introduced into the gel solution, without spreading on the gradient maker walls.

The stopcock between the chambers can be opened. Best results are reached opening at a flow rate which will drain the solutions in 3-5 minutes. Faster flow will cause turbulence in the gel which will disrupt the gradient. Slower flow rates will allow polymerization to occur before pouring is complete Order of opening is shonw in the figure below. Gel descent has been followed up near the end of the process, where the gradient maker has been inclined to grant the remaining gel buffer being aspired and inserted between the glass walls.

When all of the solution is dispensed, remove the syringe tip can be removed from the top of the cassette. Running Gel reached the level suggested by the company. A 1:1 Water/2-propanol solution has been added to grant safe and streamlined gel solidification.
It is critically important to wash *immediately* the gradient apparatus with water to prevent polymerization within the system. Polymerization happens in about one hour (Fig 2).

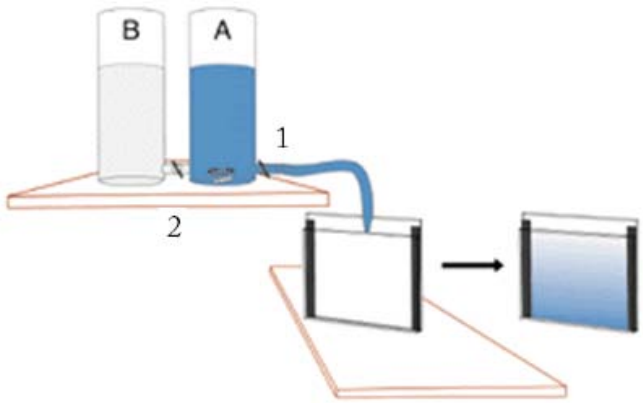

Fig. 2.

After the polymerization, gel upper surface must be washed at least three times with deionized water to remove trace of isopropanol. Even in this case, absorbing paper must be used to remove residual water.
The water/2-propanol mix has been washed 5 times with deionized water and then the glass above Running Gel has been dried with absorbent paper. Stacking gel filled the structure up to the top. A 15 wells 1 cm well comb of the same thickness of the spacers has been inserted. Stacking gel has been poured in a becker with no need of special handling. It should be noted that for an optimal polymerization and to obtain straight, well defined gels, the amount of TEMED and APS per volume compared to the Running Gel cast has been doubled.
Ater solidification, wells has been washed thrice with deionized water. Wells has been filled thereafter with storage buffers, protected by dehidratation covering them with wet paper and plastic membranes, and stored overnight at 4°C. It should be noted that the purpose of the storage buffer is to maintain the chemical and osmotic conditions of the stacking gel without adding acrylamide.

1.2.4. Electrophoresis

Wells has been washed twice with deionized water and then three times with catode buffer. This has the purpose of removing every residual acrylamide filament unneeded.

Last iteration left cathode buffer in the wells. Samples were solubilized using sample buffer in a 1:1 ratio. Solubilization occurred for 30 minutes, with vortexing once every 5 minutes. Samples where centrifugued at 14,000 rpm for 5 minutes thereafter and supernatant containing solubilized proteins has been loaded in the wells as explained in picture 1, in an amount of 40 ug per well.

SDS in the sample buffer binds to all proteins and breaks up the weak (non-covalent) bonds of the proteins, "smoothing" them out so that they exist in long rope-like SDS-polypeptide micellular chains. Each SDS molecule has 1 negative charge. Also, SDS binds at a rate of 1.4g SDS per 1g Protein which gives all SDS-bound proteins roughly the same charge to mass ratio, and hence equal mobilities in an electric field. Focused IPG strips, before separating the proteins by mass, are treated with sodium dodecyl sulfate (SDS) along with other reagents (equilibration buffer). This denatures the proteins (that is, it unfolds them into long, straight molecules) and binds a number of SDS molecules roughly proportional to the protein's length. Because a protein's length (when unfolded) is roughly proportional to its mass, this is equivalent to saying that it attaches a number of SDS molecules roughly proportional to the protein's mass. Since the SDS molecules are negatively charged, the result of this is that all of the proteins will have approximately the same mass-to-charge ratio as each other. In addition, proteins will not migrate when they have no charge (a result of the isoelectric focusing step) therefore the coating of the protein in SDS (negatively charged) allows migration of the proteins in the second dimension (NB SDS is not compatible for use in the first dimension as it is charged and a nonionic or zwitterionic detergent needs to be used).

Prior of the connection to the power source to start the Run, the gel has been assembled on the gel cassette. Upper buffer is poured into the cathode chamber and the tank is filled with the Lower (cathode) buffer. Silicone grease is used to assure tight enclosure and avoid cathode buffer loss during the run. This is always important, but is critical especially during overnight run because if Cathode becomes dry current is stopped, proteins diffuse. After a certain amount of time, the run would be wasted even if reprised because of this diffusion (see Fig 3 for a complete schematization).

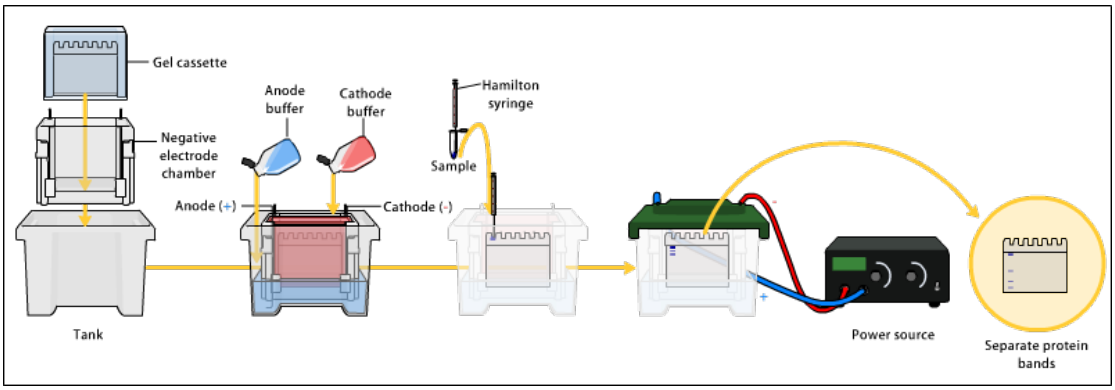

Fig. 3.

Gel has been set on the Electrophoresis apparatus and run at constant amperage of 40 mA per gel. Bromophenol blue present in the sample buffer has been used as a tracker. Run expired after six hours.

An electric field is applied across the gel, causing the negatively-charged proteins to migrate across the gel towards the positive (+) electrode (anode).

There are three important "current-carrying" anions in SDS PAGE: 1.) glycine from the Tris-Glycine buffer found in the buffer above the stacking gel and below the resolving gel; 2.) chloride ions from the Tris-Cl buffer in the sample buffer, the stacking gel, and the resolving gel; and 3.) SDS/protein micelles (from sample buffer, above). When the electric field is applied a "current-carrying" anion race through the gel is initiated.

Polyacrylamide gel has been known as a potential embedding medium for sectioning tissues as early as 1964. Two independent groups, Davis and Raymond, employed PAG in electrophoresis in 1959. It possesses several electrophoretically desirable features that make it a versatile medium. PAGE separates protein molecules according to both size and charge. It is a synthetic gel, thermo-stable, transparent, strong, relatively chemically inert, can be prepared with a wide range of average pore sizes. The pore size of a gel is determined by two factors, the total amount of acrylamide present (%T) (T = Total acrylamide-bisacrylamide monomer concentration) and the amount of cross-linker (%C) (C = Crosslinker concentration). Pore size decreases with increasing %T; with cross-linking, 5%C gives the smallest pore size.

This gel material can also withstand high voltage gradients, feasible for various staining and destaining procedures, and can be digested to extract separated fractions or dried for autoradiography and permanent recording. DISC electrophoresis utilizes gels of different pore sizes. The name DISC was derived from the discontinuities in the electrophoretic

matrix and coincidentally from the discoid shape of the separated zones of ions. There are two layers of gel, namely stacking or spacer gel, and resolving or separating gel.

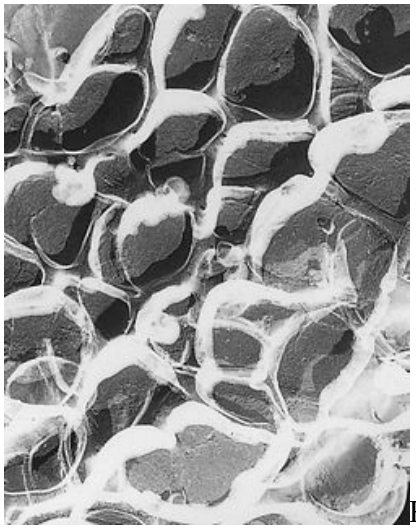 Fig. 4.

Fig 4 is a Transmission-Electron Microscopic image of a polyacrylamide gel. A polyacrylamide gel is a labyrinth of tunnels, the pore size is determined by the total amount of monomer present (%T) and the amount of cross-linker (%C).

Depending on its size, each protein will move differently through the gel matrix: short proteins will more easily fit through the gel pores, while larger ones will have more difficulty (they encounter more resistance). After a set amount of time (usually a few hours- though this depends on the voltage applied across the gel; higher voltages run faster but tend to produce somewhat poorer resolution), the proteins will have differentially migrated based on their size; smaller proteins will have traveled farther down the gel, while larger ones will have remained closer to the point of origin.

An example of several run of the same example at different T percentages is reported in Fig 5.

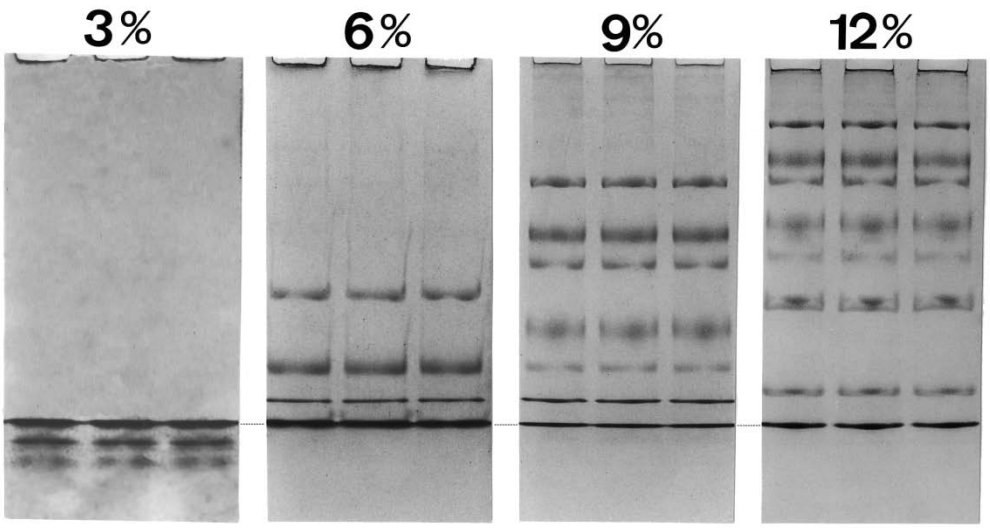

Fig. 5.

Stacking gel is a large pore PAG (4%T). This gel is prepared with Tris/HCl buffer pH 6.8 of about 2 pH units lower than that of electrophoresis buffer (Tris/Glycine). These conditions provide an environment for Kohlrausch reactions determining molar conductivity, as a result, SDS-coated proteins are concentrated to several folds and a thin starting zone of the order of 19 μm is achieved in a few minutes. This gel is cast over the resolving gel. The height of the stacking gel region is always maintained more than double the height and the volume of the sample to be applied.

Stacking occurs as a result of the differential rate of migration of the protein-micelles in the presence and absence of chloride ion "clouds" that initially surround and shield the SDS/protein micelles. To achieve this clearing of the chloride cloud, the titrate-ability of the glycine anion is employed. When the electric field is turned on, glycine, in the running buffer at pH 8.3 is slightly negatively charged and as such it carries the current in the buffer until it enters the sample buffer, pH 6.8, where the glycine becomes neutral as the amino group becomes totally protonated and the carboxyl group remains de-protonated (Fig 6 and 7).

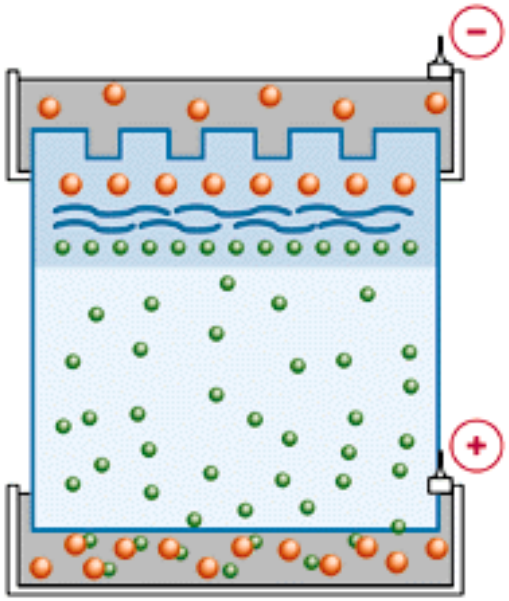

Fig. 6.

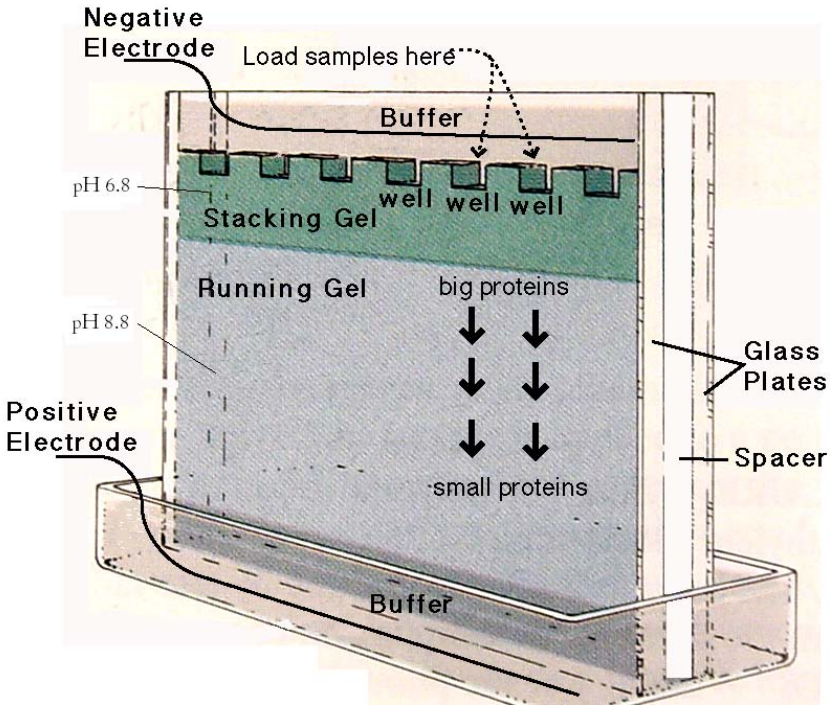

Fig. 7.

Chloride ions in the sample buffer and the gels create a "cloud" through which the SDS/proteins micelles can migrate only relatively slowly in the electric field. It is as if the chloride ions shield the micelle strings from experiencing the full force of the applied electric field (they don't move very fast). However, the chloride ions in the sample buffer and the gel buffers carry the current in these parts of the system initially, and start their migration toward the positive electrode upon the application of the electric field. As the

fastest moving species in the mix, the chloride ions, clear from the top of the sample buffer moving toward the positive electrode at the bottom of the gel, the slower moving SDS/protein micelles are left "out of the cloud of chloride". The entering glycine changes from negatively charged to neutral upon entering the pH 6.8 environment, leaving the protein-micelles unshielded so they now move faster toward the positive electrode than the micelles still in the chloride cloud lower in the sample buffer or in the gel. By the time the loaded sample reaches the Resolving (or Running) gel, the protein-micelles have managed to form a nice tight band < 1mm wide. This accounts for one component of the stacking phenomenon. The other components result from the slowing of the micelles upon encountering the various buffer-gel interfaces.

1.2.5. Staining

Gel has been removed from the support and then protein has been fixed using Fixing Solution. Gels have been inserted in to a container filled with 200 ml of fixing solution and kept 1 hour in slight agitation. After the fixation, gel has been washed three times with deionized water for approximately 15 minutes per wash.

Removal has been performed using a spacer to separate the two glasses, carfully letting the gele adhere to the larger glass (see Fig 8).

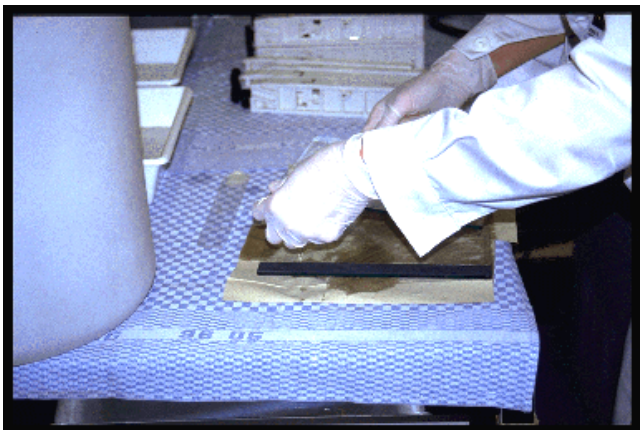

Fig. 8.

Then such spacer has been used to separate the stacking gel from the running. Stacking gel is useless from this point and is removed. Gel is thereafter submerged into a Bowl for fixation. Alimentary Bowls are perfectly suitable if endowed with hermetic enclosure (Fig 9).

Fig. 9.

Bowls are left floating on a Agitaror for 1 hour. Gels of lesser size, should be noted, are fixed in about 30 minutes, but for this kind of experiment 1 h is the best amount of time (Fig 10).

Fig. 10.

Fixing (or fixation) is the process whereby proteins are denatured and precipitated in large insoluble aggregates within the gel matrix. Fixation accomplishes several goals. Primarily, fixation prevents the diffusion of proteins, thus keeping the protein bands sharp and resolved during the staining process. In addition, fixation removes gel buffer components, most importantly SDS, which may interfere in the staining process. In some cases, fixatives are used which modify the proteins to enhance the staining reaction.

Fixing both native and SDS denatured proteins with acetic acid and alcohol results in an uncoiling of the peptide chains to produce insoluble complexes and monomers (see Fig. 11).

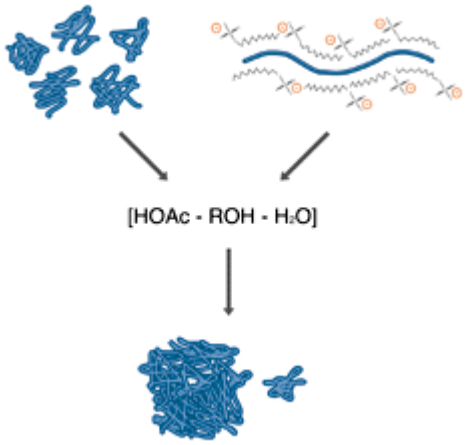

Fig. 11.

All fixatives operate by causing precipitation of the protein by converting it to an insoluble form. The most commonly used fixatives are solutions of short chain alcohols and acetic acid in water. The combination of low pH and high organic solvent content disrupts the hydrogen bonding which holds protein structures together, and exposes hydrophobic portions of the protein core. The result is an uncoiling of the peptide chain, followed by an essentially irreversible association between chains, producing a high molecular weight complex which is trapped inside the gel.

Fixation has been performed with the fixation solution described above. After the 1-hour time of fixation, gel has been washed using the same procedure described above. Each washing has been performed with 200 ml of Deionized Water. Three washing has been performed, 15 minutes long each. Washing is dramatically important because fingin solutions decrease the performance of the staining.

Several staining methods for SDS PAGE gels exist. Zinc or copper staining is a negatively staining technique able to detect Detects 6-12ng of protein. The background of the gel is stained whilst the proteins leave clear spots that can be visualised against an appropriate background, but is unstable. Silver staining can give excellent results (detecting 0.5-1.2 ng proteins). Just lately a lot of new protocols have been described that are compatible with mass spectroscopy, but is a time consuming and expensive staining technique that is not suitable for a large amount of gels present in semiquantitative analysis without special equipment.. It also suffers from a lack of dynamic range, making quantification of protein in spots highly unreliable, this can be noted in some negatively stained proteins that might appear on your gel Fluorescent stains like SYPRO ruby are very sensitive (detecting 1-2 ng proteins) but are very expensive and need special equipment.

Coomassie staining are quick, easy and cheap although making even if less sensible (Detect 36-47ng). It is important to make up fresh stain regularly as it loses its sensitivity as it gets older. It should be noted that greater sensitivity in not necessary in most cases, because a greater amount of protein should be anyway needed for successive MS analysis.

A modified Neuhoff's colloidal Coomassie Blue G-250 stain with a level of detection similar to conventional silver staining, dubbed "blue silver" on account of its considerably higher sensibility, has been reported. The main modifications, as compared to Neuhoff's protocol, were: a 20% increment in dye concentration (from 0.1% up to 0.12%) and a much higher level of phosphoric acid in the recipe (from 2% up to 10%). The "blue silver" exhibits a much faster dye uptake (80% during the first hour of coloration, vs. none with a commercial preparation from Sigma). Even at equilibrium (24h staining), the "blue silver" exhibits a much higher sensitivity than all other recipes, approaching (but lower than) the classical silver stain. Measurements of stain sensitivity after sodium dodecyl sulfate-polyacrylamide gel electrophoresis (SDS-PAGE) of bovine serum albumin (BSA) gave a detection limit (signal-to-noise ratio > 3) of 1 ng in a single zone. The somewhat lower sensitivity of "blue silver" as compared to classical silvering protocols in the presence of aldehydes is amply compensated for by its full compatibility with mass spectrometry of eluted polypeptide chains, after a two-dimensional map analysis, thus confirming that no dye is covalently bound (or permanently modifies) to any residue in the proteinaceous material. It is believed that the higher level of phosphoric acid in the recipe, thus its lower final pH, helps in protonating the last

dissociated residues of Asp and Glu in the polypeptide coils, thus greatly favoring ionic anchoring of dye molecules to the protein moiety. Such a binding, though, must be followed by considerable hydrophobic association with the aromatic and hydrophobic residues along the polypeptide backbone.

Thus, the final decision for the staining has been for the modified Coomassie Staining Blue Silver.

After the washes, the bowl is filled with 200 ml of Staining solution and left overnight floating as described above. To avoid lost of methanol by evaporation (thus altering the methanol/mother solution ratio other than being unsafe) the bowls are sealed with plastic for the overnight staining.

After the staining, gels are submerged in deionized water and let floating one whole day. Simple absorbing paper has been added (2 pieces) to the floating bowls to ensure quick removal of the coomassie excess. Water has been changed 1 time for the same purpose.

After complete destaining and background removal, gels can be scanned and analysed.

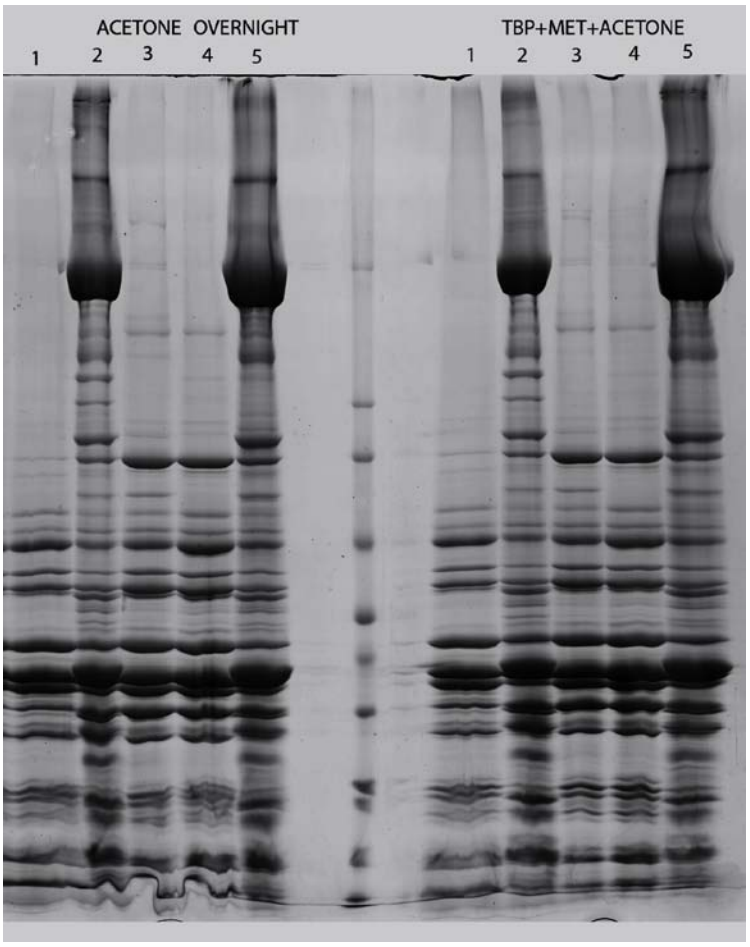

Fig. 12.

De-stained gels, with background staining removed, has been scanned by an Epson V700 photo scanner (Fig 12) and then the image has been analised by the software Progenesis Samespot. Results of the same extraction (1, 2, 3, 4, 5) and different precipitation (1, 2) has been matched in parallel to discover differencies among precipitation methods. Spot count has been used to identify the bands for each lane. A gel representative of all the kind of samples is shown above. There are 5 rows for each of the two precitpitaiton methods, separated by the marker. Molecular weight marker values have been added through graphic software. Spots count, per lane: 1-39; 2-54; 3-44; 4-45 5; 52. No difference has been found among precipitation methods (note: the image is B&W because even if Coomassien staining is blue, scanning is for image analysis is performed B&W at 8 or 16 bits- 8 in this case). Final selection is for Extraction method 2.

2. ISOELECTROFOCUSING

To separate the proteins by isoelectric point is called isoelectric focusing (IEF). Thereby, a gradient of pH is applied to a gel and an electric potential is applied across the gel, making one end more positive than the other. At all pH other than their isoelectric point, proteins will be charged. If they are positively charged, they will be pulled towards the more negative end of the gel and if they are negatively charged they will be pulled to the more positive end of the gel. The proteins applied in the first dimension will move along the gel and will accumulate at their isoelectric point; that is, the point at which the overall charge on the protein is 0 (a neutral charge).

The Immobilized pH gradient (IPG) gels are the acrylamide gel matrix co-polymerized with the pH gradient, which result a completely stable gradients except the most alkaline (>12) pH values. The immobilized pH gradient is obtained by the continuous change in the ratio of *Immobilines*. This alternative method eliminated the problems of gradient instability and poor sample loading capacity associated with carrier ampholyte pH gradient. Commercial precast IPG gels are available as the image shows. Use immobiline gels is important because avoids pre-focusing (see Fig.13).

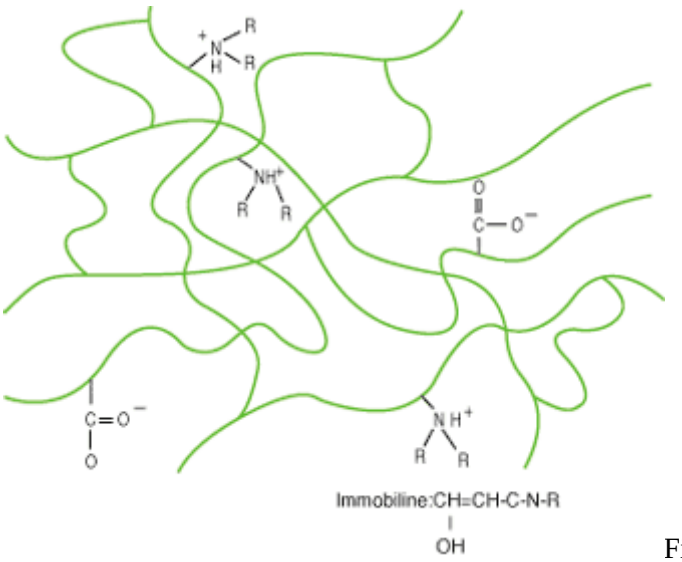

Fig. 13.

IPG strips are plastic backed, come in various lengths, but are usually 3.0mm wide and about 0.5mm thick when rehydrated. They come, dehydrated, in a variety of pH ranges. For use they must first be rehydrated, this is generally done under silicone oil. As mentioned earlier it can be beneficial to rehydrate the strips in the presence of your sample (in gel rehydration) and this is the loading method of choice in our lab and

enables us to load large quantities of protein. PH Range of precast IPG strips varies immensely and apholyte chosen should vary accordingly.

The standard procedure adopted up to the present proteome analysis calls for just reduction prior to the isoelectric focusing/immobilized pH gradient (IEF/IPG) step, followed by a second reduction/alkylation step in between the first and second dimension, in preparation for the sodium dodecyl sulfate-polyacrylamide gel electrophoresis (SDS-PAGE) step. This protocol is far from being optimal. It is here demonstrated, by matrix assisted laser desorption/ionization-time of flight (MALDI-TOF)-mass spectrometry, that failure to reduce and alkylate proteins prior to any electrophoretic step (including the first dimension) results in a large number of spurious spots in the alkaline pH region, due to "scrambled" disulfide bridges among like and unlike chains. This series of artefactual spots comprises not only dimers, but an impressive series of oligomers (up to nonamers) in the case of simple polypeptides such as the human α- and β-globin chains, which possess only one (α-) or two (β-) -SH groups. As a result, misplaced spots are to be found in the resulting two-dimensional (2-D) map, if performed with the wrong protocol. The number of such artefactual spots can be impressively large. In the case of analysis of complex samples, such as human plasma, it is additionally shown that failure to alkylate proteins results in a substantial loss of spots in the alkaline gel region, possibly due to the fact that these proteins, at their p*I*, regenerate their disulfide bridges with concomitant formation of macroaggregates which become entangled with and trapped within the polyacrylamide gel fibers. This strongly quenches their transfer in the subsequent SDS-PAGE step.

To overcome this problem, a pre-IEF reduction and alkylation method has been used.

2.1. Reagents

2.1.1. Buffers

IEF Cocktail 1(CIEF1): 7M Urea, 2M Thiourea, 2% CHAPS

IEF Cocktail 2(CIEF2): 7M Urea, 2M Thiourea, 4% CHAPS, 0.1 % EDTA, 0.85 M Tris-HCl

Iodoacetamide Cocktail: 150 ul of cockatil 2 55mM IAA

Dithioerythrol Cocktail : 150 ul of cockatil 2 55mM DTE

Strip Rehydratation Cocktail: 7M Urea 2M Thiourea 2% CHAPS 5mM DTE 1% Ampholyte

Cup Loading Cocktail: 7M Urea 2M Thiourea 4% CHAPS 1% Ampholyte
Caveat: Is *dramatically* important that *every* solution used for IEF must be prepared with DOUBLE deionized water. Failing to do this invalidates the run due to high currents.

2.2. Procedure

Sample has been extracted and precipitated with the slected method.
IEF Cocktail 1 is prepared beforehand and stored. IEF Cocktail 2 is prepared from the 1 immediately before use. Samples are resuspended into the IEF cocktail 2, in an amount of 1mg per 1,5 ml Epepndorf vial. The vial is not filled with the CIEF2, but only 250 ul are inserted for the subsequent operations relevant for the reduction and alkylation. It should be noted that the empty space is vital for the procedure since the buffer must be put in agitation three times on a rotary shaker (Fig.14).
Tris, Urea and Thiourea purpose has been explained above, whereas EDTA has the role of being a protease inhibitor. Should be noted that in CIEF2 can be added 1% ampholite, but this option is useful for helping resuspension only.

Fig. 14.

Once the sample has been resuspended (it can last several minutes in the case of muscle samples like the ones of *Longissimus lumborum*) the first step of the procedure has been performed. It should be noted that before this passage, and before the successive ones, is dramatically important spin the sample after every vortexing to be sure that minuscule drops of the sample wouldn't go dispersed after the opening of the cup – altering therefore the protein amount processed. This is even more important in the case of semiquantitative analysis.
In this study, tributyl phosphine has be used as reducing agent in the sample solution for the first-dimensional isoelectric focusing. Tributyl phosphine improves protein solubility during isoelectric focusing, which results in shorter run times and increased resolution.

Tributyl phosphine is nonionic and thus does not migrate in the IPG, therefore maintaining reducing conditions during the course of the first-dimensional separation.

Tributylphosphine is a tertiary phosphine, most commonly encountered as a ligand in transition metal complexes. It is an oily liquid at room temperature, with a nauseating odor. It reacts slowly with atmospheric oxygen, and rapidly with other oxidizing agents, to give the corresponding phosphine oxide. It is usually handled using air-free techniques, in particular aimmision of an inert gas used to counterflow additions, where air-stable reagents are added to the reaction vessel against a flow of inert gas (Fig. 15).

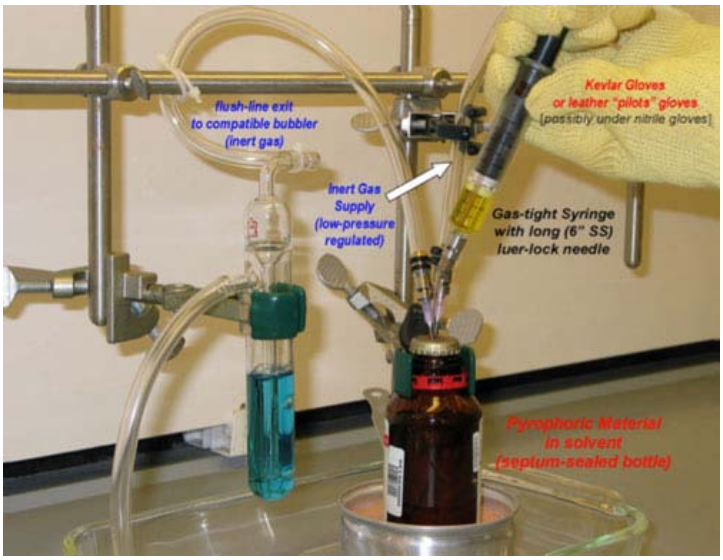

Fig. 15.

TBP is taken with a syringe and hastily inserted into a 500 ul vial. Then very quickly 0.56 ul of TBP is inserted in every vial of sample. After a brief vortexing, sample vials are protected with parafilm and inserted in a specially modified 50 ml falcon vial (covered with black insulation adhesive tape) and kept 1 hour on the rotary shaker.

TBP assures reduction (thus separation) of disulphide bonds in proteins cistheinic groups. first step to reduces all of the cysteines present in the protein, this step is undertaken to reduce any disulphide bridges that may have formed between adjacent cysteine residues (Fig 16). For this reason, once we have carried out the reduction step we then treat the sample with iodoacetamide.

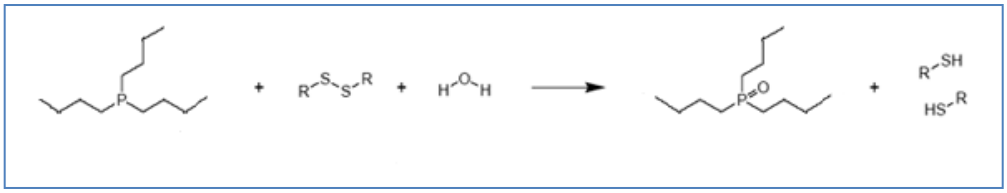
Fig. 16.

During the 1 hour step, Iodoacetamide Solution is prepared, but right near before recovering the sample(s). This is because the solution has a very high concentration and tends to precipitate very soon (Fig. 17).

After the spinning, 5 ul of the alkylating reagent Idoacetamide Solution per sample are added, and the rotary shaker procedure is repeated. Iodoacetamide purpose is to alkylate irreversibly the reduced SH groups. A non-reversible reaction occurs that places a functional group on the sulphide group, blocking it and ensuring that no further reactions can occur.

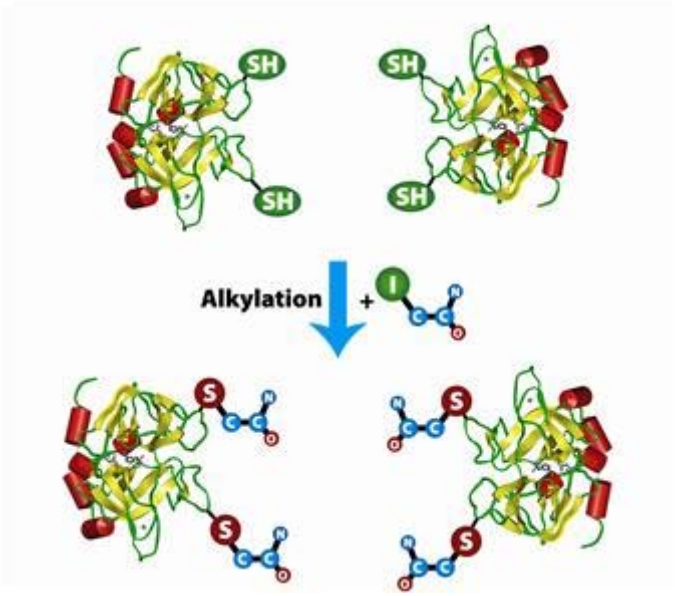

Fig. 17.

Iodoacetamide Alkylation reaction step is 1 hour long. After that, the sample is recovered from the rotary shaker as previously described. 5 ul of DTE Solution is added to proceed with the elimination of the Iodoacetamide excess. **Dithioerythritol (DTE)** is a sulfur containing sugar derived from the corresponding 4-carbon monosaccharide erythrose. It is an epimer of dithiothreitol (DTT), both molecules have a quite powerful reducing power *per se*.

The sample is precipitated with the precipitation solution above (since apparently no differences among the two precipitation methods were present, the less time-consuming one has been chosen). Precipitated proteins has been dried with a vacuum heat dryer and resuspended with cup loading cocktail and left shaking overnight.

Cup loading cocktail contains ampholite. As immobilines, Ampholytes are zwitterionic molecules able to act both as base and acids. Ampholytes have several properties; even

conductivity, high buffering capacity, soluble at isoelectric point, minimum interaction with focused proteins. All the properties help in the focusing.

Meanwhile, IPG strip rehydratation buffer is prepared. Rehydratation buffer contains ampholite. Since the pH range selected for the experiment is 3-10, every ampholyte mix added has the same pH extention. Reswelling tray is cleaned and prepared, carefully cheking balance. Rinse thoroughly with double distilled water. Use a cotton swab or a lint-free tissue to dry the holder or allow it to air-dry. Handle clean holders with gloves to avoid contamination. Note: The holder must be completely dry before use (Fig 18).

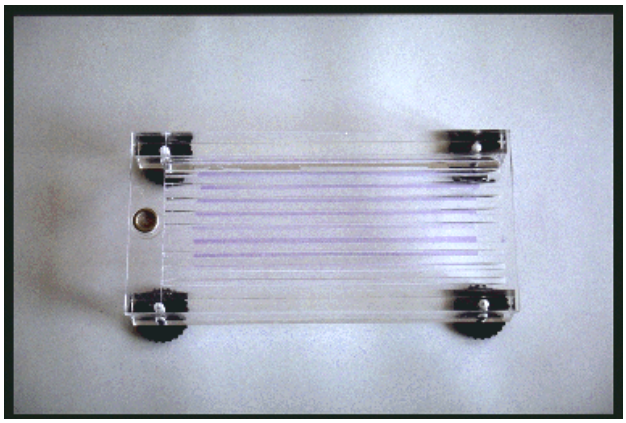
Fig.18.

Each Reaselling tray that will store a strip is filled with a variable volume of rehydratation buffer. Exact volume value is indicated by the company, but in case of cup loading method here used, since no protein is present in the rehydratation, is completely safe advised use greater values. Hence, each tray has been filled with 700 ul of buffer (400 was the minimum value). In case of passive rehydratation, ensuring complete sample uptake, without applying excess rehydration solution is important.

After that, IPG strips are removed from the storing box (Fig.19) (they are generally stored at -20°C) and carefully separated from their protective plastic layer and quickly placed in the trays. Act rapidly is dramatically important in this step because the buffer evaporates quickly invalidating the concentrations and then the experiment. Pipette the appropriate volume of rehydration solution into each well of the focusing tray. Deliver the solution slowly at a central point in the well. Remove any large bubbles.

Fig. 19.

IPG strips are placed downside into the trails using a pincer. Is vital remove carefully every bubble to grant a coherent rehidratation. IPG strips are then covered with mineral oil (to avoid dehydratation) and the tray cup is replaced. Pipette the fluid dropwise into one end of the well until one-half of the IPG strip is covered. Then pipette the fluid dropwise into the other end of the well, adding fluid until the entire IPG strip is covered. Finally, the wole structure is covered with a black drape to avoid light (since ampholites are light-sensitive).

After strips are rehydrated and samples dissolved, when the rehydration cassette had been thoroughly emptied and opened, the strips were transferred to the support. The support is a plastic grooved surface which is placed with an oiled ceramic surface able to assure cooling (the horizontal gels on their glass or plastic sheets are arranged on water-cooled plates since this allows the heat generated by electrophoresis to be readily dissipated and so avoid distortion of the separating protein bands. As with vertical polyacrylamide slab gels, multiple samples can be analysed side by side.). The support has connectrion for the current (anode and cathode, Fig. 20).

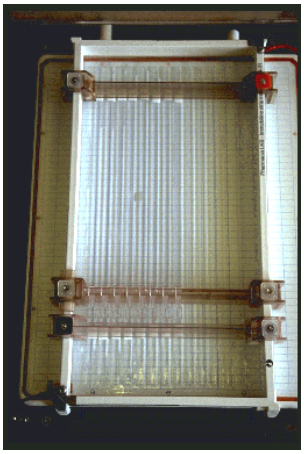

Fig. 20.

IPG strips are placed with the gel side up, having care of putting the sign up, then paper electrode wicks are wet with double deiionized water (excess is removed through laboratory absorbing water). Paper wicks are placed over the strips and then electrodes are placed on them, fimmobilizing the strips. Paper whicks purpose is to enhance and assure the current passage from the electrode to the IPG strip. Pressure blocks on the underside of the cover ensure that the IPG strip maintains good contact with the electrodes as the gel swells. A third support is added – the support for cups. Cups are small supports which vehicle the protein transfers from the buffer to the IPG strips through application of voltage (Fig 21).

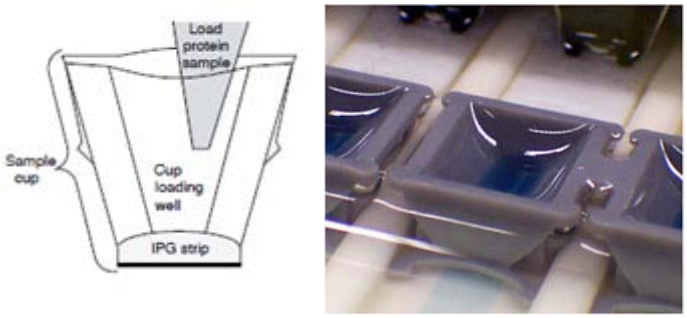

Fig. 21.

This passage is dramatically important because if the cup does not adhere completely to the strip, the sample is lost but if the strip is penetrated the runs is wasted. Hence, the cups are placed with care, and prior of the run the hold is chcked with some buffer without sample. Then sample is placed into the cups (is very recommendable sing up the order). To maximize reproducibility among samples and to be sure that all the sample is loaded, vials are spinned twice and pipette tips are slowly de-filled.

Then, a current chek is performed. If positive, cups and thereafter the whole structure are covered with mineral oil to avoid buffer dehydratation and to help cooling system and the run can start.

It advantagious to run our strips at low voltage first, then ramp up to higher voltages after the current has settled down. For strips of this length and pH range, the complete breakdown is: 150 V 1h, 300 V 1h, 500 V 1h, 800 v 1,5 h, 1500 V 1h, 2,000 V 1h, 3,000 V 1h, 3,500 V up to 85,000 V/h total (more than an overnight run generally).

All this equipment has a number of guidelines which must be adhered to. Temperatures of around 20^{o}C should be used and this should be kept constant as it is a variable and may affect the pI of sample proteins. Increasing the temperature too much above this may result in carbamylation of the proteins. Much lower temperatures may cause precipitation

of components such as urea. Cooling systems can be air or water based – in the case of the ceramic support shown, cooling is water based.

Is optimal to limit the run by amperage if possible, Bio-Rads Protean IEF is set to 50mA per gel as standard. Optimisation of each system will undoubtably be required; however, as there are so many variables you may be required to take some "leaps of faith." A good tip to ensure that the IEF is running correctly is to watch the bromophenol blue front carefully. It should slowly migrate toward the anode. If it does not migrate discretely or breaks down into a number of bands be very suspicious, you may have a problem. Should be notetd that the bromophenol blue migration cannot be used to measure the progress of the IEF run, it simply gives you a point of reference. Once the run is complete the strips can either be used immediately or frozen down at -70^{o}C for use later.

Focusing time depends on gel length, pH-gradient and gel additives (carrier ampholytes etc.). Focusing time is shorter when separation distance is shorter, or when wide-range pH-gradients are used, or when carrier ampholytes are added to the reswelling solution.

After the run, strips are ready for 2D electrophoresis, but can be strored in plastic layers and frozed (-20°C minimum), for days before the run.

As an alternative, when using the reswelling tray for in-gel rehydration, the sample volume has to be limited to the size of the IPG strip so that no superfluous sample solution is left in the tray. For a 180 mm long and 3 mm wide IPG strip, the correct sample volume is about 350 µl. When the reswelling tray is used for sample application, one should be aware that high molecular weight, alkaline and/or membrane proteins may not enter the IPG gel matrix properly

3. SECOND DIMENSION

2-D electrophoresis begins with 1-D electrophoresis but then separates the molecules by a second property in direction 90 degrees from the first. In 1-D electrophoresis, proteins (or other molecules) are separated in one dimension, so that all the proteins/molecules will lie along a lane but that the molecules are spread out across a 2-D gel (Fig. 22). Because it is unlikely that two molecules will be similar in two distinct properties, molecules are more effectively separated in 2-D electrophoresis than in 1-D electrophoresis.

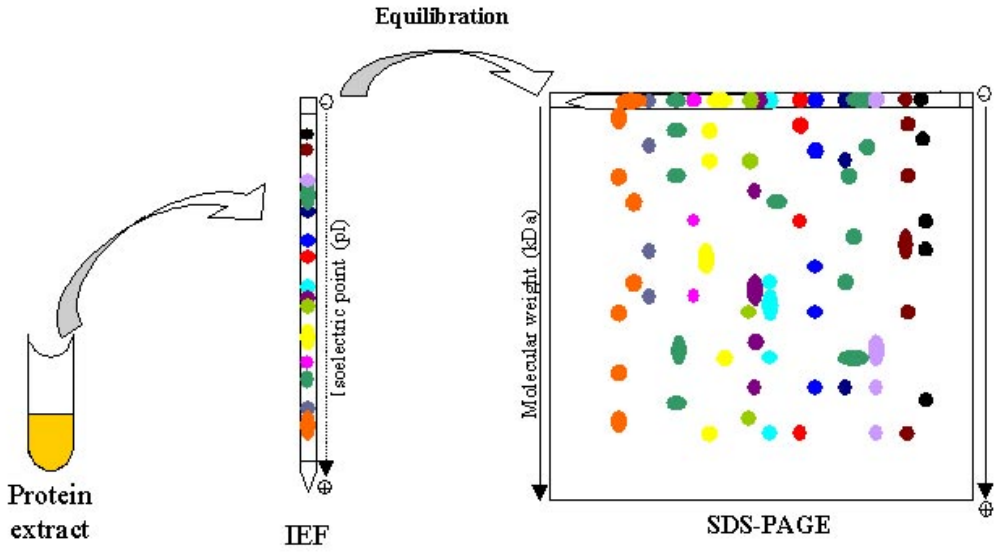

Fig. 22.

3.1. Reagents

Essentially, the mechanism is very similar to 1D SDS PAGE – Gel Casting, Run and correspondent buffers are the same. Additional reagents are:

Equilibration Buffer: 8M Urea, 30% Glycerol, 50 mM Tris-HCl, 1% SDS.

Sealing Buffer: 0.5% Agarose in Cathode Buffer, 0.2% Bromophenol Blue.

3.2. Procedure

The strips must be equilibrated before they can be used for SDS-PAGE. In fact, the equivalent of the well for 1D SDS PAGE is the focused protein band in the IPG strip. This is necessary for a number of reasons which are reflected in the components of the equilibration buffer. As the second dimension is SDS-PAGE it is important that the proteins are treated with SDS to give them a negative charge.

The pH 6.8 comes from conventional protocols, when a stacking gel was employed. Most of 2-D separations are run without a stacking gel, because it is not needed. an equilibration buffer with a higher pH works better because of several reasons: 1. The proteins are higher charged and stick thus better to the charges of the immobilized pH gradient in the IPG strips, thus you lose less proteins during equilibration. 2. The SDS sticks better to the proteins at higher pH. This is particularly important when iodoacetamide is used in the second equilibration step, considerably lowering the pH of teh buffer (even if not relevant in our case).

At this stage, equlibration should be splitted in reduction and alkylation, but since this has been already addressed before IEF, a single 30 min equilibration will occur. Glycerol (37%) are incorporated into thestacking gel to suppress electroendosmotic effects

After the equilibration, the IPG gel strips are washed with Upper Buffer and placed on a glass before being loaded on gels. Wetting the plastic back of the IPG strip with running buffer, other than stop the equilibration, makes them slide easily on the glass. The equilibrated strips with the plastic backing on the glass are placed and gently pushed the strip down onto the gel surface.

It is important not to compress the soft acrylamide strip against the opposite side of the glass, which will interfere with the protein transfer. Is optimal use carefully a spacer for this, ideally of lesser tightness compared to the Ensure that there are no air bubbles between the IPG strip and the resolving gel interface. Add a molecular weight marker that has been blotted onto a small piece of filter paper if desired. (Fig. 23).

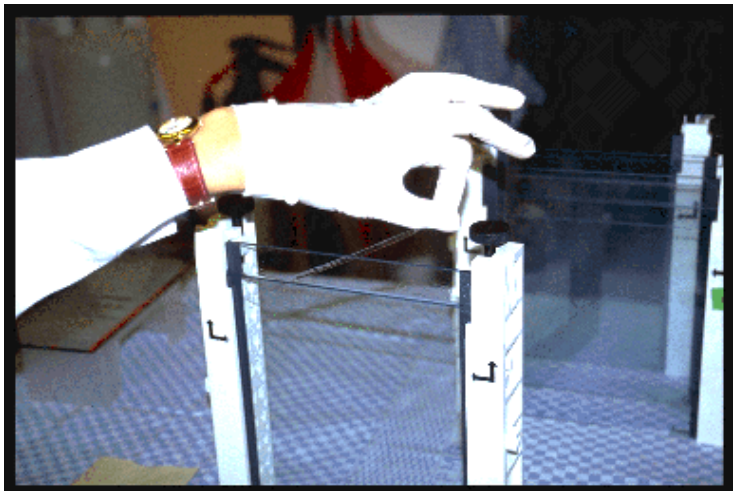

Fig. 23.

Strips are loaded on 2D gel and sealed with an agarose buffer. In the second dimension, proteins on the basis of their molecular weight with larger proteins being retained higher

in the gel and smaller proteins being able to pass through the sieve and reach lower regions of the gel (Fig. 24). Run is performed as above, but since semiquantitative electrophoresis needs several replicates, several gels are cast in the same time.

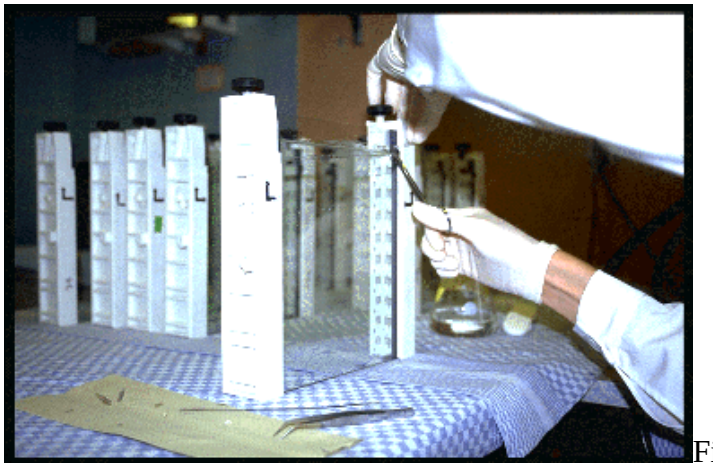

Fig. 24.

Gel multicast follows the comunicant vessels principle. Gradients are cast inserting the rubber tube in the orifice below (see figure, right) and inverting the order of the heavy and Light gel buffer. In this case, since the acrylamide percentage chosen is constant, the gel has been poured from above. Being a second dimension gel, the thickness chosen for the spacer is 1,5 mm (Fig. 25).

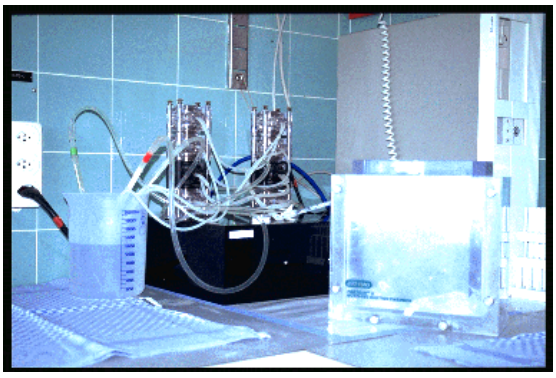

Fig. 25.

Since for reproducibility of the experiment is strongly suggested run all the gels together, or at least in comparable conditions. All the replicates of the experiment has been run with a multiple parralele run device (Fig. 27) Since gel thickness is higher, the current per gel chosen has been 40 mA. Should be noted that an even greater care should be taken to assure that there is not Upper Buffer loss – the run instead of simply stop for every gel,

would stop fo a couple and continua at an ahigh, unsitable amperage for other gels, for disateful consequences.

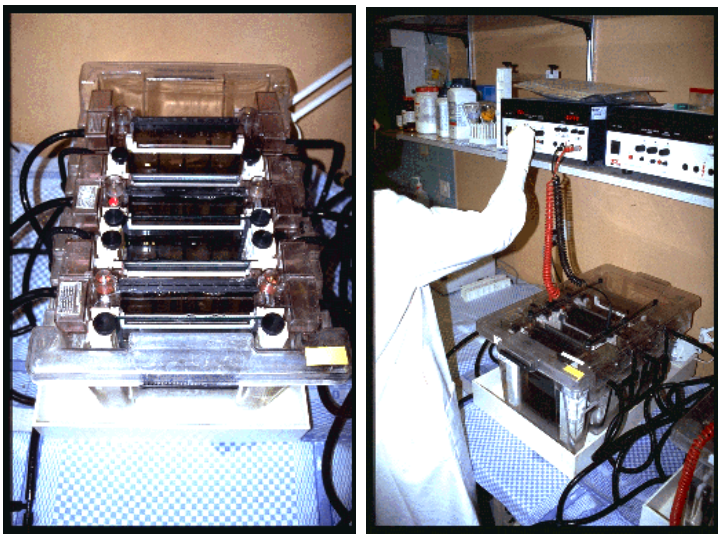

Fig.27

At the end of the run, the gels are handled in the same way as described above, staining and de-staining included. Should be noted that for statistical accuracy an huge amount of run and replicates must be performed (Fig.28).

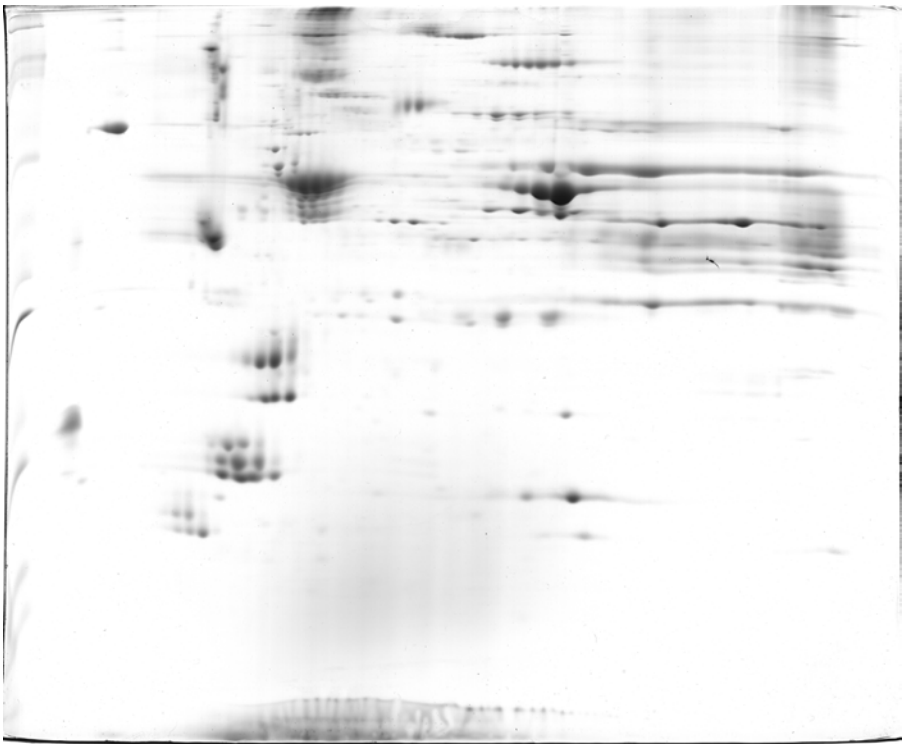

Fig. 28.

3.3. Image analysis.

Gels are analysed through Progenesis SameSpot by Nonlinear.

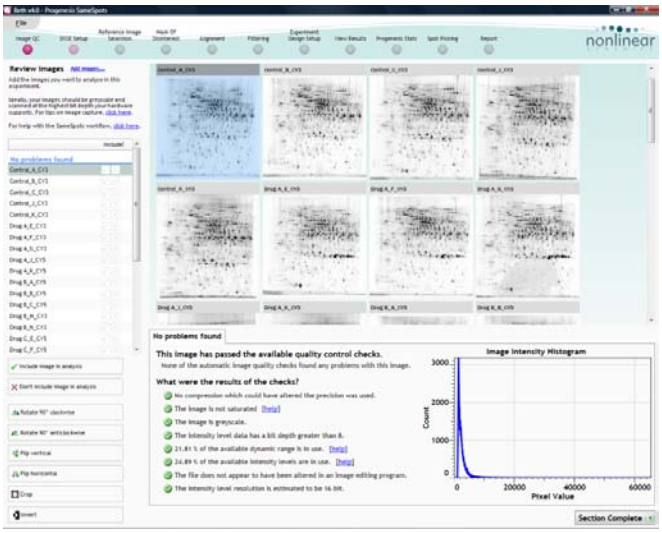

Fig. 29.

Software helps in the analysis of gel images through a process of image quality assessment with feedback to help you optimise image capture - vital for accurate image analysis (Fig 29). An image intensity histogram provides feedback on intensity levels in use and dynamic range of each image captured. Any positional errors introduced during scanning can be corrected using in-built tools (Fig. 30).

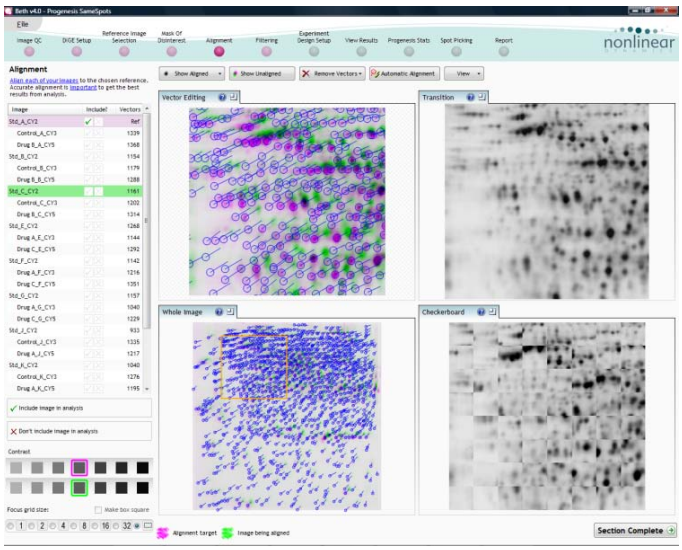

Fig. 30.

The visual tool helps the operator to perform automated image alignment. The result is perfectly aligned images at the pixel level, with 100% matching and no missing values, which radically reduces the need for editing spot detection and re-matching.

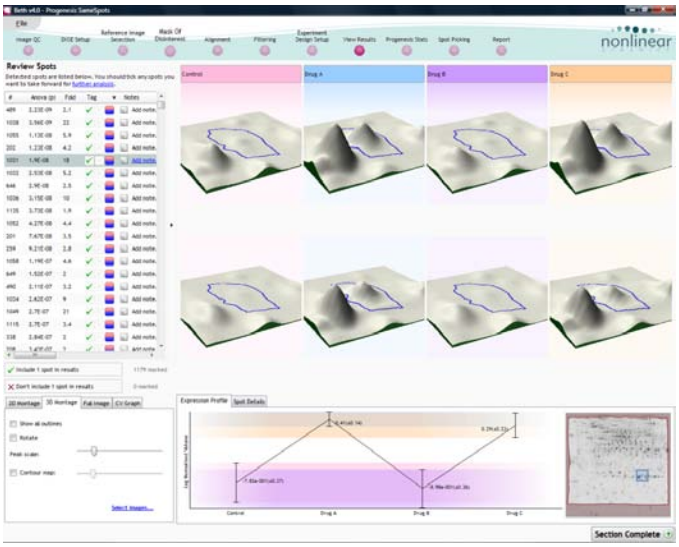

Fig. 31.

The software is endowed of a tool that allows you to apply a statistical analysis and make reliable conclusions. Principal Components Analysis (PCA), Correlation Analysis, Power Analysis and q-values (false discovery rate adjusted p-values) are included to explore the trends in data acquired (Fig. 31).

The final output points out relevant and significantly different spots eligible for excision and mass spectrometry analysis.

3.4. In Gel Digestion

The **in-gel digestion** is part of the sample preparation for the mass spectrometric identification of proteins in course of proteomic analysis.

Spot are picked using a surgeon scalpel or a custom cut pipette tip (very useful because one canset the radius of the cut gel piece (Fig. 32).


Fig. 32.

Gel pieces are cut on an illuminaing custom made surface carefully cleaned with 70% ethanol. Pieces washed two times (20 minutes, 150 ul each passage) and then dried with progressive concentration of acetonitrile (50% and 100%, 100 ul each passage, 20 minutes) prior of reduction and alkylation passage involving immersion in a 50 mM carbonate buffer, DTT 45°C heated reduction and dark IAA alkylation. Chemical mechanism is Identical to that described previously.

For every passage, samples have been shaked and heated into a laboratory shaker (Fig. 33).

Fig. 33.

After reduction and alkylation samples have been dehydrated again and then submerged in 5-12 ul of trypsin solution. Tripsin activity has been shut down keeping the samples at 4°C in ice until all the Tripsin Buffer has been absorbed and then the excess has been removed. Volume check occurs in a 45 minutes time. After the ckeck, trypsin-filled gels are submergen in 50 mM carbonate able to accept peptides.

Trypsin is a serine protease found in the digestive system of many vertebrates, where it hydrolyses proteins. It is used to fragment proteins in peptides ready for mass spectrometry analysis.

Samples have been kept overnight at 37°C (optimal for trypsin). The enzyme digests and cleaves the proteins in peptides and these are relased day thereafter surnatant has been gathered and measured for mass spectrometry analysis.

Part II

1 DIFFERENTIAL EXPRESSION IN BOVINE LIVER PROTEOME

1.1. Introduction

There is a huge amount of work currently underway on the human proteome, but little attention has been given to most animals of importance to humans. However, the importance of *Bos taurus* for the entire agricultural economy has prompted investigations into the fundamental mechanisms controlling animal health and productivity, including genetic analysis, animal physiology and susceptibility to microbial infections[43]. A combined effort of different genomic sequencing resources has now been coordinated to definitively sequence and annotate the entire bovine genome[44]. An updated bovine gene database is now available on the web at http://www.ncbi. nlm.nih.gov/genome/guide/cow[45]. The bovine genome contains about 35,000 type I coding genes arranged as 30 haploid chromosomes[46]. Almost 5,000 genes have been sequenced to date, which have shown a high degree of homology with human and mouse counterparts. As a consequence, preliminary genome projects on this species have already yielded powerful tools for the assessment of genes that specify hereditary disorders, infectious disease resistance, breedspecific quantitative loci and phenotypes of agricultural relevance[47,48]. Alongside the genetic investigation, a series of structural studies have been performed on isolated bovine proteins, depending on their easy availability or their importance as main constituents of food consumed in the human diet. In classical veterinary studies, single enzymatic activities or genetic anomalies have been associated with specific bovine physiological and pathological conditions. Limited systematic studies have been hitherto performed to evaluate the entire protein repertoire in bovine tissues and fluids during certain specific phenomena, or to detect novel markers for specific pathologies. Meanwhile, a small number of proteomic studies have been performed on bovine tissues and biological fluids, mainly focused on chondrocytes, mammary glands, cerebrospinal fluid, pulmonary endothelial cells, seminal plasma, milk and the corneal lens[49-52]. The liver has received special attention, containing as it does, enzymes involved in energy generation, carbohydrate, lipid, amino acid and xenobiotic metabolism, as well as proteins involved in polypeptide synthesis, folding and cell structure. Xu and Wang[53] carried out a comparative study on proteomic investigations of livers from ketotic cows. They found

thirtyeight different proteins between groups. Our interest in liver proteins differs, in that we are exploring the potential of this type of analysis to reveal unique profiles for different cattle breeds, despite the relatively short phylogenetic distance between Friesian and Chianina[54,55]. In this way, we purported to reveal important protein actors underlying those extreme traits that have been selected for in these breeds. Hereby we will present data about separation and identification of the differentially-expressed proteins and gene products through an integrated proteomics and transcriptomics (microarray) approach. Discussions will follow on how those changes in liver metabolism may be associated with different biological and productive aptitudes.

1.2. Material and Methods

1.2.1. Sample preparation:

Sample preparation and solubilization was performed by slight modification of the SWISS-2D PAGE sample preparation procedure. Frozen samples of liver tissue from the 6 Chianina and 6 Friesian (approximately 20 mg per sample) were crushed in a mortar containing liquid nitrogen, and to remove lipids, proteins were precipitated from a desired volume of each sample with a cold mix of tri-n-butyl phosphate/acetone/methanol (1:12:1). After incubation at 4°C for 90 min, the precipitate was pelleted by centrifugation at 2,800 g, for 20 min at 4°C. After washing with the same solution, the pellet was air-dried and then resuspended in the focusing solution containing 7 M urea, 2 M thiourea, 4% (w/v) CHAPS, 0.8% (w/v) pH 3–10 carrier ampholyte, 40 mM Tris, 5 mM TBP, 10 mM acrylamide, 0.1 mMEDTA (pH 8.5), 2% (v/v) protease inhibitor cocktail (Sigma-Aldrich), and 2 mM PMSF.

1.2.2. 2D-IEF-SDS PAGE

Before focusing, the sample was incubated in this solution for 3 h at room temperature, under strong agitation. To prevent over-alkylation, acrylamide was destroyed by adding an equimolar amount of DTE. The protein concentration of each group was determined according to Bradford[44] using BSA as a standard curve. A total of 250 μL of the resulting protein solution was then used to rehydrate 13 cm long IPG 3-10 NL (Amersham Biosciences) for 8 h. IEF was carried out on a Multiphor II (Amersham Biosciences) with a maximum current setting of 50 μA/strip at 20°C[36]. The total product time voltage applied

was 50,000 Vh for each strip. For the second dimension, the IPG strips were equilibrated for 30 min in a solution containing 6 M urea, 2% (w/v) SDS, 20% (v/v) glycerol, and 375 mM Tris–HCl (pH 8.8), with gentle agitation.

The IPG strips were then laid on a 5–16% T gradient SDS-PAGE gel with 0.5% (w/v) agarose in the cathode buffer (192 mM glycine, 0.1% w/v SDS and Tris to pH 8.3). The anode buffer was 375 mM Tris–HCl, pH 8.8. The electrophoretic run was performed at a constant current (10 mA for 60 min, followed by 40 mA until the run was completed). During the whole run, the temperature was set at 13°C. Proteins were visualized by a staining procedure: sensitive Coomassie Brilliant Blue G-250 stain[50].

1.2.3. Image Analysis

Improved staining of Sixty stained gels (3 technical replicates x 10 biological replicates x 2 breeds) were digitalized using an ImageScanner and LabScan software 3.01 (Bio-Rad Hercules, CA). The 2-DE image analysis was carried out and spots were detected and quantified using the Progenesis SameSpots software v.2.0.2733.19819 software package (Nonlinear Dynamics, New Castle UK). Each gel was analyzed for spot detection and background subtraction. Within-group comparison of protein spot numbers was determined by repeated measures analysis. Among-group comparisons were determined by ANOVA (Analysis of Variance) procedure in order to classify sets of proteins that showed a statistically significant difference with a confidence level of 0.05. Spots which were significantly different between groups (LW and CA) and not significantly different in the three technical replicate and ten biological replicate samples were identified by qTOF-MS/MS. All statistical analyses were performed with the Progenesis SameSpots software v.2.0.2733.19819 software package[52]. After the background subtraction, spot detection and match, one standard gel was obtained for each group (**Figure 1**), Large White and CA. These standard gels were then matched to yield information about the spots of differentially expressed proteins. Differential protein expression was considered significant at $P<0.05$ and the change in the photodensity of protein spots between Large White and CA samples had to be more than 2 fold.

1.2.4. In-Gel Digestion

Spots from 2-DE maps were carefully excised from the gels and subjected to in-gel trypsin digestion according to Shevchenko[56] with minor modifications. The gel pieces were swollen in a digestion buffer containing 50 mM NH_4HCO_3 and 12.5 ng/ml trypsin

(modified porcine trypsin, sequencing grade, Promega, Madison, WI, USA) in an ice bath. After 30 min, the supernatant was removed and discarded; then 20 ml of 50 mM NH_4HCO_3 were added to the gel pieces, and digestion was allowed to proceed overnight at 37°C. The supernatant containing the peptide mixture was removed and acidified with 5% formic acid before injection in the mass spectrometer.

1.2.5. Protein identification by Nano-RP-HPLC-ESI-MS/MS

Mass spectrometric procedures were performed as previously described[56]. Peptide mixtures were separated using nanoflow-HPLC system (Ultimate; Switchos; Famos; LC Packings, Amsterdam, The Netherlands). A sample volume of 10 µL was loaded by the autosampler onto a homemade 2 cm fused silica pre-column (75 µm I.D.; 375 µm O.D) Reprosil C18-AQ, 3 µm (Ammerbuch-Entringen, DE) at a flow rate of 2 µL/min. Sequential elution of peptides was accomplished using a flow rate of 200 nL/min and a linear gradient from Solution A (2% acetonitrile; 0.1% formic acid) to 50% of Solution B (98% acetonitrile; 0.1% formic acid) in 40 minutes over the precolumn in-line with a homemade 10-15 cm resolving column (75 µm I.D.; 375 µm O.D.; Reprosil C18-AQ, 3 µm (Dr. Maisch GmbH, Ammerbuch-Entringen, Germany). Peptides were eluted directly into a High Capacity ion Trap HCTplus (Bruker-Daltonik, Bremen, Germany). Capillary voltage of 1.5-2 kV and a dry gas flow rate of 10 L/min were used at a temperature of 200°C. The scan range used was from 300 to 1800 m/z. Protein identification was performed by searching in the National Center for Biotechnology Information non-redundant database (NCBInr, version 20081128, www.ncbi.nlm.nih.gov) using the Mascot program in-house version 2.2 (Matrix Science, London, UK). The following parameters were adopted for database searches: complete carbamidomethylation of cysteines and partial oxidation of methionines, peptide Mass Tolerance ± 1.2 Da, Fragment Mass Tolerance ± 0.9 Da, missed cleavages 2. For positive identification, the score of the result of (- 10 x Log(P)) had to be over the significance threshold level ($P < 0.05$). Even though high MASCOT scores are obtained with values greater than 60, when proteins were identified by one peptide only a combination of automated database search and manual interpretation of peptide fragmentation spectra was used to validate protein assignments. In this manual verification the mass error, the presence of fragment ion series and the expected prevalence of C-terminus containing ions (Y-type) in the high mass range were all taken into account. Moreover, replicate measurements have confirmed the identity of the protein hits.

1.2.6. RNA samples Collection

Samples were collected immediately after slaughtering. Samples were preserved in RNA later (Sigma-Aldrich) and stored at−80 °C. Total RNA of was extracted using the RNA easy midi kit (Quiagen).

In Casertana and large White case, RNA samples from the 10 animals of each breed were pooled as to reduce the total amount of needed material and because the primary interest was to better evidenziate breed-specific gene expression changes rather than individuals[23,24].

1.2.7. Microarray Experiment

An amount of 1μg pooled RNA was first reverse transcripted and then amplified by using the RNA ampULSe kit (Kreatech, Amsterdam, The Netherlands) following manufacturer's instructions. 4 μg of aRNA for each pool were labelled with Cy3 and Cy5 dye independently; for the repeat slide the same comparison was made with the dye assignment reversed (dyeswap)[59]. A technical replicate was performed starting from the same RNA pool (4 slides). A biological replicate of the previous experiment was obtained starting with independent RNA preparation from the same sample tissues (4 slides) [60]**.** The slides were spotted by CRIBI service with the 70mer Pig Genome Oligo Set Version 1.0 (Operon) representing the 10,665 *Bos taurus* gene sequences replicated twice. Annotations for oligo sequences were update on March 2006. The hybridizations were performed at 48°C for 18 hours by using the HybChamber (GeneMachines, San Carlos, CA).

1.2.8. Microarray data analysis

Images were obtained by a ScanArray Lite (Perkin Elmer) laser scanner and Spotfinder software (TIGR) was used to extract feature data from microarray fluorescence images. cDNA spots were automatically segmented, total foreground and background intensities of the two dyes were calculated for each spot. We filtered for poor or saturated hybridization signals, then removed systematic bias in the data by applying the dye-swap normalization[48] that makes use of the reverse labelling in the two microarray replicates and the Lowess normalization. To establish the significance of observed regulation for each gene, t-test with Welsh's correction was performed. Finally, only genes with Fold-Change over |1.5|) were considered (**Table 2**).

1.2.9. Network analyses

A preliminary analysis was carried out using the Pathway Studio Enterprise software Edition 5.0 (Ariadne Genomics). Differentially-expressed proteins shown in **Table 1** and gene products from microarray data have been used to perform the pathway analysis. Protein and gene groups have then been inserted in the Pathway Genomics Built Pathway function to evaluate their connectivity, finding all the shortest paths between them and finding all the entities directly connected to the inserted proteins.

The networks were generated through the use of Ingenuity Pathway Analysis (Ingenuity® Systems, www. ingenuity.com)[26]. A data set containing gene identifiers and corresponding expression values was uploaded into in the application, basing on either proteomics or transcriptomics results. Each gene identifier was mapped to its corresponding gene object in the Ingenuity Pathways Knowledge Base. The significance of the association between the data set and the canonical pathway was measured in 2 ways: 1) a ratio of the number of proteins from the data set that map to the pathway divided by the total number of proteins that map to the canonical pathway is displayed. 2) Fischer's exact test was used to calculate a P-value determining the probability that the association between the proteins in the dataset and the canonical pathway is explained by chance alone. Proteins/ gene products are represented as nodes, and the biological relationship between two nodes is represented as an edge (line).

All edges are supported by at least 1 reference from the literature, from a textbook, or from canonical information stored in the Ingenuity Pathways Knowledge Base. Nodes are displayed using various shapes that represent the functional class of the gene product. Grey nodes represent the proteins/ genes from the submitted dataset which have a match in the canonical pathway from the database, while white nodes represent gene products that the software attributed to the same networks, although they were not present in the submitted dataset. Continuous lines (edges) represent direct interactions, while indirect ones are represented by interrupted lines.Circular lines around onenode describe a feed-back loop of activity of that node on itself (e.g. by self-modulating its activity or expression). Grey edges represent interactionswithin a single network, while orange edges cross-link nodes from multiple interacting networks. The program could either graph single networks alone or merged together to stress their interactions.

The Ingenuity Pathway Analysis software allows performing an unbiased elaboration of the experimental data, in order tofocus subsequent analyses and discussions on the pivotal

networks which are revealed upon the experimental phase (in this case: differentially-expressed liver proteins and gene transcripts).

1.3.Results

On the basis of Talamo et al.[61] who compared proteomic analysis of bovine liver, kidney, skeletal, plasma and red blood cells, we analyzed differential proteome profiles of livers from two bovine breeds, Chianina and Friesian. For the analysis a sampling of 12 animals (six Chianina and six Friesian) was examined using immobilized pH gradient-based 2-DE and ESI-TOF-MS. The 2-DE protein extraction step was performed separately for each animal. To reduce the technical variance, each sample was analyzed in 3 technical replicates. **Figure 1** shows the well-resolved and reproducible 2-DE maps of liver tissue obtained from Chianina and Friesian. The maps show similar 2-DE patterns and only high-quality protein spots that were present in at least 24 out of 36 (both biological and technical) replicates were considered for quantification. A total of 560±57 protein spots were found to be commonly expressed in both cattle breed liver samples, without any significant quantitative difference. On the other hand, 39 different spots were found to be differentially expressed between Chianina and Friesian (**Table 1**). In detail, 12 spots were found to be up-regulated in Chianina, 13 spots were up-regulated in Friesian (ratio>2), 7 spots were only expressed in Chianina (Chianina ON), while 7 in Friesian only (Friesian ON). Data were statistically elaborated with cluster analysis, which stressed the up/on-regulation trend of these 39 proteins. No problems of reproducibility or calibration of the gels occurred during image processing, thus confirming the suitability of these 2-DE gels as reference standards. The aim of the study was to provide molecular evidences of the physiological differences in liver metabolism in these two beef (Chianina) and dairy (Friesian) cattle breeds. Therefore, differentially-expressed rather than commonly-detected proteins intuitively reflect the molecular basis of such differences. Hence, only modulated spots were cut out of the second dimension gel, digested with trypsin and analysed with MS tools, as described in the materials and methods section. In **Table 1** the identities are listed of the successfully identified proteins, together with the standard spot number (SSP), the identification parameters, and the indication of their gene ontology (GO) annotation (molecular function). In order to complement and validate proteomic results, we performed a thorough microarray analysis of the same liver samples.

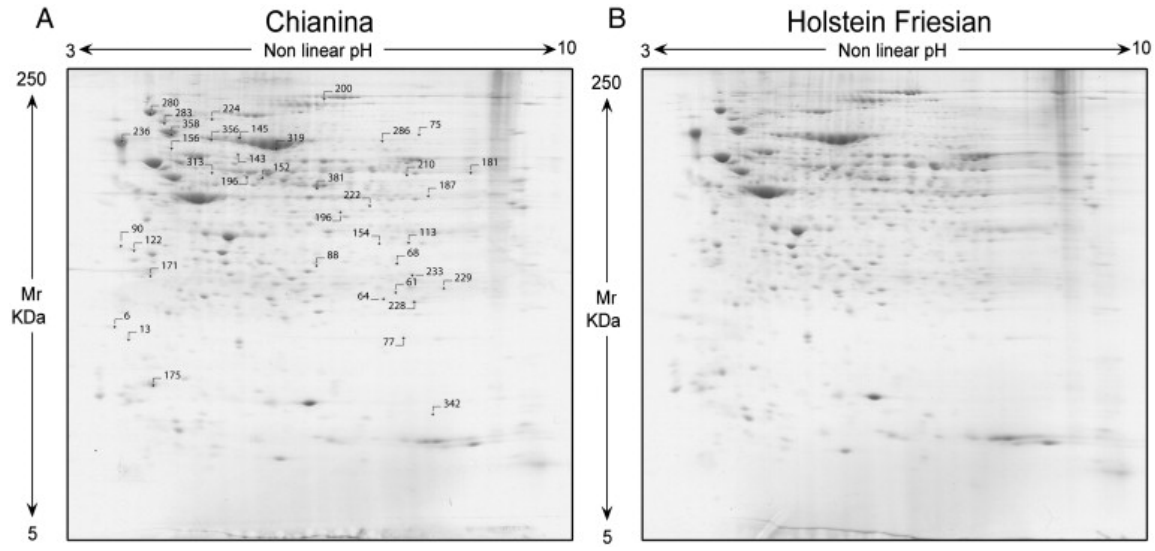

Fig. 1 – 2-DE of liver extracts from Chianina and Friesian breeds. Each gel image has been elaborated with Progenesis SameSpots (Nonlinear Dynamics, NewCastle, UK) and represent an average of 18 gels (3 technical replicate for 6 biological replicate samples), upon background subtraction.

.

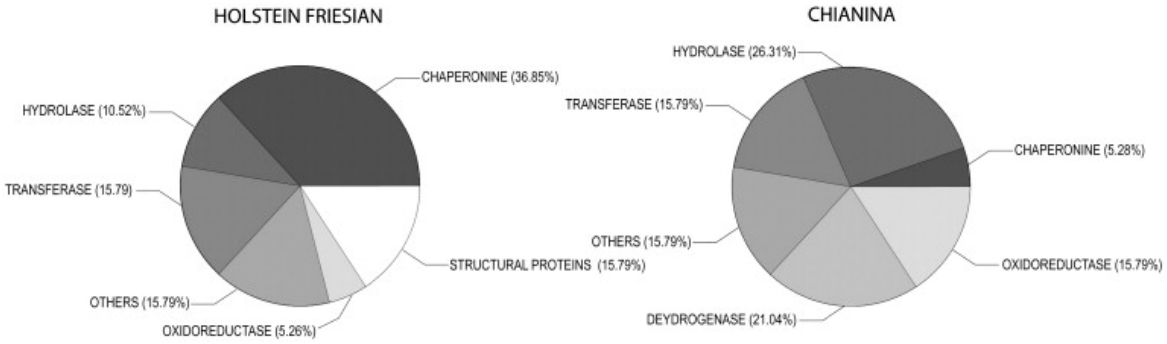

Fig.2– Elaboration of differentially-expressed proteins between Friesian and Chianina livers by means of Pathway Studio Enterprise software Edition 5.0 (Ariadne Genomics). The former (left side) cattle breed was characterized by an increase in chaperonines, mainly heat shock proteins, in line with its reduced thermoregulatory capacity. The latter (right side) was characterized by an increase in metabolic and anabolic enzymes, such as hydrolases, which are involved in fatty acid metabolism.

.

Table 1. Proteins were identified on the basis of **Figure 1**. Proteins highlighted in green have been confirmed to be up-regulated through microarray analysis

N	SSP	MwkDa	pI	No. of peptides identified	Mascot Score	NCBI Accession Number	Protein ID [Bos taurus]	Protein Function	Gene
Holstein Friesian Up									
3.	145	62861	5.62	5	172	gi|119910189	Similar to esterase 31	Chaperonine	Es31
4.	236	46524	4.31	14	532	gi|631545	Calreticulin, brain isoform 1	Chaperonine	CALR
5.	280	92654	4.76	38	1770	gi|27807263	Tumor rejection antigen (gp96) 1	Chaperonine	TRA1
6.	175	11044	5.15	5	209	gi|353817	Cytochrome b5	Hemoprotein	CYB5A
7.	200	165833	6.28	33	1668	gi|76659916	Similar to carbamoyl phosphate synthetase 1 isoform 1	Transferase	CAD
8.	156	42084	5.22	9	370	gi|116242946	Actin, cytoplasmic 1 (Beta-actin)	Structural Protein	ACTB
9.	319	76197	5.60	8	342	gi|2914360	Chain, Bovine Annexin Vi (Calcium Bound)	Lipid Binding	1AVC
10.	122	24902	4.54	2	75	gi|58760396	Eukaryotic translation elongation factor 1 beta 2-like	Transferase	EF1B
11.	356	71424	5.37	26	1051	gi|146231704	Heat shock 70kDa protein 8	Chaperonine	HSPA8
12.	171	27946	4.80	18	764	gi|2852383	14-3-3 protein beta	Oxydoreductase	YWHAB
13.	283	85077	4.93	28	668	gi|60592792	Heat shock 90kD protein 1 , alpha	Chaperonine	HSPCA
Holstein Friesian On									
14.	152	53078	5.60	3	94	gi|78042564	Hypotetical protein LOC512626	Peptidase	CNDP2
15.	90	48120	5.88	5	223	gi|77735583	S-Adenosylhomocysteine hydrolase	Hydrolase	AHCY
16.	196	47116	5.49	6	197	gi|6980816	Chain C, the Crystal structure of modified bovine fibrinogen	Structural Protein	FGA
17.	6	18813	4.33	2	87	gi|51493666	Cytosolic Prostaglandin E synthase	Chaperonine	cPGES
18.	381	48120	5.88	17	843	gi|77735583	s-Adenosylhomocysteine hydrolase	Hydrolase	AHCY
19.	88	35062	6.00	13	583	gi|124249242	Hypothetical Protein LOC783020	Transferase	SULT1C4
20.	13	23356	4.51	4	257	gi|62460528	Hypothetical Protein LOC513312	Structural Protein	NACA

.

Table 2. Microarray results..in green have been confirmed to be up-regulated through microarray analysis.

N	SSP	MwkDa	pI	No. of peptides identified	Mascot Score	NCBI Accession Number	Protein ID [Bos taurus]	Protein Function	Gene
Chianina Up									
1.	210	61992	8.03	22	1040	gi|74354891	GLUD1 protein	Dehydrogenase	GLUD1
2.	113	33115	6.78	10	407	gi|230290	Chain rhodanese	Transferase	1RHD
3.	286	61774	7.55	6	313	gi|89574195	Succinate dehydrogenase subunit A	Dehydrogenase	SDHA
4.	75	79870	6.75	13	562	gi|2501351	Serotransferrin precursor (Transferrin) (siderophylin) (beta-1-metal-binding globulin)	Metal Binding Globulin	TF
5.	77	57664	8.45	4	165	gi|229299	Catalase	Oxidoreductase	CAT
6.	313	53959	5.50	3	94	XP_001787596.1	Similar to cytosolic beta-glucosidase, partial	Hydrolase	GBA
7.	233	34410	7.71	10	429	gi|78369248	Hypothetical protein LOC509274	Hydrolase	HAGH
8.	222	43302	6.44	22	1152	gi|76639590	Similar to beta-ureidopropionase	Hydrolase	UBP1
9.	224	71423	5.49	6	109	gi|123644	Heat shock cognate 71 kDa protein (Heat shock 70 kDa protein 8)	Chaperonine	HSPA8
10.	228	40045	8.20	3	98	gi|29135271	Ornithine carbamoyltransferase	Transferase	OTC
11.	229	44809	8.82	3	63	gi|77735757	Acyl-Coenzyme A dehydrogenase, C-2 to C-3 short chain	Dehydrogenase	ACADS
12.	342	43302	6.44	9	206	gi|76639590	Similar to beta-ureidopropionase	Hydrolase	BUP1
Chianina On									
13.	61	26901	6.45	12	677	gi|62888856	Triosephosphate isomerase	Isomerase	TP1
14.	64	25810	6.45	12	574	gi|76613071	Similar to class mu glutathione S-transferase isoform 1	Transferase	GSTM1
15.	68	27294	8.45	3	169	gi|27805907	Hydroxyacyl-Coenzyme A dehydrogenase, type II hydroxyacil-Coenzyme A	Oxydoreductase	HADH
16.	187	46673	7.14	13	629	gi|27806925	Argininosuccinate synthetase	Ligase	ASS
17.	181	46943	8.31	6	258	gi|115497690	Acyl-coenzyme A dehydrogenase, C-4 to C-12 straight chain	Dehydrogenase	ACADM
18.	196	46491	6.49	3	122	gi|119913765	Similar to Fumarylacetoacetate (FAA) Hydrolase	Hydrolase	FAH
19.	154	55426	6.24	7	280	gi|27806321	aldehyde dehydrogenase 1 family, member A1	Oxydoreductase	ALDH1
Holstein Friesian Up									
1.	358	72470	5.07	23	977	gi|115495027	Heat shock 70kDa protein 5	Chaperonine	HSPA5
2.	143	33287	5.39	8	391	gi|77736137	Chaperonin containing TCP1, subunit 5 (Epsilon)	Chaperonine	CCT5

1.4. Discussion

Our aim was to outline a molecular trend paralleling the physiological differences between the analyzed dairy and cattle breeds. Although we could not manage to find a perfect match among proteins and gene products from the proteomics or transcriptomics approach, respectively, we purported to outline that this integrated approach could evidence whole pathways, which were turned on in livers from Chianina beef and Friesian dairy cattle breeds. Delving into network complexity Pathway analyses have been performed on proteomics and microarray data, either merged or alone, for Chianina and Friesian cattle breeds. Most of the up/on-regulated proteins and gene transcripts in Chianina (with respect to Friesian) were found to be involved in anabolic and catabolic pathways. Pathway analysis of the Chianina-related differentially- expressed proteins and gene transcripts revealed their connection with lipid metabolism, aminoacid metabolism and molecular transport. Notably, although transcriptomics and proteomics data did not match, pathway analyses of either differentially-expressed gene transcripts or proteins for Chianina samples delivered identification of a central network, namely the "Lipid Metabolism, Amino acid metabolism and Molecular Transport" network. Indeed, hydroxiacyl-Coenzyme A dehydrogenase (HADH, spot 68), Acyl Co A dehydrogenase straight chain, C-4 to C-12 straight chain (ACADM, spot 181) and Acyl-Coenzyme A dehydrogenase C-2 to C-3 short chain (ACADS, spot 229) from the differential proteomics analysis, and protein tyrosine phosphatase-like A domain containing 1 (PTPLAD1), 5,10- methenyltetrahydrofolate synthetase (MTHFS) from the microarray analysis are all proteins involved in fatty acid catabolism, in valine, leucine and isoleucine and carbon metabolism, respectively. In general these enzymes catalyze the oxidative dehydrogenation of different substrates present in the mitochondrial matrix and thus exert a key role in the fatty acid beta-oxidation pathway, converting fatty acid reserves to energy, especially during periods without food (fasting). ACADS, for example, is an essential enzyme for fatty acid metabolism (lipid metabolism) because it catalyzes the alpha, beta-dehydrogenation of acyl-CoA. Its inhibition causes low blood sugar (hypoglycemia), a lack of energy (lethargy), poor feeding, and failure to gain weight and grow at the expected rate (failure to thrive). HADH and ACADS are also involved together with in the degradation of isoleucine and valine, together with ACADM, a homotetramer, which also catalyzes the key step in leucine degradation. MTHFS had already been observed in human liver as well

and it catalyzes the ATP- and Mg (2+)-dependent conversion of 5-formyltetrahydrofolate (5-FTHF) to 5,10-methenyltetrahydrofolate (5,10- MTHF), which is subsequently interconverted into other reduced folates involved in carbon metabolism. Other up-regulated enzymes in Chianina take part in the amino acid metabolism and map on the network, such as Glutamate dehydrogenase (GLUD1, spot 210), Arginine Succinate Synthetase (ASS, spot 187) and Ornithine Carbamoyltransferase (OTC, spot 228). These basic enzymes act in the arginine and proline biosynthesis. In particular ASS and OTC are involved in the urea cycles. ASS is responsible for the third step of the urea cycle and one of the reactions of the Citrulline-NO cycle and is a precursor to fumarate in the citric acid cycle via argininosuccinate lyase. OTC is an enzyme that catalyzes the reaction between carbamoyl phosphate and ornithine to form citrulline and phosphate. GLUD1 represents a key link between catabolic and anabolic pathways: ammonia incorporation in animals occurs through the actions of glutamate dehydrogenase and glutamine synthetase. The product α-Ketoglutarate can be exploited to provide energy through the citric acid cycle, in order to ultimately produce ATP. Catalase (CAT, spot 77) and Oxydoreductase (HADH, or HSD17B) are enzymes involved in the final step of tryptophan degradativemetabolismto acetil-CoA.HADHin this case catalyzes the dehydrogenation of 3-hydroxy-butanoyl-CoA to acetoacetil-CoA and its over-expression can improve the Glycolitic pathway. Finally ACADAM and Beta-Ureidopropionase (UBP1, spot 222) are proteins that link the metabolism of beta-alanine to pyrimidine and propanoate metabolism, respectively. In fact Beta-ureidopropionase, also known as betaalanine synthase, catalyzes the last step in pyrimidine degradation and its depletion causes muscular hypotonia, dystonic movements. Degradation of uracil is the only pathway to provide b-alanine inmammals[62]. The net result of the alanine cycle is the transport of nitrogen from muscle to liver. In conclusion, the metabolic functions of the up/onregulated proteins in the Chianina breed with respect to Friesian seem to indicate a mobilisation of nonconventional energy supplies (proteins, fatty acids) regarding the use of glycogen. In parallel, the increased levels of PTPLAD1 from microarray observations, which is known to take part in the NRF2-mediated oxidative stress response pathway, and of transferrin (TF), a pivotal iron transporter, are consistent with catalase up-regulation in Chianina livers[63], and may account for an increased resistance to oxidative stress[64] also in consequence to fatty acid oxidation[65] All this information has been retrieved from the KEGG pathway Database Kanehisa Laboratory, Bioinformatics Center, Institute for Chemical Research, Kyoto University (http://www.genome.jp/kegg/pathway.html) [66,67] and the Ingenuity Pathways Knowledge

Base (Ingenuity® Systems, www.ingenuity.com). In contrast, a wider series of proteins and transcripts were expressed in Friesian which were absent in Chianina. These gene and proteins were mainly related to protein folding and degradation, hormone homeostasis and ability to thermoregulate. Indeed, in a recent paper, Sevi and colleagues[68] suggested that high ambient temperature may markedly modify the lipid composition of ewe's milk and that provision of shade, but not feeding management, can improve the milk fatty acid profile in dairy sheep raised in hot climates. Therefore, it is worthwhile to underline the identification of the hypothetical protein LOC78302 in Friesian (SULT1C), but not in the Chianina. LOC783020 is a protein belonging to the sulfotransferase (SULT1C4, spot 88) family that plays a key role in the biosynthesis and homeostasis of a number of hormones, including estrogens and iodothyronines. The gene structure (number and length of exons) is similar among family members. This gene encodes a protein that belongs to the SULT1 subfamily, responsible for transferring a sulfo moiety from PAPS to phenol-containing compounds. Two alternatively spliced transcript variants, encoding different isoforms, have been described for this gene. The final protein enzymes catalyze the sulfate conjugation of many neurotransmitters, drugs, xenobiotic compounds and, above all, hormones. Involvement of the thyroid hormones in adapting metabolism postpartum in calves is now a generally accepted idea: changes in the blood levels of T3 and T4 are detectable in calves suffering from ketosis[69]. For example blood levels of thyroid hormones were reduced in milk from post-partum cows[70]. Furthermore, several papers have reported studies on bovine milk investigating the relationship between the presence of iodine, thyroid metabolism and fertility problems[71]. For example, Wemheuer found that TRH increased the production of milk and lactose slightly (as well as milk enzymes)[71]. However Whitaker and co-workers[72] concluded that, although several texts have reported that iodine deficiency in bovine milk has an influence on fertility, more research is required to establish a firm link[73,74]. Over-expression of Calreticulin (HSP90AA1), a protein that binds calcium, has been observed in Friesian both with the proteomics and transcriptomics approach. HSP90AA1 is probably in correlation with SULT1C4. HSP90AA1 has a chaperonin-like activity and binds transcription factors of the thyroid (TTF-1), a homeodomain-containing protein implicated in the differentiation of lung and thyroid. HSP90AA1 mRNA levels in thyroid cells are under strict control by the thyroid-stimulating hormone, thus implicating calreticulin in the modulation of thyroid gene expression by thyroid-stimulating hormone. HSP90AA1 is a ubiquitously expressed and multifunctional Ca2+-binding protein that regulates diverse vital cell functions, including

Ca2+ storage in the ER and protein folding. Calreticulin deficiency in mice is lethal in utero due to defects in heart development and function. Interestingly, HSP90AA1 is closely located on the same map of SULT1C4 and takes part in a sub-pathway involving casein kinase 2 (ck2) and Furin, the latter known to cleave the proparathyroid hormone[75], for an indirect control on the thyroid hormone, and superoxide dismutase (SOD3 in the map), thus reducing the capacity to protect against oxidative stress[76]. The presence of Heat shock 70 kDa protein 5 (HSAPS, spot 358 in **Table 1**), as well as of HSP90, and HSPE1 were also observed in Friesian. It is worthwhile to underline that HSPs represented the central network individuated upon pathway analysis of either proteomics/transcriptomics data alone or taken together. Increased levels of HSPs occur in response to environmental stresses, infection, normal physiological processes, and gene transfer. Stress can disrupt the physiology and productive performance of an animal. The increase in body temperature caused by heat stress has direct, adverse consequences on cellular function, such as an increased glucose and amino acid oxidation and a reduced fatty acid metabolism[76]. This unbalance might favour trygliceryd deposition and, finally cause fatty liver. Fatty liver (i.e., hepatic lipidosis) is a major metabolic disorder of many dairy cows in early lactation and is associated with decreased health status and reproductive performance. In severe cases, milk production and feed intake are decreased. Therefore, a practical preventative or an efficacious treatment of fatty liver could help dairy farmers yearly save millions of dollars in treatment, replacement, and production losses. Since even mild fatty liver is associated with decreased health status and reproductive performance of dairy cows, prevention of fatty liver by supplying cows with sufficient nutrients and a clean and health-promoting environment in the peripartal period would reduce production losses of cows more than any subsequent treatment of fatty liver. This, however, might not be enough for those cows suffering from additional complications such as obesity, poor appetite, metabolic disorders, infectious diseases, calving difficulty or twin birth, or severe negative energy balance because of high milk production immediately after calving. Changes in the genetics and physiology of food animals for increased production are making these animals less able to regulate body temperature, i.e., less adapted to warm environments. This is especially true for dairy cattle. Selection for milk yield reduces the ability to thermoregulate in the face of heat stress[77] and magnifies the seasonal depression in fertility caused by heat stress[78]. Besides, use of bovine somatotropin (BST) as a lactational promotant can increase body temperatures during heat stress[79-83]. Moreover, adaptation of both beef and dairy cattle is reduced when native, genetically adapted cattle in tropical or

semitropical regions are replaced by higher producing, maladapted breeds. Chronic elevation of uterine temperature has long been known to increase embryo mortality in dairy cattle. Shortterm elevation in temperature of mouse embryos to 43°C (acute) has been shown to induce intracellular production of heat-shock proteins (HSPs). HSP 90 kDa beta member is important for converting certain fats to energy with a shortage (deficiency) of functional medium-chain acyl-CoA dehydrogenase. This causes that medium-chain fatty acids are not metabolized properly. As a result, these fats are not converted to energy, which can lead to several symptoms such as lack of energy (lethargy) and low blood sugar. **Figure 2** summarizes the nature of the identified polypeptide species and the differences in expression profiles between up/ on proteins from Friesian and Chianina. In general, the livers of both breeds have revealed a large number of protein species, in accordance with the numerous specialized biochemical and physiological functions of this organ. However, relative abundances vary between the two: in Friesian the largest group of proteins are chaperonines (36.85% of total proteins), whilst in Chianina they only represent 5.28%; hydrolases follow the opposite trend representing 10.52% and 26.31% respectively. Hydrolases perform a wide range of different digestive functions, though they are most prevalent in fatty acid metabolism, in agreement with pathway analysis elaborations for Chianina cattle livers; in contrast chaperonines are most involved in protein folding and consequently in the synthesis of new molecules or protection from denaturing stress (e.g. heat or oxidative stress) of the yet existing ones (as stressed by the pathway analysis elaboration for Friesian cattle livers). Although current proteomic methodologies applied to mammalian cell analysis still suffer from several technical limitations, which prohibit a systematic comprehensive description of the entire protein expression profile and result in non-detection of many important low soluble or less abundant components, these preliminary tissue analyses by conventional 2-DE procedures are still able to yield useful data on poorly characterized animals. Relevant information could be retrieved when performing both proteomics and transcriptomics analyses simultaneously, even when the experimental datasets display low to absent overlap, due to a series of intrinsic technical limitations—last but not least, the inadequacy of available statistical tools to compensate for biases in the data collection methodologies, as it has already been pointed out before[50]. Even in this case, however, interaction pathway analysis of those datasets allows the individuation of central networks sharing the same biological meaning, but not necessarily the same molecular actors. Hereby, we pinpointed at two main networks which undergo primary modifications in cattle breeds with different productive aptitudes, such as Chianina

and Friesian. This kind of approach definitely eases data analysis and final discussions, other than bridging the gap between the arid experimental phase and its biological interpretation (in this case, bovine liver).

2. DIFFERENTIAL EXPRESSION IN PIG MUSCLE PROTEOME

2.1. Introduction

Europe and China are the origin of about 70% of breed diversity in the world[84]. In both China and Europe, pig has been and remains a major meat producer. Molecular approaches to improve pig meat quality have been rapidly emerging and gaining momentum[85], especially those kinds of investigations which are oriented towards comparisons between different breeds through integrated proteomics and transcriptomics analyses[86,87].

Europe has 228 listed existing breeds, plus 105 now extinct; China has 118 listed breeds and 10 more extinct as it has been reported in the World Watch List for Domestic Animal Diversity[75]. In the late 18th century many new pig breeds, such as the Large White (LW) and the Berkshire in the UK came into existence and were distributed globally to replace or improve local breeds[85]. Indeed, many of the European local breeds have been heavily altered and three-quarters of local or traditional breeds are extinct or marginalized. This is the case of the black pigs of Italy, which have been long questioned to be influenced by pigs imported from China – although it is still controversial, as they appear to be closely related to the Iberian groups[84] or rather belong to an independent area of domestication on the Italian peninsula, which is opposed to the rest of Europe[85]. Italian black pigs might date back to Roman times or, more likely, to the 17th century[86]. One Italian breed in particular, the Neapolitan, played a pivotal role in the formation of some of the English breeds such as the Berkshire and the Large Black[35]. The Casertana and Calabrese directly descend from the Neapolitan lineage, which is formally extinct. Casertana is an endangered pig breed, very ancient and absolutely singular. It has been raised for centuries in semi-wild conditions in the forests near Caserta and Benevento, where it fed on acorns, chestnuts and other vegetables of the brush, and any other food it could find with his long snout.

CA and Large White exhibit an opposite genetic profile with respect to the energy metabolism. Chemical composition of muscles from Casertana and its crossbreeds (also with Large White) has already been investigated,[87] underlying that Casertana muscles are characterized by a higher lipid content and a lower protein content. Zullo et al. reported that Casertana and Landrace x (Landrace x Large White) pigs provided a product with the lowest chewing value; moreover, CA x (Landrace x Large White) pigs produced meat

with the highest water holding capacity, while CA pigs produced lighter commercial cuts[88]. Studies with Casertana pigs may shed light on the physiological process of fat deposition because these animals are prone to adipogenesis and have a strong aptitude for fat deposition. Indeed, Casertana pigs have a higher percentage of body fat and produce more than double backfat thickness as Large White pigs[89]. Since this breed did not undergo selection programmes, Casertana pigs retain the traits of a slow growing and high fat depositing pig compared to the genetic lines actually exploited in the pig industry. Comparison with Large White pigs demonstrated that the Casertana is far less competitive regarding growth performance, reaching a commercial slaughter weight at a considerably greater age, and with a 2 fold increase in backfat thickness[89].

Skeletal muscle is a heterogeneous tissue which is made up of several fiber types[90]. These compositional differences determine distinct metabolic and physiological functions and affect body composition as well as meat quality[91,92]. Muscles are traditionally distinguished among slow-twitch oxidative, fast-twitch glycolytic/ oxidative (red muscles) and fast-twitch glycolytic only (white muscles) [93].

Red muscles (for example *soleus* and *psoas*) are adapted to undertake chronic contractile activity without fatigue under aerobic respiratory conditions and are characterized by a higher percentage of capillaries, myoglobin, lipids and mitochondria than white skeletal muscles.

On the other hand, white muscles, such as the *gastrocnemius* and *Longissimus lumborum*, are recruited sporadically during the brief periods of intense muscular activity[92,93]. White and red muscles also differ in their fiber type composition.

A preliminary proteomics portrait of the *Longissimus lumborum* muscle has been recently provided, mainly aiming at determining the molecular characteristics influencing meat quality, on the basis of a comparative analysis on the role of alternative genetic backgrounds[94,95].

The proteome analysis based on 2-DE and mass spectrometry is a method of choice for the quantitative differential display of large numbers of proteins and is a promising and powerful tool in meat science. Differential proteomics analyses between different pig breeds have already been performed (Meishan vs Large White, Pietrain vs Duroc x (LWxHampshire))[96, 97].

In the present study, we performed proteomics, transcriptomics and interactomics network/pathway analyses, along with functional enrichment of GO terms, to the end of characterizing and comparing expression profiles in the *Longissimus lumborum* of

Casertana and Large White. Our aim was to reveal the differences of breed-related protein/transcript expression patterns between the Casertana and the Large White. These observations might be useful to deepen our understanding of the genetic differences among these breeds, as well as the molecular mechanisms responsible for breed-specific peculiar growth performance.

2.2. Material and Methods

2.2.1 Sample preparation

All animals used in this study were treated according to International Guiding Principles for Biomedical Research Involving Animals. We selected 20 animals (10 per breed) which were of the same age.

Sample preparation and solubilization was performed by slight modification of the SWISS-2D PAGE sample preparation procedure[97]. Frozen samples of *Longissimus lumborum* from 10 Large White and 10 Casertana (approximately 20 mg per sample) were crushed in a mortar containing liquid nitrogen, and to remove lipids, proteins were precipitated from a desired volume of each sample with a cold mix of tri-n-butyl phosphate/acetone/methanol (1:12:1). After incubation at 4 C for 90 min, the precipitate was pelleted by centrifugation at 2,800g, for 20 min at 4 C. After washing with the same solution, the pellet was air-dried and then resuspended in the focusing solution containing 7M urea, 2M thiourea, 4% (w/v) CHAPS, 0.8% (w/v) pH 3–10 carrier ampholyte, 40mM Tris, 5mM TBP, 0.1 mM EDTA (pH 8.5), 2% (v/v) protease inhibitor cocktail (Sigma-Aldrich, Basle, Switzerland), and 2mM PMSF. Before focusing, the sample was incubated in this solution for 3 h at room temperature, under strong agitation. Alkylation has been performed with 7.7 mM Iodoacetamide in a solution of 7 M urea, 2 M thiourea, 4% CHAPS, 20 mM Tris, pH 3-10 carrier ampholyte, 40 mM Tris, 5 mM TBP, 0.1 mM EDTA (pH 8.5), 2% (v/v) protease inhibitor cocktail (Sigma-Aldrich). To prevent over-alkylation, iodoacetamide excess was destroyed by adding equimolar amount of DTE. The protein concentration of each group was determined according to Bradford[10] using BSA as a standard curve.

2.2.2. Semiquantitative IEF-SDS PAGE

A total of 250 µL of the resulting protein solution was then used to rehydrate 18 cm long IPG 3-10 NL (Amersham Biosciences) for 8 h (1 mg of protein each strip). IEF was

carried out on a Multiphor II (Amersham Biosciences) with a maximum current setting of 50 µA/strip at 20°C. IEF was performed using ready-to-use Immobiline Dry-Strips linear pH gradient 3–10 length 18 cm (Biorad, CA, USA) and the in gel sample rehydration method. IEF was run on an Protean IEF BIORAD at 20°C constant temperature and 8000 V for 99,000 Vh. After IEF, the IPG gel strips were incubated at room temperature for 30 min in 6 M urea, 30% w/v glycerol, 2% w/v SDS, 5 mM Tris-HCl, pH 8.6. The strips were sealed at the top of a 1.0 mm vertical second dimensional gel (Biorad) with 0.5% agarose in 25 mM Tris, 192 mM glycine, 0.1% SDS, pH 8.3. SDS-PAGE was carried out on homogeneous running gels 12 % T 3% C The running buffer was 25 mM Tris, 192 mM glycine, 0.1% SDS, pH 8.3 and running conditions were 40 mA/gel until the bromophenol blue reached the bottom of the gel. Molecular weight marker used was Wide Range Weight Electrophoresis Calibration Kit (Amersham Biosciences, UK). Gels were automatically stained with Brilliant Blue G colloidal (Sigma, St. Louis, MO, USA) following the manufacturer's instructions. Gels have been de-stained overnight in deionized water with blotting paper meant to gather Coomassie excess. Three technical replicates per sample were performed.

2.2.3. Pig Longissimus lumborum gels.

Thirty-six stained gels were digitalized using an ImageScanner and LabScan software 3.01 (Bio-Rad Hercules, CA). The 2-DE image analysis was carried out and spots were detected and quantified using the Progenesis SameSpots software v.2.0.2733.19819 software package (Nonlinear Dynamics, New Castle UK). Each gel was analyzed for spot detection and background subtraction. Within-group comparison of protein spot numbers was determined by repeated measures analysis. Among-group comparisons were determined by ANOVA (Analysis of Variance) procedure in order to classify sets ofproteins that showed a statistically significant difference with a confidence level of 0.05. Spots which were significantly different between groups (Chianina vs Friesian) and not significantly different in the three technical replicate and six biological replicate samples were identified by qTOF-MS/MS. All statistical analyses were performed with the Progenesis SameSpots software v.2.0.2733.19819 software package[52].

After the background subtraction, spot detection and match, one standard gel was obtained for each group. These standard gels were then matched to yield information about the spots of differentially expressed proteins. Differential protein expression was

considered significant at $P<0.05$ and the change in the photodensity of protein spots between Chianina and Friesian samples had to be more than 2 fold.

2.2.4. In-Gel Digestion

Spots from 2-DE maps were carefully excised from the gels and subjected to in-gel trypsin digestion according to Shevchenko[56] with minor modifications. The gel pieces were swollen in a digestion buffer containing 50 mM NH_4HCO_3 and 12.5 ng/ml trypsin (modified porcine trypsin, sequencing grade, Promega, Madison, WI, USA) in an ice bath. After 30 min, the supernatant was removed and discarded; then 20 ml of 50 mM NH_4HCO_3 were added to the gel pieces, and digestion was allowed to proceed overnight at 37°C. The supernatant containing the peptide mixture was removed and acidified with 5% formic acid before injection in the mass spectrometer.

2.2.5. Protein identification by Nano-RP-HPLC-ESI-MS/MS

Mass spectrometric procedures were performed as previously described[56] Peptide mixtures were separated using nanoflow-HPLC system (Ultimate; Switchos; Famos; LC Packings, Amsterdam, The Netherlands). A sample volume of 10 µL was loaded by the autosampler onto a homemade 2 cm fused silica pre-column (75 µm I.D.; 375 µm O.D) Reprosil C18-AQ, 3 µm (Ammerbuch-Entringen, DE) at a flow rate of 2 µL/min. Sequential elution of peptides was accomplished using a flow rate of 200 nL/min and a linear gradient from Solution A (2% acetonitrile; 0.1% formic acid) to 50% of Solution B (98% acetonitrile; 0.1% formic acid) in 40 minutes over the precolumn in-line with a homemade 10-15 cm resolving column (75 µm I.D.; 375 µm O.D.; Reprosil C18-AQ, 3 µm (Dr. Maisch GmbH, Ammerbuch-Entringen, Germany). Peptides were eluted directly into a High Capacity ion Trap HCTplus (Bruker-Daltonik, Bremen, Germany). Capillary voltage of 1.5-2 kV and a dry gas flow rate of 10 L/min were used at a temperature of 200°C. The scan range used was from 300 to 1,800 m/z. Protein identification was performed by searching in the National Center for Biotechnology Information non-redundant database (NCBInr, version 20081128, www.ncbi.nlm.nih.gov) using the Mascot program in-house version 2.2 (Matrix Science, London, UK). The following parameters were adopted for database searches: complete carbamidomethylation of cysteines and partial oxidation of methionines, peptide Mass Tolerance ± 1.2 Da, Fragment Mass Tolerance ± 0.9 Da, missed cleavages 2. For positive identification, the score of the result of (- 10 x Log(P)) had to be over the significance threshold level ($P < 0.05$). Even though high MASCOT scores are obtained

with values greater than 60, when proteins were identified by one peptide only a combination of automated database search and manual interpretation of peptide fragmentation spectra was used to validate protein assignments. In this manual verification the mass error, the presence of fragment ion series and the expected prevalence of C-terminus containing ions (Y-type) in the high mass range were all taken into account. Moreover, replicate measurements have confirmed the identity of the protein hits.

2.2.6. Phosphorylated proteins identification

Gels have been washed three times with double distilled water and then stained with ProQ diamond[88] (Invitrogen, Carlsbad, CA) for 2 hours, following manufacturer's instructions. Stained gels have been washed three times with a 100 mM Sodium Acetate, 20% Acetonitrile solution for destaining. Images have been acquired with a *Gel Doc*™ XR System (Biorad), through UV-ray fluorescence and matched against coomassie stained gels.

2.2.7. RNA Samples Collection

Longissimus lumborum muscle samples of Large White and Casertana individuals (see above) were collected immediately after slaughtering. Samples were preserved in RNA later (Sigma-Aldrich) and stored at –80°C. Total RNA was extracted by using TRIzol Plus RNA purification kit (Invitrogen). RNA integrity was assessed by electrophoretic analysis of 28S and 18S rRNA subunits. RNA purity and concentration were assessed with the spectrophotometer GeneQuant*pro* (Amersham Pharmacia Biotech, Uppsala, Sweden); A260/A280 ratio was >1.9. Besides RNA concentration was measured by using the Quant-iT RNA Assay kit (Molecular Probes) on the DTX 880 fluorometer (Beckman Coulter, Brea, USA).

2.2.8. Microarray experiments

An amount of 1μg pooled RNA was first reverse transcripted and then amplified by using the RNA ampULSe kit (Kreatech, Amsterdam, The Netherlands) following manufacturer's instructions. 4 μg of aRNA for each pool were labelled with Cy3 and Cy5 dye independently; for the repeat slide the same comparison was made with the dye assignment reversed (dyeswap)[99] A technical replicate was performed starting from the same RNA pool (4 slides). A biological replicate of the previous experiment was obtained starting with independent RNA preparation from the same sample tissues (4 slides) [24] The slides

were spotted by CRIBI service with the 70mer Pig Genome Oligo Set Version 1.0 (Operon) representing the 10,665 *Sus scrofa* gene sequences replicated twice. Annotations for oligo sequences were update on March 2006. The hybridizations were performed at 48°C for 18 hours by using the HybChamber (GeneMachines, San Carlos, CA).

2.2.9. Microarray data analysis

Hybridization images were scanned with the Packard™ ScanArray® Express Line of Microarray Scanners (PerkinElmer Life Sciences, Waltham, Massachussets). Spotfinder software (TIGR) was used to extract feature data from microarray fluorescence images. Slides were first pre-processed filtering spots with poor hybridization signals, saturated signals, or signal to background ratio lower than two. Then lowess and dye-swap normalizations were applied[60,100]. To establish the significance of observed regulation for each gene, t-test with Welsh's correction was performed. Finally, only genes with Fold-Change over |1.3| were considered (Benjamini/-/Hochberg adjusted P<0,05).

2.2.10. Network analyses

The networks were generated through the use of Ingenuity Pathway Analysis (Ingenuity® Systems, www. ingenuity.com)[60]. A data set containing gene identifiers and corresponding expression values was uploaded into in the application, basing on either proteomics or transcriptomics results. Each gene identifier was mapped to its corresponding gene object in the Ingenuity Pathways Knowledge Base. The significance of the association between the data set and the canonical pathway was measured in 2 ways: 1) a ratio of the number of proteins from the data set that map to the pathway divided by the total number of proteins that map to the canonical pathway is displayed. 2) Fischer's exact test was used to calculate a P-value determining the probability that the association between the proteins in the dataset and the canonical pathway is explained by chance alone. Proteins/ gene products are represented as nodes, and the biological relationship between two nodes is represented as an edge (line).

All edges are supported by at least 1 reference from the literature, from a textbook, or from canonical information stored in the Ingenuity Pathways Knowledge Base. Nodes are displayed using various shapes that represent the functional class of the gene product. Grey nodes represent the proteins/ genes from the submitted dataset which have a match in the canonical pathway from the database, while white nodes represent gene products that the software attributed to the same networks, although they were not present in the submitted

dataset. Continuous lines (edges) represent direct interactions, while indirect ones are represented by interrupted lines.Circular lines around onenode describe a feed-back loop of activity of that node on itself (e.g. by self-modulating its activity or expression). Grey edges represent interactionswithin a single network, while orange edges cross-link nodes from multiple interacting networks. The program could either graph single networks alone or merged together to stress their interactions.

The Ingenuity Pathway Analysis software allows performing an unbiased elaboration of the experimental data, in order tofocus subsequent analyses and discussions on the pivotal networks which are revealed upon the experimental phase (in this case: differentially-expressed liver proteins and gene transcripts).

For Casertana and Large white, preliminary network analyses were performed as above. Two original lists of proteins and gene transcripts were obtained from proteomics and transcriptomics differential analyses. The lists (either merged or alone) were submitted for elaboration of network analyses to the Ingenuity Pathway Analysis (IPA) software (Ingenuity® Systems, www.ingenuity.com) [101]. Each gene identifier from the submitted list was mapped to its corresponding gene object in the Ingenuity Pathways Knowledge Base. The significance of the association between the dataset and the canonical network was measured in 2 ways:

1) A ratio of the number of proteins from the data set that map to the pathway divided by the total number of proteins that map to the canonical pathway is displayed.

2) Fischer's exact test was used to calculate a p-value determining the probability that the association between the proteins in the dataset and the canonical pathway is explained by chance alone.

Highest scores are proportional to a lower probability of casual association. The IPA software allowed us to perform an unbiased elaboration of the available data, in order to focus subsequent analyses and discussions on the pivotal networks.

Network analysis delves into protein-protein interactions and exploits them to give an intuitive portrait of the relationships among pivotal molecules and, on a higher level, among networks. The software determines and graphs unbiased networks, in which gene products are represented as nodes, and the biological relationship between two nodes is represented as an edge (line). All edges are supported by at least 1 reference from the literature, from a textbook, or from canonical information stored in the Ingenuity Pathways Knowledge Base. Nodes are displayed using various shapes that represent the functional class of the gene product. Grey nodes represent the proteins from the submitted dataset

which have a match in the canonical pathway from the database, while white nodes represent gene products that the software attributed to the same networks, although they were not present in the elaborated dataset. Continuous lines (edges) represent direct interactions, while indirect ones are represented by interrupted lines. Circular lines around one node describe a feed-back loop of activity of that node on itself (e.g. by self-modulating its activity or expression). Grey edges represent interactions within a single network (intra-network), while orange edges cross-link nodes from multiple interacting networks (cross-network).

In a general point of view, IPA software was initially developed for the study of pathologies and mainly focused on cancer. As a consequence, many of the retrieved pathways are related to diseases, in particular to cancer. Clearly, this software is not well adapted for the study of pig proteins. To fix this difficulty, IPA or equivalent software should firstly be used to establish some group of proteins. Therefore, proteomics data were also elaborated for network analysis with Cytoscape[102], exploiting the APID2NET plugin[103]. Data were treated as to include all the proteins individuated upon the experimental phase, including isoforms and excluding redundant entries. The software interrogates freely available online database for interactomics analysis, namely BioGrid (version 2.0.47), BIND (version 04-05-06), DIP (version 14-10-08), HPRD (version 7), IntAct (version 2008-12-12), MINT (version 2008-10-23). Interaction data are compared against standard proteomics databases for protein identification through IDs, names and descriptions, such as UniProt, and validated with iPfam (for domain-domain interaction-pattern recognition. Cut-off values were set as to include in the protein-protein interaction analyses only those nodes which have been reported as interactors in at least 3 experimental publications and with at least two different techniques. Experimentally-individuated proteins are represented as red nodes, while white nodes represent those proteins which the software has individuated as likely interactors through stringent analysis.

2.3. Results

We investigated protein composition of *Longissimus lumborum* muscle samples from Large White and Casertana pig breeds. In parallel, samples were also analyzed with transcriptomics techniques.

Proteomics analyses (2-DE and MS/MS identification) yielded a total of 473 $\pm$ 44 spots which were commonly expressed by both breeds, and 36 differentially-expressed spots ($P \leq 0.05$) upon comparison of 60 gels (30 per breed, 10 biological replicates and 3 technical replicates each). In particular, 14 spots were up-regulated in Casertana and 20 in Large White (**Table 3**). Approximately 95% of these spots were identified via ESI-MS/MS. Notably, mass spectrometric identification of those spots revealed that most of those spots accounted for the same protein (mainly glycolytic enzymes in Casertana and myosin light chain isoforms in Large White**)**, as to yield a total of 10 different up-regulated proteins in Casertana and 10 counterpart entries for Large White. Some proteins have multiple duplicate entries in the table, such as creatine kinase M chain for Casertana (3 entries) and myosin light chain 1f in Large White (4 entries).

For example, spots 29 and 47 from Large White, accounting for the same protein (myosin light chain 1f), displayed a similar quantitative trend. Analogous observations could be made for spots 21, 473 and 54 (creatine kinase M-type), which are reported in **Figure 3**. These observations could suggest that breed-specific characteristic probably rely on further differential post-translational modifications of pivotal enzymes, other than on their specific differential expression. However, ProQ diamond staining for the characterization of the phosphorylation pattern through specific staining of 2D gels confirmed that most of these duplicate entries showing only slight differences in pH were represented by differently phosphorylated proteins (**Figure 4** for details).

Microarray analyses have individuated a total of 105 differentially-expressed gene transcripts with a fold change > 1.3 (**Table 4**). In detail, 66 gene transcripts were up-regulated in Casertana and 39 in Large White pigs. Little or no direct overlap between transcriptomics and proteomics data was observed, as previously reported[103,104]. These differences may arise from annotation errors or differential regulation of translation, turnover or alternative splicing.[69] However, in addition to various biological factors, it should be considered that the poor correlation between transcriptomic and proteomic data could be quite possibly due to the inadequacy of available statistical tools to compensate for biases in the data collection methodologies as well as to the different bioinformatic approaches employed to analyze and integrate data from either proteomics or genomics studies,[14] but is more likely to be due to the difficulties in evaluating on a global level which biological factor, translational efficiency or protein half-life influences the correlation between mRNA and protein abundances to time-course differences between mRNA changes and protein responses[84,105].

It has been previously suggested and observed[106] that, although massive proteomics and transcriptomics studies on the same biological model seldom directly match, they likely converge when it comes to the biological pathway in which the individuated proteins/gene transcript products utterly map.

Although modest direct overlap was observed between analyses from different platforms, many of the individuated proteins and gene transcripts could be regrouped under the same functional category and take part in the same biological networks. Under this perspective, proteins and gene transcripts indirectly converged in Casertana, as they mainly belonged to metabolic pathways - glycolytic and glycolysis-related enzymes, such as Enolase 3 (ENO3), Triosephosphate Isomerase (TPI), Phosphoglucomutase1 (PGM1), Lactate Dehydrogenase (LDHA), Glucose 3-Phosphate Dehydrogenase (GPDH) and Creatine Kinase (CK-M)**;** Ketoexokinas**e (**KHK) - enzymes involved in fatty-acid oxidation responses - glutaredoxin 3 (GRX3), thioredoxin 2 TRX2 - calcium homeostasis - Calsequestrin, (CASQ1) S100 calcium binding protein A2 (S100A2), hormone inducers/growth factors/regulators of transcription (hydroxy-delta-5-steroid dehydrogenase (HSD3B2), NFKB inhibitor interacting Ras-like 1 (NKIRAS1), bromodomain containing 4 (BRD4), leucine-rich repeat kinase 1 (Lrrk1), silent mating type information regulation 2 homolog 2 (SIRT1).

Conversely, proteins and gene transcripts which were found to be over-expressed in Large White *Longissimus lumborum* muscle mainly accounted for structural muscle proteins - myosin light chain (MLC) isoforms 1f, 2, 2V and 3; alpha-actin (ACTA1), proteins involved in the maintenance of the balance between protein synthesis and degradation - E3 ubiquitin-protein ligase (MARCH5), ring finger protein 128 (RNF128), SERPINA3 fatty-acid oxidation and oxidative stress response - carnitine palmitoyltransferase 1C (CPT1), Glutathione peroxidase 5 (GPRX5), Peroxiredoxin-2 (PRX2), transcription regulators - retinoic acid receptor alpha (RARA), estrogen related receptor alpha (ESRRA), basic leucine zipper and W2 domain-containing protein 2 (BZW2), zinc finger protein 212 (ZNF212).

These preliminary observations were confirmed upon GO term enrichment of biological function in Casertana *Longissimus lumborum* up-regulated proteins and transcripts (Tables **3-5**). Indeed, Casertana muscles appeared to be particularly enriched in GO terms involving glycolytic catabolism (catabolic process, cellular catabolic process, glycerol metabolic process, glycerol-3-phosphate metabolic process, cellular carbohydrate catabolic

process, hexose metabolic process and vitamin metabolism (vitamin metabolic process, L-ascorbic acid metabolic process.

GO term enrichment for biological functions confirmed the role of muscle growth (developmental maturation, regulation of cell proliferation, muscle development and contraction/response to stress (muscle contraction, response to stress, lipid metabolism (lipid metabolic process, regulation of lipid metabolic process and, adding a further detail, oxidative metabolism (oxygen and reactive oxygen species metabolic process, oxidative phosphorylation). Whether a molecular correlation between predisposition to adipogenesis and molecular profiles surely exists, it is more likely distributed on wide networks of proteins instead of relying on single specific molecules. This is the reason why we focused on protein-protein interaction networks of the individuated datasets. A multi-platform network analysis was performed with IPA for Casertana (**Figure 5**) and Large White (**Figure 6**).

Merging both proteomics and transcriptomics datasets allowed us to graph a detailed map of the Casertana differential interactome, dissected in 4 sub-groups, namely Nfkβ-related pathways (A), solute carriers (B – Vitamin carriers such as SCL23A2), glycolytic metabolism (D – PGM1, LDH, ENO3, GPDH) and muscle stress and contraction (D – CASQ, CASQ2; Lipoxygenase; thioredoxin 2, glutaredoxin). It is immediately evident that the very heart of the map, harbouring a series of transcription factors, is mainly characterized by white nodes, that is to say proteins missing in the submitted dataset. However, it should be considered that only differentially expressed proteins and gene transcripts were included in the present analysis. Inclusion of non- or less-significantly differently expressed proteins in the dataset would solve this minor issue of the IPA analysis.

In like fashion to the Casertana map, the Large White interactome could be dissected in 3 sub-groups, namely cell growth-related pathways: a series of transcriptional regulators and proliferation-related molecules are present (A); lipid metabolism/mobilization (B); muscle growth, myosin isoforms in particular (C).

The Cytoscape/APID2NET analysis confirmed observations from IPA and revealed two main sub-groups of nodes in the CA map, which accounted for proteins devoted to glycolysis (north) and Muscle contraction (center, south). Likewise, the Large White protein-protein interaction map could be divided in 3 domains, the first including proteins involved in muscle protein synthesis and degradation (north), in muscle contraction the second (south), and lipid mobilization (center).

A detailed discussion of the main proteins/gene transcripts which emerged upon pathway, network and functional GO analyses is provided as follows.

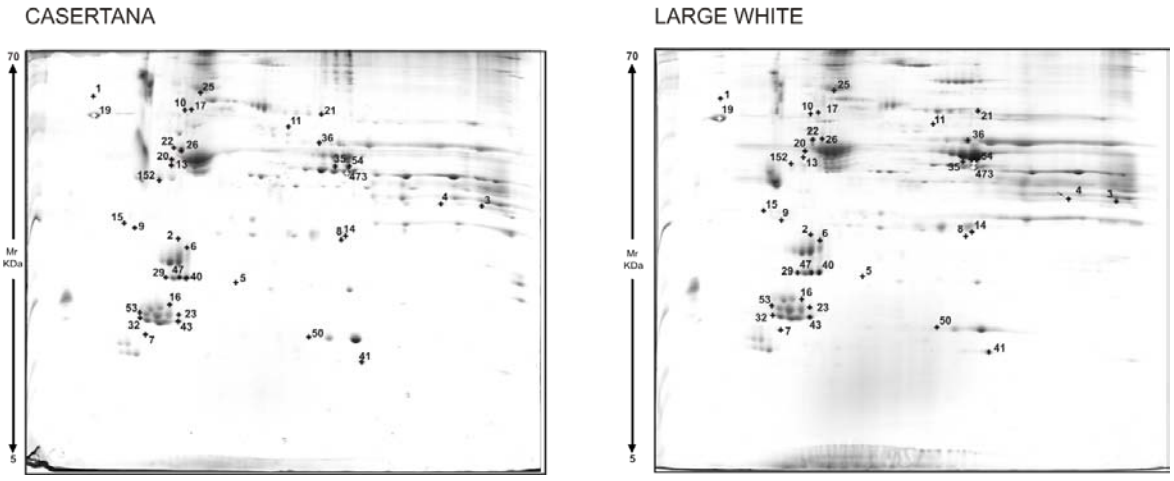

Figure 3. 2-DE of *Longissimus lumborum* extracts from Large White and Casertana pig breeds. IEF pH range is 3-10, 12% T 3% C Acrylamide. Gels have been stained with Colloidal Coomassie. Each gel image has been elaborated with Progenesis SameSpots (Nonlinear Dynamics, NewCastle, U.K.) and represent an average of 30 gels (3 technical replicate for 10 biological replicate samples), upon background subtraction.

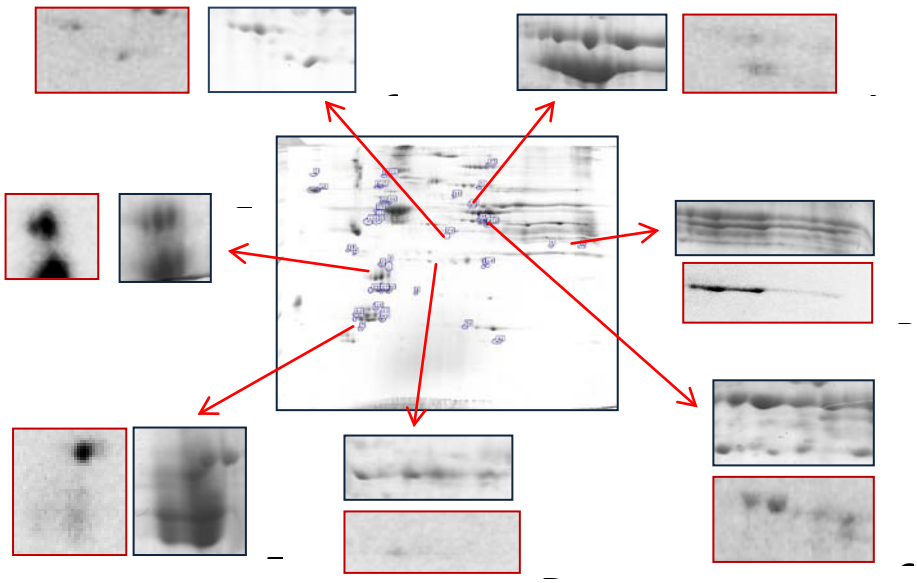

Figure 4. Phosphorylated proteins recognized by ProQ-Diamond staining are shown. (A) Enolase; (B) Lactate Dehydrogenase; (C) Creatine Kinase; (D) NI; (E) Myosin Regulatory Light Chain 2; (F) Myosin Light Chain 1, Fast; (G) cytosolic glycerol-3-phosphate dehydrogenase. Coomassie staining is shown squared in blue, corresponding ProQ Diamond staining squared in red.

Table 3. Protein differentially expressed from Large White and Casertana pig breeds.

Differential proteomics analysis						
Casertana						
N Spot	Mr, kDa theor/exper	pI theor/exper	No. of peptides identified	Mascot Score	NCBI Accession Number	**Protein ID [Sus scrofa]**
CTspot1	45.0/70.0	4.0/3.9	2	73	gi|118150866	Calsequestrin 1 [Bos taurus]
CTspot3	36.9/32.0	8.2/9.2	9	460	gi|1170740	L-lactate dehydrogenase A chain (LDH-A) (LDH muscle subunit) (LDH-M) [Sus scrofa]
CTspot4	36.9/32.0	8.2/8.7	6	388	gi|1170740	L-lactate dehydrogenase A chain (LDH-A) (LDH muscle subunit) (LDH-M) [Sus scrofa]
CTspot7	15.1/17.0	4.9/4.7	5	463	gi|3746944	phosphoglucomutase 1 [Sus scrofa]
CTspot8	22.1/25.8	6.0/7.3	12	655	gi|91214448	triosephosphate isomerase 1 [Sus scrofa]
CTspot11	54.1/54.0	6.0/6.6	5	266	gi|119917044	Similar to tripartite motif-containing 72 [Homo sapiens]
CTspot14	22.1/25.8	6.0/7.4	17	973	gi|91214448	triosephosphate isomerase 1 [Sus scrofa]
CTspot15	20.3/29.0	5.0/4.7	8	380	gi|2149959	cytosolic glycerol-3-phosphate dehydrogenase [Sus scrofa]
CTspot 21	43.3/54.7	6.6/7.3	20	1021	gi|62286641	Creatine kinase M-type (Creatine kinase M chain) [Sus scrofa]
CTspot35	47.4/40.5	8.0/7.3	19	1079	gi|113205498	enolase 3 [Sus scrofa]
CTspot36	44.8/44.0	8.0/7.0	10	564	gi|47169448	Chain A, Structure Of Pig Muscle Pgk Complexed With Mgatp [Sus scrofa]
CTspot50	17.1/17.1	6.8/7.0	2	72	gi|230253	Chain A, The Determination Of The Crystal Structure Of Recombinant Pig Myoglobin By Molecular Replacement And Its Refinement [Sus scrofa]
CTspot54	43.3/40.5	6.6/7.4	15	866	gi|62286641	Creatine kinase M-type (Creatine kinase M chain) [Sus scrofa]
CTspot473	43.3/39.0	6.6/7.4	14	843	gi|62286641	Creatine kinase M-type (Creatine kinase M chain) [Sus scrofa]
Large White						
N spot	Mw kDa	pI	No. of peptides	Mascot Score	NCBI Accession Number	**Protein ID**

			identified			[Sus scrofa]
LWspot2	21.0/26.1	4.9/5.2	13	782	gi|117660874	MLC1f [Sus scrofa]
Lwspot5	22.9/23.1	5.8/5.7	4	217	gi|9968807	alpha-1-antichymotrypsin 3 [Sus scrofa]
LWspot6	21.0/26.1	4.9/5.3	12	824	gi|117660874	MLC1f [Sus scrofa]
LWspot9	26.4/29.0	4.8/4.7	5	268	gi|530049	14-3-3 protein [Ovis aries]
LWspot10	42.2	5.3/5.2	4	210	gi|6653228	skeletal alpha-actin [Sparus aurata]
LWspot13	30.3/41.0	5.4	13	638	gi|164359	apolipoprotein A-I [Sus scrofa]
LWspot16	19.1/20.5	4.9/5.1	16	884	gi|54607195	myosin regulatory light chain 2 [Sus scrofa]
LWspot17	42.2/55.2	5.2/5.2	4	239	gi|30268609	skeletal alpha-actin type-2b [Coryphaenoides yaquinae]
LWspot19	44.9/55.0	4.0/3.8	2	109	gi|118150866	calsequestrin 1 [Bos taurus]
LWspot20	42.4/41.5	5.3/5.2	7	578	gi|27819614	actin, alpha 1, skeletal muscle [Bos taurus]
LWspot22	45.7/44.1	5.8/5.3	4	218	gi|61553131	alpha 2 actin [Bos taurus]
LWspot23	19.1/19.0	4.9/5.2	5	353	gi|54607195	myosin regulatory light chain 2 [Sus scrofa]
LWspot26	42.3/44.2	5.2/5.4	9	663	gi|268607671	actin, alpha skeletal muscle [Sus scrofa]
LWspot29	21.0/23.4	4.9/5.0	14	868	gi|117660874	MLC1f [Sus scrofa]
LWspot32	19.1/18.0	4.9/4.7	12	767	gi|54607195	myosin regulatory light chain 2 [Sus scrofa]
LWspot40	14.3/23.4	4.7/5.3	3	128	gi|1717797	Peroxiredoxin-2 (Thioredoxin peroxidase 1) (Thioredoxin-dependent peroxide reductase 1) (Thiol-specific antioxidant protein) (TSA) [Sus scrofa]
Lwspot41	16.1/14.0	6.8/7.4	11	886	gi|809283	Chain B, Structure Determination Of Aquomet Porcine Hemoglobin At 2.8 Angstrom Resolution
LWspot43	19.1/18.0	4.9/5.2	12	929	gi|54607195	myosin regulatory light chain 2 [Sus scrofa]
LWspot47	21.0/23.4	4.9/5.2	13	803	gi|117660874	MLC1f [Sus scrofa]

LWspot53	16.7/19.0	4.6/4.7	5	244	gi|127135	Myosin light chain 3, skeletal muscle isoform (A2 catalytic) (Alkali myosin light chain 3) (MLC3F) [Oryctolagus cuniculus]

Table 4. Microarray Output.

Large White						
N.	**Gene Id**	**Unigene Sus**	**Gene**	**Gene Encoding**	**Fold Change**	**p value**
1.	gi|194044553	Ssc.49967	NP_115590.1	milar to Srclikeadaptor 2 isoform a	1,30215	0,001452
2.	gi|194034423	Ssc.48760	L2HGDH	Similar to L-2-hydroxyglutarate dehydrogenase precursor	1,30235	0,000268
3.	gi|194040450	Ssc.1094	GLO1	Similar to glyoxalase I	1,30615	0,002367
4.	gi|190360625	Ssc.8984	ARHGEF2	rho/rac guanine nucleotide exchange factor (GEF) 2	1,30895	0,012928
5.	gi|22748777	Ssc.18511	CPT1C	Strongly similar to carnitine palmitoyltransferase 1C isoform 2	1,3153	0,013585
6.	gi|219522004	Ssc.54776	MAPKAPK3	Mitogen-activated protein kinase activated- protein kinase 3	1,32111	0,028946
7.	gi|37588873	Ssc.18929	RNF128	ring finger protein 128	1,32246	0,022308
8.	gi|194035579	Ssc.5132	FAM84B	family with sequence similarity 84, member B	1,32584	0,00897
9.	gi|51873031	Ssc.11130	NCLN	strongly similar to nicalin precursor [Homo sapiens]	1,3287	0,004981
10.	gi|237681314	Ssc.3153	NP_001020461.1	developmental pluripotency associated 5	1,33176	0,018456
11.	gi|10092639	Ssc.18546	LOC100070329	similar to cysteine-rich motor neuron 1 protein precursor [Homo sapiens]	1,34622	0,001207
12.	gi|194037340	Ssc.15828	RARA	Retinoic acid receptor, alpha	1,34798	0,000997
13.	gi|31083243	Ssc.6731	PPP2R5C	protein phosphatase 2, regulatory subunit B', gamma isoform	1,34823	0,021911
14.	gi|24797065		ZNF212	zinc finger protein 212	1,35108	0,036852
15.	gi|1469874	Ssc.61966	LOC100050625	similar to Uncharacterized protein KIAA0146	1,3546	0,033324
16.	gi|149193321	Ssc.12808	GRSF1	Grich RNA sequence binding factor 1	1,35556	0,002732
17.	gi|13938355	Ssc.7378	ATP6V1B2	ATPase, H+ transporting, lysosomal 56/58kDa, V1 subunit B2	1,35894	0,00147
18.	gi|8923900	Ssc.1763	CMAS	cytidine monophosphate Nacetylneuraminic acid synthetase	1,37176	0,000527
19.	gi|220732380		FREM1	FRAS1 related extracellular matrix 1	1,37538	0,010872
20.	gi|29788758	Ssc.39944	LOC652955	similar to goliath Homolog precursor [Homo sapiens]	1,37623	0,012116
21.	gi|55859666	Ssc.18510	XP_001493829.1	Similar to actin binding LIM protein 1 [Homo sapiens]	1,37654	0,046034
22.	gi|148763347	Ssc.70866	XP_001713795.1 replaced in database by NP_076916	similar to cell division protein kinase 11A isoform 1 [Homo sapiens]	1,37909	0,048123
23.	gi|209915561	Ssc.60309	LOC506315	similar to dynamin 3 [Homo sapiens]	1,37985	0,012045
24.	gi|239049447	Ssc.6166	LOC100061008	similar to malic enzyme 3, NADP(+)dependent, mitochondrial precursor [Homo sapiens]	1,38554	0,010694
25.	gi|171465894	Ssc.2330	SLC3A2	Solute carrier family 3 (activators of dibasic and neutral amino acid transport), member 2	1,40501	0,005402
26.	gi|33636756	Ssc.40278	MARK4	Similar to MAP/microtubule affinity regulating kinase 4	1,40557	0,049369

27.	gi|209977023	Ssc.15262	LOC100068640	moderately similar to NP_872425.2 secretory protein LOC348174 precursor [Homo sapiens]	1,40972	0,036035
28.	gi|47523090	Ssc.14513	GPX5	Glutathione peroxidase 5 (epididymal androgenrelated protein)	1,41346	0,015261
29.	gi|168229161	Ssc.60909	CORO7	Similar to coronin 7 (Homo sapiens)	1,4171	0,011396
30.	gi|18860920	Ssc.55256	Esrra	strongly similar to NP_004442.3 estrogen-related receptor alpha [Homo sapiens]	1,43313	0,017213
31.	gi|21389315	Ssc.17264	SLC25A1	Similar to solute carrier family 25 (mitochondrial carrier; citrate transporter), member 1[Homo sapiens]	1,43735	0,010343
32.	gi|229577398	Ssc.51869	LOC100053031	similar to Basic leucine zipper and W2 domaincontaining protein 2	1,44724	0,017316
33.	gi|119570479	Ssc.7478	LOC788125	similar to E3 ubiquitinprotein ligase MARCH5 (Membraneassociated RING finger protein 5) (Membraneassociated RINGCH protein V) (MARCHV) (RING finger protein 153)	1,45647	0,044993
34.	gi|6634023	Ssc.29073	LOC531863	similar to Pleckstrin Homology domaincontaining family M member 1 (162 kDa adapter protein) (AP162)	1,45783	0,003205
35.	gi|89353283	Ssc.6230	SDCCAG3	Moderately similar to serologically defined colon cancer antigen 3	1,46199	0,000443
36.	gi|189083684	Ssc.6514	Gale	Strongly similar to galactose4 epimerase, UDP	1,49271	0,000377
37.	gi|144922657	Ssc.6826	SELK	Selenoprotein K	1,51373	0,020642
38.	gi|113205850	Ssc.57041	RGS2	regulator of G protein signaling 2, 24kDa	1,51615	0,017288
39.	gi|194038117	Ssc.49381	4930573I19Rik	RIKEN cDNA 4930573I19 gene	1,54825	0,019928

Casertana

N.	Gene Id	Unigene Sus	Gene	Gene Encoding	Fold Change	p value
1.	gi|34577087	Ssc.2212	RNF13	ring finger protein 13	1,93087	0,011911
2.	gi|62420888	Ssc.49801	LOC100059924	similar to Dipeptidylpeptidase 7	1,91137	0,014412
3.	gi|194036051	Ssc.54527	LOC719341	similar to LOC526125 protein (Dingo protein isoform 1)	1,80105	0,000741
4.	gi|5902134	Ssc.13176	Coro1a	coronin, actin binding protein 1A	1,76507	0,009432
5.	gi|194035490	Ssc.50346	LOC100064627	hypothetical protein LOC100064627 similar to RecQ protein-like 4 isoform 1	1,69498	0,002568
6.		Ssc.14202		Transcribed locus	1,64555	0,003126
7.	gi|194038510	Ssc.5780	LOC100054565	similar to pecanex-like protein 1	1,61993	0,001504
8.	gi| 18390344	Ssc.19644	ATRIP	ATR interacting protein	1,61518	0,004452
9.	gi|19923621	Ssc.11534	NP_079469.2	Hydroxy-delta-5-steroid dehydrogenase, 3 beta and steroid deltaisomerase 7	1,61352	0,033153
10.	gi| 47523440	Ssc.57585	SLC23A2	Solute carrier family 23 (nucleobase transporters), member 2	1,57817	0,009305
11.	gi| 256773260	Ssc.54720	TIMM8B	mitochondrial import inner membrane translocase subunit Tim8 B	1,55179	0,004532
12.	gi|194034004	Ssc.18454	TLE1	Similar to transducin-like enhancer protein 1 (LOC100157241)	1,5299	0,004166
13.		Ssc.54014		Transcribed locus	1,52761	0,03567
14.	gi| 55741443	Ssc.70373	PAG6	Similar to pregnancy-associated glycoprotein 6	1,52585	0,001232
15.	gi| 255759955	Ssc.21896	LOC100072409	Similar to WD repeat domain 81 isoform 4	1,5155	0,012373
16.	gi|22547159	Ssc.11419	LOC100073148	similar to tetratricopeptide repeat domain 19	1,50752	0,023896
17.	gi| 194044705	Ssc.12924	NCOA5	Similar to nuclear receptor	1,49957	0,000886

				coactivator 5		
18.	gi| 256838109	Ssc.70871 (retired) New: Ssc.42571	LOC608816	Similar to solute carrier family 25 (mitochondrial carrier; phosphate carrier), member 3	1,49845	0,015786
19.	gi| 178056229	Ssc.55376	RBM4	RNA binding protein 4	1,49104	0,035514
20.	gi| 9966809	Ssc.12641	NKIRAS1	Similar to kappa B-ras 1	1,48267	0,001218
21.	gi| 4506967	Ssc.27983	CSKI	Similar to v-ski sarcoma viral oncogene Homolog	1,48264	0,001322
22.	gi|156120132	Ssc.54918	NR1H3	Nuclear receptor subfamily 1, group H, member 3	1,47355	0,003882
23.	gi|4503563	Ssc.11016	LOC717867	similar to Epithelial membrane protein 3	1,46876	0,012115
24.	???	Ssc.2047	FNDC3A	fibronectin type III domain containing 3A	1,46643	0,02612
25.	gi| 55741813	Ssc.211	TRAINA	Putative pancreatic ribonuclease precursor	1,45406	0,012041
26.		Ssc.35609		Transcribed locus	1,45282	0,006403
27.	gi| 148231223	Ssc.49478	MAVS	Mitochondrial antiviral signaling protein	1,44677	0,010636
28.	gi| 133922600	Ssc.59509	SFRS16	splicing factor, arginine/serinerich 16	1,44532	0,014511
29.		Ssc.54615		Transcribed locus	1,44353	0,040486
30.	gi|33695078		LOC709587	similar to protein phosphatase 2, regulatory subunit B, beta isoform 1	1,44178	0,024297
31.	gi| 194043140	Ssc.25105	CRYBB3	similar to beta-B3 crystallin	1,44117	0,038394
32.	gi| 166796035	Ssc.6381	SIRT2	Sirtuin (silent mating type information regulation 2 Homolog) 2	1,43879	0,042071
33.	gi|15147240	Ssc.24837	BOC	strongly similar to NP_150279.1 brother of CDO precursor	1,43443	0,000755
34.	gi| 47523436	Ssc.16086	OPRL	Orphanin FQ/nociceptin receptor	1,42946	0,017954
35.	gi| 298104080	Ssc.60025	RAB11FIP4	similar to ribosomal protein L30 isoform 2	1,42871	0,044632
36.	gi| 80971504	Ssc.55003	NPAL3	ribosomal protein SA	1,4263	0,014475
37.	gi| 115430241	Ssc.9051	LTBP3	similar to SCY1-like 1 isoform A	1,41497	0,002041
38.	gi|194042067	Ssc.18510		similar to actin binding LIM protein 1	1,4131	0,040943
	gi|145701012		LOC703083	similar to EGL nine (C.elegans) Homolog 2	1,41288	0,000814
39.	gi| 156416005	Ssc.2256	COMMD9	COMM domain containing 9	1,41273	0,028578
40.	gi|5670342	Ssc.5996	KHK	ketohexokinase (fructokinase)	1,40936	0,02108
41.	gi| 28416946	Ssc.54531	LOC519634	myosin-XVIIIa isoform a	1,40696	0,02938
	gi| 66347768		LOC612166	similar to Absent in melanoma 1 protein	1,39789	0,013524
42.	gi| 47522674	Ssc.14550		matrix metalloproteinase 25 precursor	1,39241	0,010134
43.	gi|21361403	Ssc.14827	LOC100069490	similar to thioredoxin 2 precursor	1,38949	0,033595
44.	gi| 194035143	Ssc.55109		Similar to Uncharacterized protein C6orf203 (LOC100157575)	1,38203	0,025584
45.	gi|90991702	Ssc.25233	LRRK1	leucine-rich repeat serine/threonine-protein kinase 1	1,37715	0,001965
46.	gi| 46575934	Ssc.28748	LOC616908	KIAA1680 protein isoform 2	1,37613	0,029454
47.	gi| 17149842	Ssc.54360	FKBP2	FK506 binding protein 2, 13kDa precursor	1,37603	0,014657
48.	gi| 7661622	Ssc.68154	LOC782016	hypothetical protein LOC25906 [Homo sapiens]	1,37502	0,010824
49.	gi| 157671951	Ssc.44921	SLC4A3	solute carrier family 4, anion exchanger, member 3	1,37466	0,02771
50.	gi|34335194	Ssc.58414	LOC100018119	cAMP responsive element modulator isoform g	1,36276	0,025195
51.	gi|239835767	Ssc.48672	LOC100071758	similar to Developmental pluripotency associated 2	1,35267	0,014497
52.	gi| 194040419	Ssc.7179	LOC618886	similar to Uncharacterized protein	1,35163	0,000348

				C6orf89 Homolog		
53.	gi| 194036153	Ssc.12269	S100A2	similar to Protein S100-A2 (S100 calcium-binding protein A2) (Protein S-100L) isoform 2	1,34902	0,011624
54.	gi| 7657218	Ssc.28006	BRD4	bromodomain-containing protein 4 isoform short	1,34479	0,019024
55.	gi|187607085		LOC100054101	similar to E3 ubiquitin-protein ligase LNX isoform a	1,33575	0,027296
56.	gi|110815802	Ssc.60174	LOC709210	hypothetical protein LOC84267	1,33436	0,003368
57.	gi| 50979297	Ssc.5575	ELS1	Pancreatic elastase I precursor	1,33051	0,019014
58.	gi| 171460918	Ssc.24428	DNM1L	dynamin 1-like isoform 3	1,32822	0,00286
59.	gi| 224809399	Ssc.50353	LOC511316	Strongly similar to hypothetical protein LOC729991 isoform 1	1,31815	0,028298
60.	gi|144226847	Ssc.48643	OBSL1	obscurin-like 1	1,31806	0,00608
61.	gi|194272180	Ssc.40232	PLXNB1	Similar to plexin B1 precursor	1,30931	0,020747
62.	gi| 47522778	Ssc.5053	CD163	CD163 antigen	1,30663	0,03586
63.	gi|95113651	Ssc.20426	NP_006532.2	strongly similar to glutaredoxin 3	1,30587	0,0136
64.	gi| 29826282	Ssc.54826	LOC100055191	strongly similar to protein phosphatase 1G	1,30433	0,006456

Table 5 – GO term enrichment in Large White and Casertana pigs

GO term	
Casertana	**Large White**
catabolic process (GO:0009056)	muscle contraction (GO:0006936)
vitamin metabolic process (GO:0006766)	response to stress (GO:0006950)
cellular catabolic process (GO:0044248)	developmental maturation (GO:0021700)
glycerol metabolic process (GO:0006071)	lipid metabolic process (GO:0006629)
L-ascorbic acid metabolic process (GO:0019852)	oxygen and reactive oxygen species metabolic process (GO:0006800)
glycerol-3-phosphate metabolic process (GO:0006072)	regulation of lipid metabolic process (GO:0019216)
tricarboxylic acid cycle intermediate metabolic process (GO:0006100)	regulation of cell proliferation (GO:0042127)
cellular carbohydrate catabolic process (GO:0044275)	muscle development (GO:0007517)
hexose metabolic process (GO:0019318)	oxidative phosphorylation (GO:0006119)

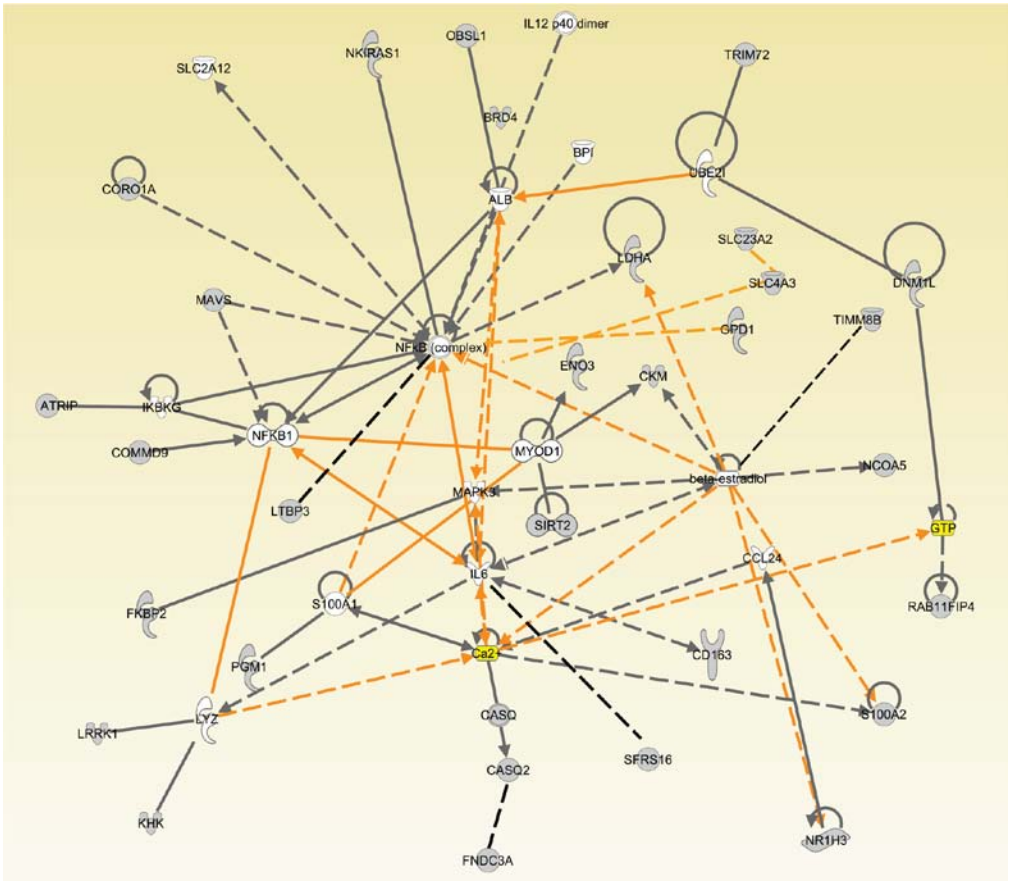

Figure 5. Top network from network analysis via Ingenuity Pathway Analysis in Casertana merged protein and microarray data. Gray nodes: proteins from the data set having a match in the databas. White nodes: proteins from the database which were not identified (if present) upon the experimental phase. Yellow nodes: nonprotein molecules. Gray edges: interactions within a network. Continuou line - edge: direct interaction. Interrupted line - edge: indirect interaction.

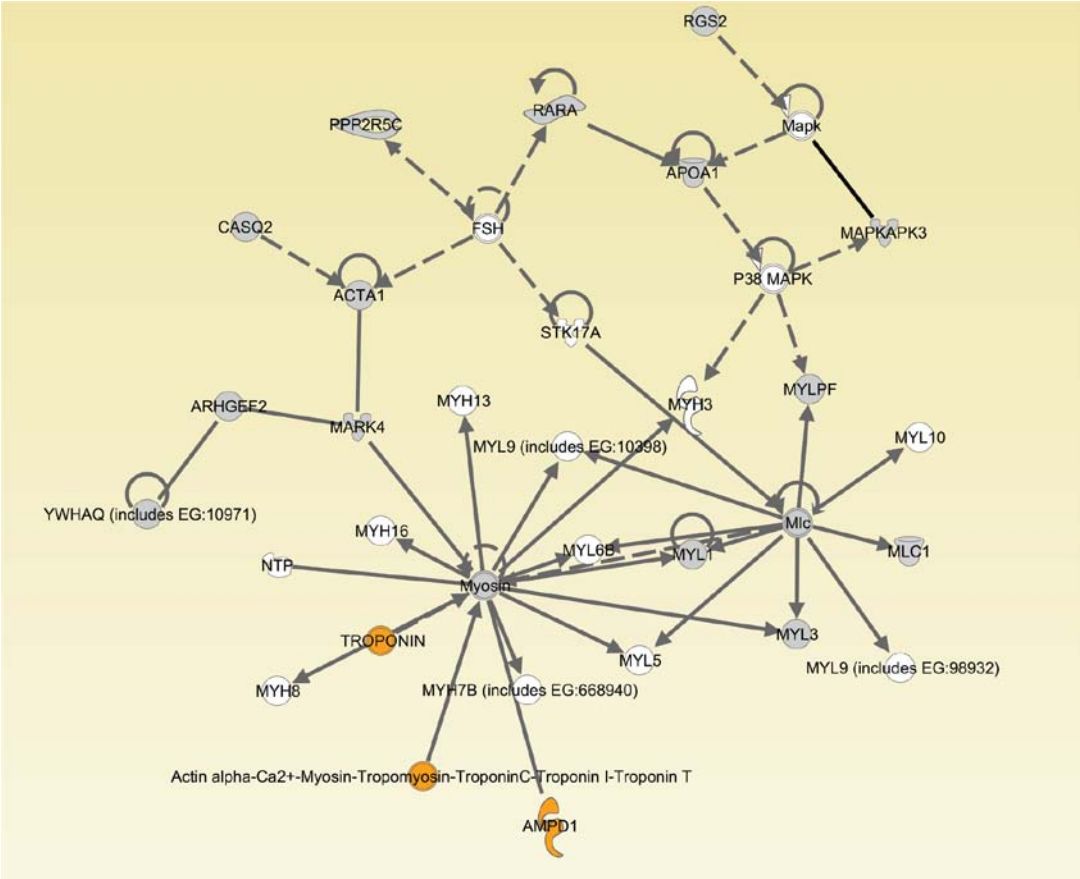

Figure 6. Top network from network analysis via Ingenuity Pathway Analysis in Large White merged protein and microarray data. Gray nodes: proteins from the data set having a match in the database. White nodes: proteins from the database which were not identified (if present) upon the experimental phase. Orange nodes: nondifferentially expressed protein molecules. Gray edges: interactions within a network. Continuous line - edge: direct interaction. Interrupted line - edge: indirect interaction.

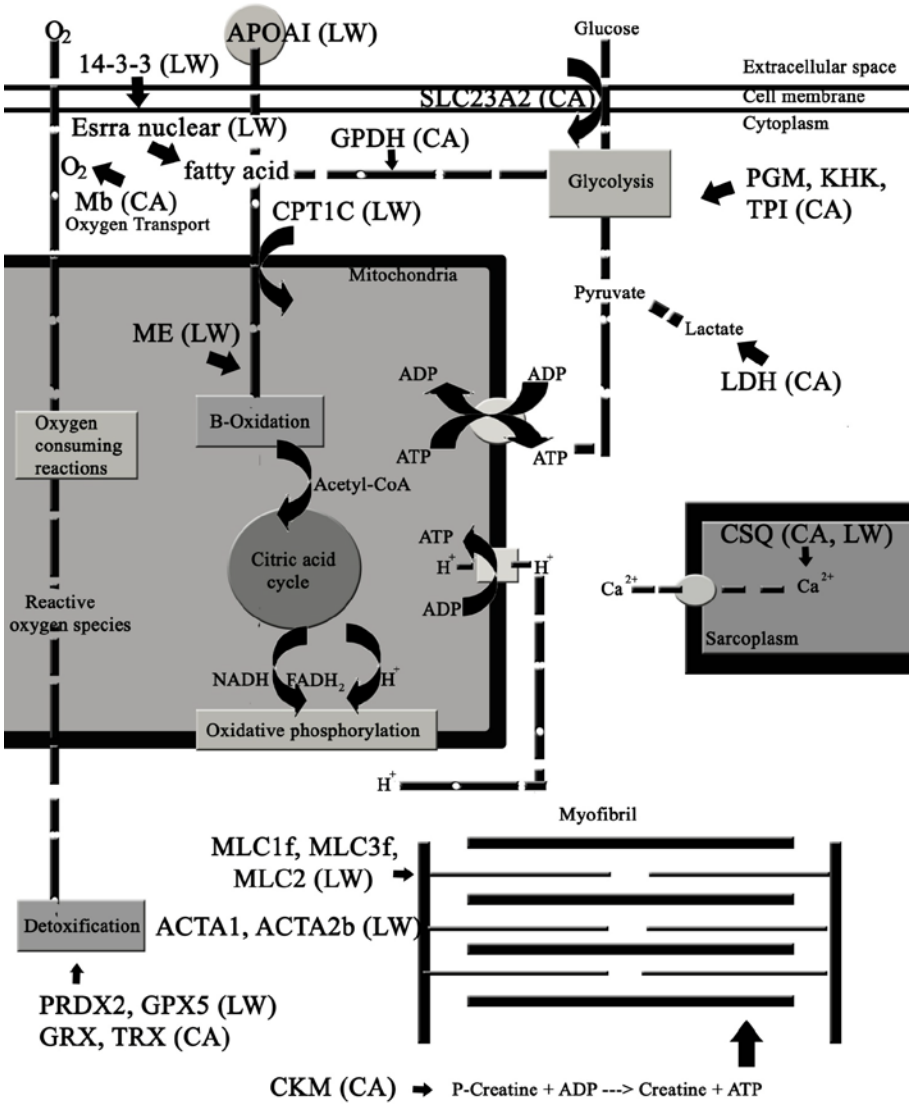

Figure 7. Schematic view of the experimentally individuated differentially-expressed proteins/gene transcripts Casertana and Large White pigs which might influence meat quality.

2.4. Discussion

Casertana: glycolysis, vitamin transport and fat deposition

CA pig breed is certainly the most precious among Italian breeds, being able to provide large amounts of fat[108]. As pathway and functional analyses have pointed out, most of the proteins and gene transcripts individuated in Casertana *Longissimus lumborum* muscle accounted for metabolic functions. It is worthwhile to underline that glycolytic enzymes or glycolysis-related proteins (PGM1, KHK, GPDH, TPI, ENO3, LDH, CK-M) were individuated through both proteomics and transcriptomics approaches.

Glycolysis is the major metabolic pathway that provides cells with metabolic precursors and a rapid source of energy. Following the glycolytic order, phosphoglucomutase (PGM), ketohexokinase (KHK), glycerol-3-phosphate dehydrogenase (GPDH) and triosephosphate isomerase (TPI) are closely involved in shifts in the main pathway of glycolysis.

Glycerol-phosphate dehydrogenase (GPDH)–catalyzes the conversion of glycerol-3-phosphate into the glycolytic intermediary DHAP and viceversa. Working in the former direction this enzyme constitutes a positive switch for glycolysis, while in the latter it produces glycerol-3 phosphate which could be exploited to esterify fatty acids in order to form triglycerides[107]. Indeed, the requirement for net balance of synthesis, degradation and transport for all intermediates in the pathways from glucose to fat imposes constraints on the balance of fluxes between different pathways[94]. The central role of GPDH in the triglyceride synthesis makes this enzyme a useful marker of late adipogenesis extensively used in mammals[108]. This is in agreement with the marked tendency in Casertana to accumulate a fat mass.

The triosophosphate isomerase (TPI) enzyme is an essential housekeeping enzyme in all living cells and tissues, catalyzing the interconversion of DHAP and glyceraldehyde 3-phosphate. TPI functions at a metabolic cross-road ensuring the rapid equilibration of the triosephosphates produced by aldolase in glycolysis, which is interconnected to lipid metabolism, to glycerol-3-phosphate shuttle and to the pentose phosphate pathway[109]. TPI connection to lipid metabolism has been suggested to positively relate with a tender meat[110].

Pig muscle enolase 3 (ENO3) has been thoroughly investigated over the last decades[111]. ENO is a metalloenzyme responsible for the catalysis of 2-phosphoglycerate to phosphoenolpyruvate, the ninth and penultimate step of glycolysis.

ENO levels have been shown to increase in high fat accumulating pigs[97,110], although Duroc (high intramuscular fat) pigs displayed higher levels of enolase 3 when compared to Large White[94,95,110], although most of the observed differences were indicated by the Authors to be related to gender and rearing environment conditions rather than intrinsic pig breed characteristics[94,95,11].

ENO correlation with creatine kinase-M (CK-M) has been observed *in vitro*, suggestive of a likely role in the modulation of glycolytic metabolism[112].

CK has a key role in the energy metabolism of cells with intermittent high-energy requirements, such as skeletal muscle fibers. M-CK is located in the cytosol, where a

small fraction of the enzyme binds specifically to the M-band of the sarcomere[113]. A small proportion of enolase is also tightly bound to the M-band of muscle, although a direct correlation between them is possible, albeit not yet fully demonstrated[113]. Fast-twitch glycolytic skeletal muscle (such as *Longissimus lumborum*) fibers have very low mitochondrial content and mainly rely on quickly mobilisable energy sources (mainly phosphocreatine and glycogen) to develop strong and fast contractions, although this is only possible for short periods of time because of limited reserves. These muscles are thus quickly fatigable and should recover their energy reserves through anaerobic glycolysis and, less importantly, through mitochondrial oxidations. CK catalyses the conversion of creatine and consumes adenosine triphosphate (ATP) to create phosphocreatine and adenosine diphosphate (ADP). This CK enzyme reaction is reversible, such that also ATP can be generated from phosphocreatine and ADP. In tissues and cells that consume ATP rapidly, especially skeletal muscle, but also brain, photoreceptor cells of the retina, hair cells of the inner ear, spermatozoa and smooth muscle, phosphocreatine serves as an energy reservoir for the rapid buffering and regeneration of ATP *in situ*, as well as for intracellular energy transport by the phosphocreatine shuttle or circuit[114]. It has been suggested that CK during evolution because it could provide an advantage in the search of food and to escape from predators[115].

Interestingly, CK-M, along with myoglobin, is also a marker of muscular damage, thus it is also used as a suitable marker for heart infarction[116]. Myoglobin has been found to be over-expressed in Casertana muscle as well. However, myoglobin is also the major protein as oxygen carrier in muscle and usually distributed uniformly throughout muscle. Generally, a high myoglobin concentration in muscle is associated with a high level of muscular activity and high capability for aerobic metabolism[117]. High levels of myoglobin and mitochondria are believed to exist in slow twitch oxidative fibers[118]. This is partly in contrast with the fast-twitch glycolytic nature of the *Longissimus lumborum* muscle and with the glycolytic-oriented molecular behavior outlined by functional analysis results. Nevertheless, this is coherent with previous observations about a direct correlation of M-CK, myoglobin, GPDH and lactate dehydrogenase (LDH) with outdoor rearing of pig breeds[115], as it is the case of Casertana breeds. Moreover, even if high levels of myoglobin and mitochondria are believed to exist in slow oxidative fibers, Takemasa and colleagues have shown that myoglobin can be considerably richer in some fast type fibers[119].

LDH converts pyruvate to lactate and indicates the anaerobic-glycolytic capacity in muscles. LDH has been reported to increase its expression in a model of adipogenesis induced through peroxisome proliferator-activated receptor γ (PPARγ) activation[120].

In this respect, it is worthwhile to underline that, although many molecular evidences support the physiological observation of an increased likelihood of fat deposition in Casertana pigs, only indirect functional approaches (see the end of previous paragraph) but none of the proteomics and transcriptomics approaches has directly detected an over-expression of PPARγ in samples from this breed. Nonetheless, this is not totally unexpected, as previous observations on high fat deposition breeds did not show to correlate with PPARγ expression changes[38]. In this respect, Nuclear receptor subfamily 1, group H, member 3 (NR1H3) is known to take part in PPAR cascades and induce cholesterol and fat accumulation[119,120].

Other up-regulated proteins in Casertana might be related with adipogenesis, mainly transcription factors such as cAMP responsive element modulator and hydroxysteroid dehydrogenase, which both have been shown to induce adipogenesis in 3T3-L1 pre-adipocytes[121-124].

Finally, proteomics observations about an increased expression of calcium-binding proteins, such as calsequestrin (CSQ), is in line with other evidences in that CSQ is known to inhibit calreticulin expression[125], which in turn would inhibit adipocyte differentiation through a negative feedback on PPAR-mediated signaling[126].

Obesity and, in general, high fat accumulation physiological behaviours are highly correlated with an increased risk of lipid peroxidation and inflammatory cascades[126, 127]. In this respect, the role of Nfkβ-mediated pathways is relevant in combating inflammation[126], in agreement with network analysis observation of Casertana data. In parallel, NFkβ operates as a primary antagonist of PPAR cascades, through regulation of cytokine production during inflammation[128]. Negative regulation of NFkβ signaling would result in triggering on the adipogenetic cascades. Therefore, it is notably that gene transcripts for NFKB inhibitor interacting Raslike 1(NKIRAS1) and COMMD have been individuated as over-expressed in Casertana. NKIRAS has been shown to interfere with activation of transcription factor NFkβ, through binding to IkappaB proteins, natural inhibitors of NFkβ, and delaying their stimulus-dependent degradation[129].

COMMD proteins terminate NFkβ-mediated transcriptional responses by destabilizing the interaction between NFkβ and its binding sites on chromatin[130]. Therefore, although proteins involved in PPAR cascades are only partially over-expressed, Nfkβ negative

regulation could reduce antagonism of PPAR pathways and thus switch on pro-adipogenetic cascades.

The presence of SLC23A2, a specific carrier for glucose and ascorbic acid cellular intake, could be pivotal, as pinpointed by functional analyses (GO terms: vitamin metabolic process, L-ascorbic acid metabolic process) Indeed, if in the one hand glucose uptake could be related to the glycolytic-centered metabolism of Casertana pigs, ascorbate uptake could be related to protection against oxidative stress, since ascorbate is an anti-oxidant, mainly tackling lipid and protein peroxidations[131,132]. Analogous function could be played by thioredoxins and glutaredoxins, which have been already related to lipid mediated inflammation, oxidative stress and nuclear transcription signaling cascades[133-137].

Large White: lipid mobilization, protein synthesis and proliferation pathway for a constant growth and low fat deposition

LW pigs are distinguished by their erect ears and slightly dished faces. They are long-bodied with excellent hams and fine white hair and, as their name suggests, they are characterized by large size. The Large White has proved itself as a rugged and hardy breed that can withstand variations in climate and other environmental factors. Their ability to cross with and improve other breeds has given them a leading role in commercial pig production systems and breeding pyramids around the world.

While the Large White was originally developed as an active and outdoor breed, they do very well in intensive production systems. Large White pigs excel in growth rate and lean meat percentage. These main characteristics were reflected in Large White molecular proteomics and transcriptional profiles, as emerged from pathway, functional and network analyses**..**

At a rapid glance, proteomics data clearly hint at a differential modulation of muscle fiber content in Large White pigs when compared against Casertana (e.g. several myosin light chain isoforms, actin; muscle contraction; None of the experimental approaches individuated any significant difference between Casertana and Large White pig muscles, as far as myosin heavy chains are concerned. This is suggestive of a likely fine tuning through modulation of myosin light chain isoforms in muscle fibers from these breeds, instead of a dramatic structural re-organization. Fiber composition dramatically affects muscle properties and thus meat quality[138]. For example, myosin light chain 2 modulates calcium-sensitive cross-bridge transitions in vertebrate skeletal muscle[139], thus

influencing contraction properties of the muscle. Although they are transcribed from two different widely-spaced promoters, myosin light chain 1f and 3 definitely share their biological function and are extremely evolutionary conserved in all vertebrates, from mammals to birds[139]. Myosin has an heavy chain (I or II, slow or fast), and two ligh chains alkali (1 or 3) and regulatory (MLC2). Heterogeneity in myosin isoform expression, with respect to both heavy and light chain (MHC and MLC) subunits, exists in all types of vertebrate muscle. The results of several studies have demonstrated associations between isoforms of MHC and/or MLC isoforms with shortening velocity and/or power output in skeletal muscles. It is now widely accepted that MHC isoform composition plays a primary role in the determination of maximal shortening velocity and power output of the muscle, while the MLC isoform complement has a modulatory influence on regulating these properties[139-141]. In humans, a transcriptome analysis on control patients (body fat 14.6 % $\pm$ 4.3 standard deviation) versus endurance athletes (body fat 11.2 % $\pm$ 2.2) clearly shows how skeletal muscles from athletes display higher levels of myosin light chain 2 (as in our Large White pigs) and lower levels of glycolytic enzymes (such as, for example, enolase 3) [142]. Notably enough, it is known from literature that differential phosphorylation of myosin light chain 2 is fundamental in regulating muscle contraction properties: based on the introduction of negative charges by phosphorylation, it has been hypothesized that the cross-bridges move away from the filament backbone, thus increasing the probability of attachment and force generation[143]. Intriguingly, ProQ Diamond Staining evidenced abundant phosphorylation for myosin light chain (**Figure 4**) from 2DE gels in Large White.

Accordingly, it is long known that alpha-actin positively correlates with synthesis of muscle fiber proteins and, ultimately, with muscle growth[144]. Since Approximately 50% of the protein content of the muscle fiber is made up of the contractile machinery, mostly consisting of myosin complexes of the thick filaments and actin strings of the thin filaments, the upregulation of ACTA1 in Large White LM is completely coherent with the greater tendency to mass accumulation of the breed. ACTA1 is indirectly modulated by MYLPF, whose over-expression in Large White has been individuated through proteomics approaches[145].

Skeletal muscle mass is a balance between protein synthesis and degradation. An imbalance such that proteolysis prevails over synthesis is associated with skeletal muscle atrophy. Along with other muscle homeostasis regulators, Large White overexpresses a Serpine Peptidase inhibitor 3 (SERPINA3) [146].

Besides, the over expression of non-canonical proteins has been correlated with muscle functioning modulation and myogenesis as well. For example, rho/rac guanine nucleotide exchange factor (ARHGEF) is a guanine nucleotide exchange factor for Rho whose activity is regulated through a cycle of microtubule binding and release. Phosphorylation of ARHGEF at Ser(885) by PAK1 induces 14-3-3 binding to the exchange factor and relocation of 14-3-3 to microtubules[147]. The 14-3-3 protein γ is member of the 14-3-3 protein family, which are conserved regulatory proteins that bind a multitude of functionally diverse signaling proteins including kinases and phophatases[148]. It has been proposed that the 14-3-3 proteins have a role in the regulation of myosin light chain kinase that becomes phosphorylated during muscle contraction, and it can be speculated that 14-3-3 protein may play a role in the muscle contraction during rigor[149]. ARHGEF also binds MARK4[150], which is known to modulate actin cytoskeleton in cell polarity and cell structural development[151].

As one of the peculiar characteristics of Large White breeds is their constant growth during their lifespan, it is not unexpected that both pathway and network analyses stressed the role of several proteins/gene transcripts involved in cell cycle regulation and proliferation control. One of these is PPP2R5C, of the phosphatase 2A regulatory subunit B family. PPP2R5C is one of the four major Ser/Thr phosphatases, and it is implicated in the negative control of cell growth and metabolism[152].

In parallel, Large White showed to over-express RGS2, a simple RGS protein with the potential to integrate multiple signaling networks. Recently, the amino-terminal domain of RGS2 was shown to interact with and regulate three different effector proteins: adenylyl cyclase, tubulin, and the cation channel TRPV6. RGS2 is a key point of integration for multiple intracellular signaling pathways, which has a dynamic role in the fine tuning of a diverse range of cellular functions[153]. RGS2 has been associated with the modulation of the thickness of skeletal muscle fibers[154].

Peroxiredoxin 2 (oxygen and reactive oxygen species metabolic process, apoptosis is a member of the peroxiredoxin family of antioxidant enzymes, which reduce hydrogen peroxide and alkyl hydroperoxides. Its over-expression in Large White muscles could be related to cellular growth, as it has been observed that peroxiredoxin 2 can reduce hydrogen peroxide generated in response to growth factors and tumor necrosis factor-alpha[155].

Downstream of mitogen-activated protein kinases, MAPKAPK3 (MAP kinase kinase activity is ubiquitously over-expressed in large Diannan pigs compared to smaller

ones[156]. MAPKAPK3 is thought to regulate gene expression at the transcriptional and post-transcriptional level, control cytoskeletal architecture and cell-cycle progression, and are implicated in inflammation[157].

Retinoic acid can combine with the nuclear retinoic acid receptor (RAR) or PPARs, leading to cell growth inhibition or stimulation[158,159].

Estrogen-related receptor alpha (ERRα)was over-expressed in Large White pigs. Transcriptional control in Large White pigs is not only strictly related to muscular growth, but also in regulation of its metabolism. ERRα has wide tissue distribution but it is most highly expressed in tissue that preferentially use fatty acids as energy sources such as kidney, heart, cerebellum, intestine, and skeletal muscle[160] ERRα regulates genes involved in mitochondrial biogenesis[161], gluconeogenesis[162], oxidative phosphorylation[163] and fatty acid metabolism[164]. Furthermore ERRα knockout mice display impaired fat metabolism and absorption[165]. This is relevant in that although displaying higher levels of ERRα transcripts, Large White pigs are less prone to adipogenesis. This could be explained when dissecting the pivotal molecules which are indicated by network analyses, in which a high tendency is observed in Large White pigs to mobilize and consume lipids instead of increasing their deposition. Apolipoprotein A1 (APOA1), carnityne carnitine palmitoyltransferase 1C (CPT1C), malic enzyme (ME), and Glyoxalase I perfectly fit in this framework. Apolipoprotein A-I is the major protein component of high density lipoprotein in plasma. The protein promotes cholesterol efflux from tissues to the liver for excretion[165] It is a cofactor for lecithin cholesterol acyltransferase which is responsible for the formation of most plasma cholesterol esters. APOAI has been associated with insulin resistance (APOI-A -/- mice show increase in fat content) [166].

An important step in beta-oxidation of long-chain fatty acids, CPTI is believed to contribute to the transport of fatty acids across the mitochondrial membranes. This transport is L-carnitine dependent and is catalyzed by the carnitine palmitoyltransferase enzyme system, which consists of CPT I, carnitine-acylcarnitine translocase, and CPT II. CPT I is located in the outer mitochondrial membrane and catalyzes the conversion of acyl-CoA to acylcarnitine, which is then transported across the inner mitochondrial membrane via carnitine-acylcarnitine translocase[167]. A greater expression of this transporter suggests a larger utilization of long chain fatty acids by Large White pigs.

ME catalyzes the reductive carboxylation of pyruvate to malate. The malate can then be oxidized to oxaloacetate, through the catalytic activity of the TCA cycle enzyme, malate

dehydrogenase. Pyruvate can also be directly carboxylated to oxaloacetate by the enzyme pyruvate carboxylase. The generated oxaloacetate can undergo a condensation reaction with acetyl-CoA (which can be formed by the oxidative decarboxylation of pyruvate, catalysed by pyruvate dehydrogenase), resulting in citrate production[168].

Glioxalase I is part of the glyoxalase system present in the cytosol of cells, catalyzing the conversion of reactive, acyclic α-oxoaldehydes like malonic dialdehyde (MDA), a cytosolic aldehyde produced in cells into the corresponding α-hydroxyacids. The rise of the amount of MDA is associated to lipid peroxidation as well as to cell damage, which is particularly high at the protein level (protein turn-over) in fast growing muscle tissues[169].

Taken together, these observations prompt a series of considerations of a more oxidative-oriented metabolism for this muscle in Large White pigs, against an inefficient strict glycolytic tendency of Casertana ones (**Figure 7**).

3. PROTEIN EXPRESSION IN BOVINE MILK MFGM

3.1. Introduction

Bovine milk is a major component of human diet as well as an important agricultural resource deeply affecting the economy of a country. A major objective of research on dairy cattle genomics is the identification of genes underlying the variability of milk production traits, as well as of genes which are relevant for a deeper understanding of mammary gland evolution and involution mechanics. The dairy industry has invested enormous resources into the identification of Quantitative Trait Loci (QTL) for milk production traits in cattle, particularly milk, protein and fat yield, protein and fat percentage. A recent review reports a list of 238 milk QTLs which have been related to these five traits[170]. Several genes, like alpha casein and acyl-CoA diacylglicerol acyltransferase, have been suggested to be relevant in physiological pathways; and are employed in some breeding programs[171]. As it's well known, one of the economically and biologically most important component of milk are proteins.

Bovine milk proteins are generally classified as caseins (80% of the total milk protein content), whey proteins (16%), peptones/low molecular weight peptides (3%) and milk fat globule membrane (MFGM) proteins (1%)[172].

Milk-fat globules (MFG) are secreted from the apical surface of the cell, surrounded by the MFGM. These are formed by lipids and a subcategory of milk proteins, which mainly function as carriers of lipids in the milk medium[172]. Wu et al. obtained evidence[173] that lipid droplets in milk-secreting cells originate from endoplasmic reticulum and lipid droplets resembling MFGs in morphology and composition have been released from mammary gland endoplasmic reticulum in an experimental cell-free system. MFGMs constitute a docking site for a wide range of membrane proteins, and their proteomic analysis highlighted some of the possible signaling and secretory pathways used by the mammary gland[174].

Protein-oriented investigations on milk have recently relied on "omic" strategies, such as proteomics, which aims at investigating all the proteins within a biological sample simultaneously. Some proteomics studies have been so far conducted on the MFGM and whey fractions, as it has been extensively reviewed[175].These studies advanced the understanding of mammary function and milk secretion. Recently, papers on MFGM proteomics in cattle have been published, showing development changes during early

lactation phases[142, 143] However, comparative proteomic analyses on MFGM from dairy and beef cattle breeds have not been hitherto performed and the time span of lactation taken into consideration has been quite limited.

A series of studies have highlighted the nutraceutical and biological relevance of MFGM [176-178].

While quantitative investigations are still under development, especially for the least abundant protein species, preliminary functional classifications and protein-protein interaction maps have been recently proposed. Besides, only a handful of investigations addressed the variations in MFGM-protein expression levels across the early stages of lactation (but not over the whole period), mainly focusing on colostrum versus bovine milk[144]. or on specific protein classes (growth factors, for example[177]). On the other hand, no proteomic study has been performed so far to compare MFGM of *Bos taurus* breeds with different productive attitudes. Therefore, in the present study we exploited a proteomic approach to compare the expression levels of the most abundant MFGM proteins from milk samples from Friesian and Chianina cattle breeds, representative of selection for milk and meat traits, respectively. We considered a wide lactating period (up to six months) in order to capture variation in mammary gland MFGM both in evolution and involution and compared the observed differences to the productive attitudes of the two breeds and the physiological characteristics of the analyzed milk.

3.2. Materials and Methods

3.2.1. Sample Preparation:

All animals used in this study were treated according to the International Guiding Principles for Biomedical Research Involving Animals. Fresh milk samples of individuals belonging to breeds of different origins and selected for different purposes (beef, Chianina, and dairy, Friesian) were collected. All individuals were raised in the same farm. Samples from three animals per breed (three replicates per sample) were collected at three lactation phases: seven days (1), seven weeks (2) and six months (3) after calving (for a total of 18 samples) and transported in ice to the laboratory. MFGM were isolated according to literature[181-184]. 500 ml of milk were centrifuged at 2,000*g* for 30 min at 4°C to remove cells, obtaining skim. The recovered cream layer was washed five times with 7.4 pH Phosphate Saline Buffer solution to remove caseins. Washed globules were stored at

−20°C until used. To extract the MFGM proteins, the washed skim was mixed 1:3 with a solution containing 7 M urea, 2 M thiourea, 4% CHAPS, 1% Triton X-100, 20 mM Tris, 1% DTT and 0.5% IPG buffer, following Quaranta[151], incubated in ice for 60 min with periodic vortexing, then centrifuged at 10,000 g for 1 hour. After removing the floating skim layer, the solubilised proteins were precipitated with methanol and chloroform following Wessel and Flügge[186]. Before focusing, the sample was incubated for 3 h at room temperature, under strong agitation, to perform alkylation with 7.7 mM iodoacetamide in a solution of 7 M urea, 2 M thiourea, 4% CHAPS, 20 mM Tris, pH 3–10 carrier ampholyte, 40 mM Tris, 5 mM TBP, 0.1 mM EDTA (pH 8.5), 2% (v/v) protease inhibitor cocktail (Sigma-Aldrich). To prevent over-alkylation, iodoacetamide excess was destroyed by adding an equimolar amount of DTE.

3.2.2. IEF_SDS PAGE of MFGM protein fraction.

Isoelectrofocusing (IEF) has been performed using ready-to-use Immobiline Dry-Strips linear pH gradient 3–10 length 18 cm (BioRad, Hercules, CA, USA) and the in gel sample rehydration method. An amount of 600 µg of proteins was loaded per strip. IEF was run on a BioRad Protean IEF at 20°C constant temperature and 8,000 V for 99,000 Vh. After IEF, the IPG gel strips were incubated at room temperature for 30 min in 6 M urea, 30% w/v glycerol, 2% w/v SDS, 5 mM Tris-HCl, pH 8.6. The strips were sealed at the top of a 1.0 mm vertical second dimensional gel (BioRad, Hercules, CA, USA) with 0.5% agarose in 25 mM Tris, 192 mM glycine, 0.1% SDS, pH 8.3. SDS-PAGE was carried out on homogeneous running gels 12 % T 3% C. The running buffer was 25 mM Tris, 192 mM glycine, 0.1% SDS, pH 8.3; running conditions were 40 mA/gel until the bromophenol blue reached the bottom of the gel; the molecular weight marker was Wide Range SigmaMarker™ (Sigma, St. Louis, MO, USA). Gels were automatically stained with Brilliant Blue G colloidal (Sigma, St. Louis, MO, USA) following the manufacturer's instructions.[187] Three technical replicates per sample and three biological replicates per breed across three lactation phases were performed, for a total of 54 (27 x 2 breeds) gels. The 2-D image analysis was carried out and spots were detected and quantified using the Progenesis SameSpots software v.2.0.2733.19819 package (Nonlinear Dynamics, Newcastle, UK). Each gel was analysed for spot detection and background subtraction. Within-group comparison of protein spot numbers was determined by repeated measure analyses. Among-group comparisons were determined by ANOVA (Analysis of Variance) procedure in order to classify sets of proteins that showed a statistically significant

difference with a confidence level of 0.05. Spot intensities were normalized to the minimum average value for each spot (calculated from three replicates for each lactation phase for each breed).

3.2.3. Friesian versus Chianina gels

Sixty stained gels (3 technical replicates x 10 biological replicates x 2 breeds) were digitalized using an ImageScanner and LabScan software 3.01 (Bio-Rad Hercules, CA). The 2-DE image analysis was carried out and spots were detected and quantified using the Progenesis SameSpots software v.2.0.2733.19819 software package (Nonlinear Dynamics, New Castle UK). Each gel was analyzed for spot detection and background subtraction. Within-group comparison of protein spot numbers was determined by repeated measures analysis. Among-group comparisons were determined by ANOVA (Analysis of Variance) procedure in order to classify sets of proteins that showed a statistically significant difference with a confidence level of 0.05. Spots which were significantly different between groups and not significantly different in the three technical replicate and ten biological replicate samples were identified by qTOF-MS/MS. All statistical analyses were performed with the Progenesis SameSpots software v.2.0.2733.19819 software package[188]. After the background subtraction, spot detection and match, one standard gel was obtained for each group.. These standard gels were then matched to yield information about the spots of differentially expressed proteins. Differential protein expression was considered significant at $P<0.05$ and the change in the photodensity of protein spots between Large White and CA samples had to be more than 2 fold.

3.2.4. In-Gel Digestion

Spots from 2-DE maps were carefully excised from the gels and subjected to in-gel trypsin digestion according to Shevchenko[56] with minor modifications. The gel pieces were swollen in a digestion buffer containing 50 mM NH_4HCO_3 and 12.5 ng/ml trypsin (modified porcine trypsin, sequencing grade, Promega, Madison, WI, USA) in an ice bath. After 30 min, the supernatant was removed and discarded; then 20 ml of 50 mM NH_4HCO_3 were added to the gel pieces, and digestion was allowed to proceed overnight at 37°C. The supernatant containing the peptide mixture was removed and acidified with 5% formic acid before injection in the mass spectrometer.

3.2.5. Protein identification by Nano-RP-HPLC-ESI-MS/MS

Mass spectrometric procedures were performed as previously described[22]. Peptide mixtures were separated using nanoflow-HPLC system (Ultimate; Switchos; Famos; LC Packings, Amsterdam, The Netherlands). A sample volume of 10 µL was loaded by the autosampler onto a homemade 2 cm fused silica pre-column (75 µm I.D.; 375 µm O.D) Reprosil C18-AQ, 3 µm (Ammerbuch-Entringen, DE) at a flow rate of 2 µL/min. Sequential elution of peptides was accomplished using a flow rate of 200 nL/min and a linear gradient from Solution A (2% acetonitrile; 0.1% formic acid) to 50% of Solution B (98% acetonitrile; 0.1% formic acid) in 40 minutes over the precolumn in-line with a homemade 10-15 cm resolving column (75 µm I.D.; 375 µm O.D.; Reprosil C18-AQ, 3 µm (Dr. Maisch GmbH, Ammerbuch-Entringen, Germany). Peptides were eluted directly into a High Capacity ion Trap HCTplus (Bruker-Daltonik, Bremen, Germany). Capillary voltage of 1.5-2 kV and a dry gas flow rate of 10 L/min were used at a temperature of 200°C. The scan range used was from 300 to 1800 m/z. Protein identification was performed by searching in the National Center for Biotechnology Information non-redundant database (NCBInr, version 20081128, www.ncbi.nlm.nih.gov) using the Mascot program in-house version 2.2 (Matrix Science, London, UK). The following parameters were adopted for database searches: complete carbamidomethylation of cysteines and partial oxidation of methionines, peptide Mass Tolerance ± 1.2 Da, Fragment Mass Tolerance ± 0.9 Da, missed cleavages 2. For positive identification, the score of the result of (- 10 x Log(P)) had to be over the significance threshold level ($P < 0.05$). Even though high MASCOT scores are obtained with values greater than 60, when proteins were identified by one peptide only a combination of automated database search and manual interpretation of peptide fragmentation spectra was used to validate protein assignments. In this manual verification the mass error, the presence of fragment ion series and the expected prevalence of C-terminus containing ions (Y-type) in the high mass range were all taken into account. Moreover, replicate measurements have confirmed the identity of the protein hits.

3.3. Results

A gel sample from each lactation phase per breed is shown in **Figure 8**. Spots identified as differentially expressed between the breeds or across lactation phases were automatically numbered by Progenesis SameSpots software, as it is shown in **Figure 9**. Proteins identified through mass spectrometry are listed in **Table 6**, along with their gene IDs, Uniprot Ids, expected molecular weights and p*Is*. We identified and analysed a total of 20 spots which displayed the highest photodensity intensities (most abundant species) and significant differential-expression (*p*-value > 0.05) between breeds or across lactation phases. Out of these spots, 13 different proteins were identified.

K-Means algorithm for functional clusterization through STRING 8.3 allowed to distinguish 5 main functional categories, including i) MFG lipid droplet proteins (Butyrophilin subfamily 1 member A1 -BTN1A1; Fatty acid binding protein 3 - FABP3; Milk fat globule-EGF factor 8 protein - MFGE8; adipose differentiation-related protein/perilipin 2 - PLIN2); ii) structural proteins (beta-actin –ACTB; Peptidylprolyl cis-trans isomerase A - PPIA); iii) signaling proteins (14-3-3 protein gamma beta/alpha - YWHAB); iv) and proteins involved in innate and humoral immunity (Glycosylation dependent cell adhesion molecule 1/proteose peptone component 3 - GLYCAM1; Glycoprotein 2 - GP2; beta-lactoglobulin – LGB; Polymeric immunoglobulin receptor – PIGR; Fibrinogen beta chain – FGB; Immunoglobulin J chain – IGJ). Some of the identified proteins cross-interact with others from different functional categories, since they are known to take part in different biological cascades, such as MFGE8 (lipid droplet/immunity), GLYCAM1 (immunity/lipid droplet secretion), PLIN2 (lipid droplet/lipolysis) and PPIA (structural/signaling), as it will be extensively discussed below.

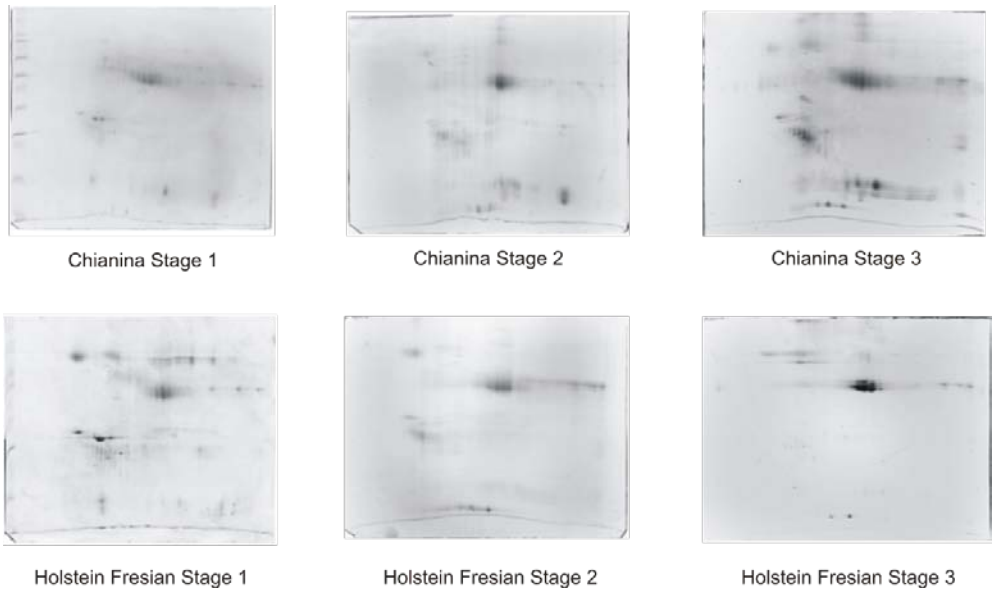

Figure 8. 2-DE of MFGM protein extracts from Chianina and Friesian cattle breeds. IEF pH range is 3-10, 12%T 3% C Acrylamide. Gels has been stained with Colloidal Coomassie. One gel for each breed and each studied lactation phase is shown.

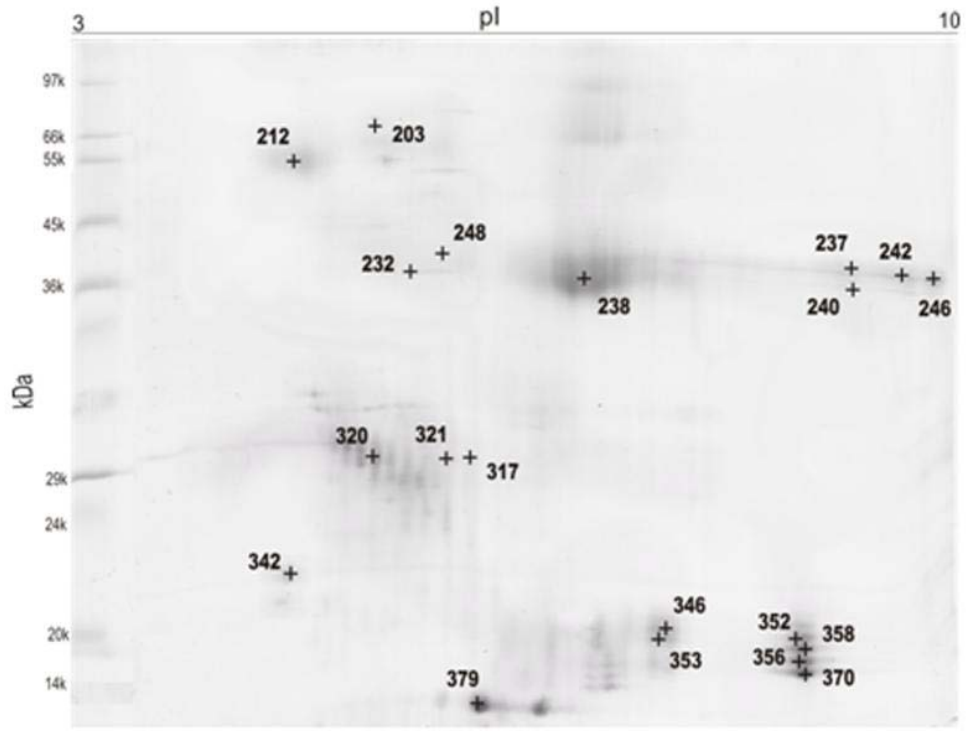

Figure 9. 2-DE of MFGM protein extracts from Chianina and Friesian cattle breeds. IEF pH range is 3-10, 12%T 3% C Acrylamide. Differentially expressed proteins spot are shown.

Table 6. MFGM Proteins identified by MS/MS.

N	Spot	Mw kDa	pI	Peptides	Mascot Score	NCBI Accession Number	Uniprot ID	Protein ID
1	352	16580	8,71	6	424	gi|28189246	PPIA	Peptidylprolyl cis-trans isomerase A, cyclophilin A, rotamase
2	356	17150	8,37	3	161	gi|8699209	PPIA	Peptidylprolyl cis-trans isomerase A, cyclophilin A, rotamase
3	358	18086	8,34	7	524	gi|47523764	PPIA	Peptidylprolyl cis-trans isomerase A, cyclophilin A, rotamase
4	370	16580	8.71	3	161	gi|28189246	PPIA	Peptidylprolyl cis-trans isomerase A, cyclophilin A, rotamase
5	346	15295	5,98	2	131	gi|741536	GLYCAM1	Glycosylation dependent cell adhesion molecule 1, lactophorin, proteose peptone component 3
6	353	15295	5,98	2	112	gi|741536	GLYCAM1	Glycosylation dependent cell adhesion molecule 1, lactophorin, proteose peptone component 3
7	379	14774	7.00	3	412	gi|227994	FABP3	Fatty acid binding protein 3, mammary-derived growth inhibitor
8	317	59912	6.11	4	313	gi|125662132	BTN1A1	Butyrophilin subfamily 1 member A1
9	342	18541	4.83	5	340	gi|223165	LGB	Beta-lactoglobulin
1	320	27946	4.80	3	215	gi|2852383	YWHAB	14-3-3 protein gamma beta/alpha, protein kinase C inhibitor
1	248	42096	5.31	6	496	gi|161376754	ACTB	Actin beta (cytoplasmic)
1	232	47116	5.49	3	111	gi|6980816	FGB	Fibrinogen beta chain
1	240	49622	8,72	14	1601	gi|27806759	PLIN2	Perilipin 2, adipophilin, adipose differentiation-related protein
1	246	49622	8,72	20	1822	gi|27806759	PLIN2	Perilipin 2, adipophilin, adipose differentiation-related protein

1	242	49622	8,72	14	1605	gi|27806759	PLIN2	Perilipin 2, adipophilin, adipose differentiation-related protein
1	237	49622	8,72	13	1649	gi|27806759	PLIN2	Perilipin 2, adipophilin, adipose differentiation-related protein
1	212	60734	4.69	6	669	gi|115495209	GP2	Glycoprotein 2, zymogen granule membrane, pancreatic secretory granule membrane major glycoprotein
1	238	45704	7.10	8	1155	gi|213676 0	MFGE8	Glycoprotein 2, zymogen granule membrane, pancreatic secretory granule membrane major glycoprotein
1	203	83695	5.12	10	635	gi|391434 6	PIGR	Polymeric immunoglobulin receptor;
2	321	25032	5.84	2	136	gi|15088675	IGJ	Immunoglobulin J chain, linker protein for immunoglobulin alpha and mu polypeptides

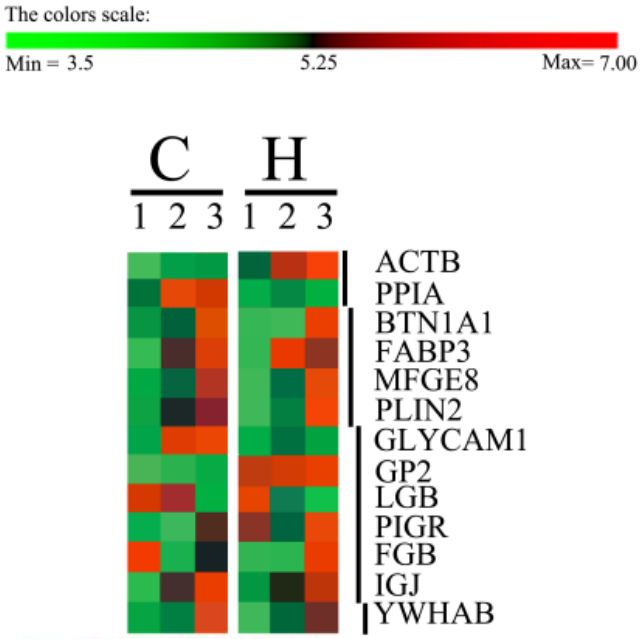

Figure 10. MCL functional clustering analysis of the 20 differentially-expressed protein spots (13 proteins) in Chianina versus Friesian MFGs. The clustering analysis was performed with PermutMatrix graphical interface, plotting the averages of relative spot values and clustering through functional classification through String 8.3. Each cell represents the average of the relative spot value, according to the greyscale scale above.

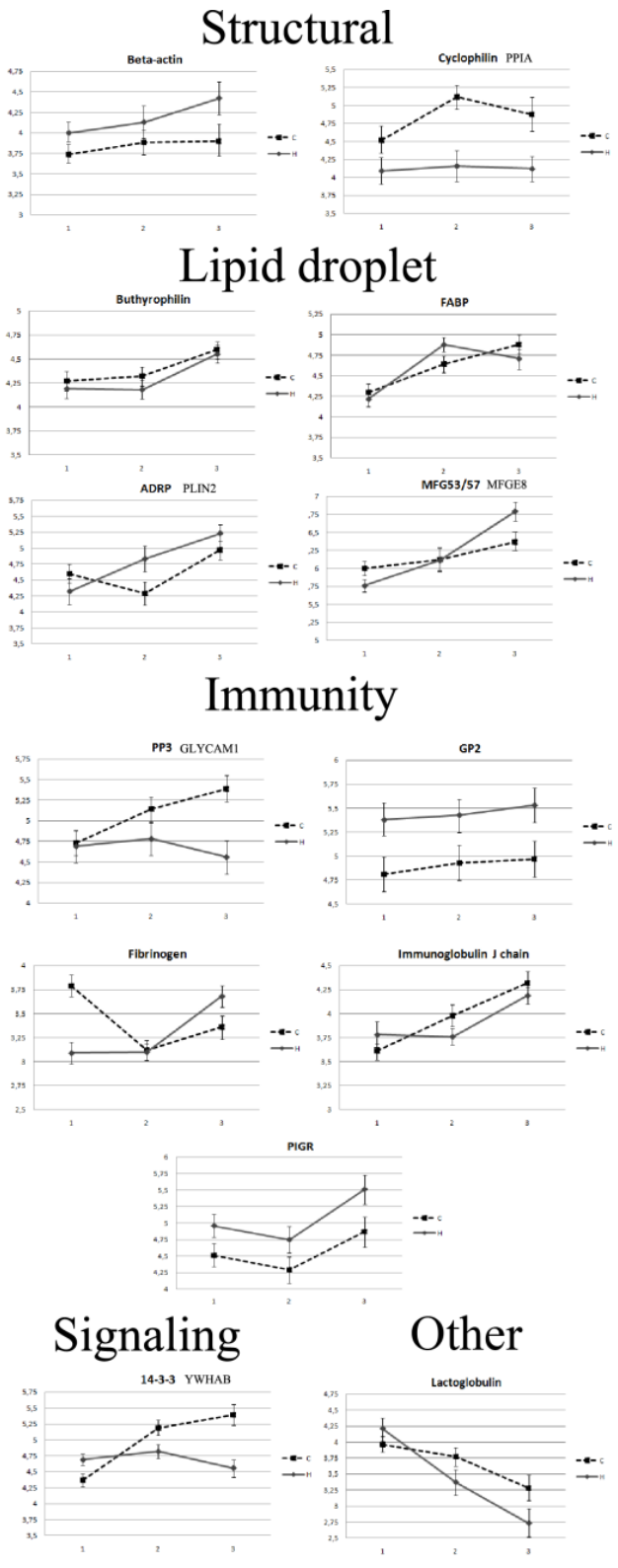

Figure 11. Graphical representation of the expression trend for each protein in each breed. In the abscissa are found lactation phases (labelled with 1, 2 and 3) and in ordinate the spot intensity.

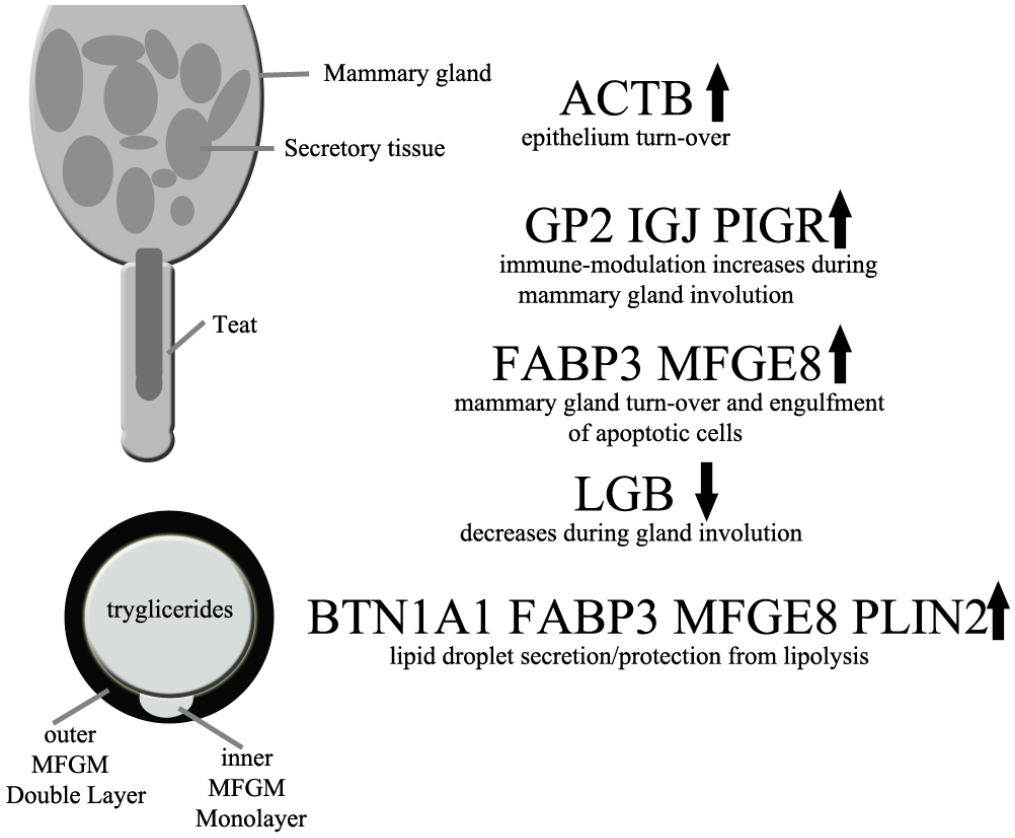

Figure 12. Mammary gland involution model: differently expressed proteins between breeds and across lactation phases are reported, along with indications of their trend during mammary gland involution (A) and lactation (B) (arrows; up = increase; down = decrease).

3.3.1. Intra-breed Comparison Results

Friesian In Friesian, ACTB (structural); MFGE8, FABP3 and PLIN2 (lipid droplet); FGB, PIGR and IGJ (immune system) concentrations increased from phase 1 to 3. GP2 remained constant, while LGB decreased. BTN1A1 was significantly higher at phase 3 than in phase 1 and 2.

Chianina PPIA, GLYCAM1, IGJ, PIGR; FABP3 and MFGE8 concentrations in Chianina followed a positive trend, increasing over lactation phases. Conversely, FGB and LGB spot intensities decreased across lactation phases (from 1 to 3).

GP2 concentration remained almost unaltered throughout the phases, while PLIN2 expression decreased significantly in phase 2 and rose again in phase 3.

Notably enough, three proteins followed a completely opposed pattern and trend of expression in Friesian and in Chianina, namely GLYCAM1, FBG and YWHAB. In all cases, it was possible to observe a positive trend in Chianina, while the expression of these proteins remained almost constant from phase 1 to 2 in Friesian. In the case of GLYCAM1

and FGB, in phase 3 a minor drop of concentrations was observed. BTN1A1 was significantly higher at phase 3 than in phase 1 and 2.

3.3.2. Intra Lactation Phases Comparisons Results

Phase 1: Seven Days At day 7, Chianina significantly expressed a larger amount of PPIA, MFGE8 and FGB, Friesian a greater amount of GP2, PIGR, ACTB and YWHAB.

Phase 2: Seven Weeks At the seven weeks phase, MFGM from Chianina milk showed a larger amount of PPIA, LGB, IGJ and YWHAB proteins compared to Friesian. Friesian MFGM proteins of GP2, PIGR, PLIN2 and FABP3 are significantly more expressed in the seven weeks phase.

Phase 3: Six Months At the six months after calving phase, in Chianina we detected a larger amount of PPIA, GLYCAM1, LGB and YWHAB. On the opposite, GP2, PIGR, ACTB, FGB and MFGE8 levels were higher in Friesian.

3.4. Discussion

Comparative studies on biological samples from *Bos taurus* through the 2D-IEF-SDS electrophoresis approach have been recently published for kidney, muscle, plasma, red blood cells[189] and liver[190]. In particular, liver from Friesian and Chianina cattle breeds have been recently investigated through complementary proteomic, transcriptomic and interactomic approaches[191]. Meanwhile, proteomic strategies have been growingly demonstrated to represent a valuable asset in bovine milk investigations[192,193]. which holds relevant economic considerations and potential pitfalls. In the present study, we investigated the variations in the 2D-electrophoretic patterns of the most abundant MFGM proteins in milk from Chianina (beef) and Friesian (dairy) breeds, to monitor whether physiological changes are reflected in MFGM protein composition. Three lactation stages were investigated: 7 days (phase 1), 7 weeks (phase 2) and 6 months (phase 3) after calving. To our knowledge, this is the first report covering such a long time span, complementing previous observations on colostrums and 7 days MFGM[194] Intra-breed and inter-breed expression patterns were individuated for 13 differently-expressed proteins (**Table 6**). The main changes observed involved the progress of the lactation stages (**Figures 10-11**), while only a handful of proteins followed a breed-specific trend.

Lipid droplet structure Differences observed in ACTB protein spots in Friesian 2DE gels, especially between phase 1 and 3, could be related to cytoskeletal changes occurring in mammary gland cells during lactation. In mammary glands, MFGs are known to be uni-directionally transported to apical cell regions by a mechanism which involves cytoskeletal elements[195]. It has been suggested that these constraints may be communicated to the cell interior through mechanical changes in the cytoskeleton[196]. An increased concentration of ACTB parallels an improved capacity of lipid droplet formation as actin is known to contribute to cytoskeletal reorganization and trafficking which is associated with lipid secretory granule formation. Indeed, PPIA, PLIN2, MFGE8, BTN1A1 and FABP3 [197-199], which contribute to intracellular/apical membranes formation, assist granule transport, vesicle budding and secretion and protect the MFG from lypolysis[199], show a positive trend of concentrations.

Alternatively, the mechanism of milk production, leading to epithelial cell destruction, could be related to release of ACTB in milk; therefore, a greater amount of actin might be a symptom of an increased rate of mammary cells depletion.

In detail, PLIN2, also known as adipocyte differentiation-related protein (ADRP), is considered one of the earliest markers of adipocyte differentiation[200,201]. In mammary cells, PLIN2 seems to be concentrated mainly in cellular components involved in the generation of milk lipid globules. The expression of this protein in milk-secreting cells, as well as in adipocytes, implies that it might be involved in the deposition of triacylglycerols droplets in the cytosol[202]. During secretion, droplets interact with areas of plasma membrane enriched with butyrophilin (BTN1A1)[203,204] and xanthine oxidase/reductase (XOR)[205] BTN1A1 is highly expressed in the lactating mammary gland and secreted with MFGM[206]. Buthyrophilin family (BTN) proteins have been originally identified for their ability to aid production of milk fat globules. BTN1A1 has been linked to the secretion of milk lipid droplets being highly expressed in the mammary epithelium during lactation and its expression has been shown to be regulated in several human immune cells [198]. Moreover, BTN1A1 *in vivo* stabilizes the association of XOR with the MFGM.

In our study, BTN1A1 amount increases significantly at lactation phase 3. Buthyrophilins increase in later stages of lactation has been confirmed by literature[209].XOR amount does not seem to increase through lactation phases in the MFGM fractions analyzed in our study (data not shown). It should be remembered that XOR is not firmly anchored to MFGM membrane. Even if the tendency of XOR to concentrate in MFGM is well-known[210] and has led to the assumption that XOR is present primarily in the skim fraction of milk this is

certainly not the case with bovine milk[211] where it has been several times individuated in the whey fraction[212].

Key proteins involved in triacylglycerol synthesis in tissues such as adipose tissue and mammary gland include fatty acid binding proteins (FABP), carriers for fatty acids. Bionaz et al. reported a significant increase of expression of FABP3, FABP4 and FABP5 mRNA during lactation[213]. We observed an increase of FABP3 from phase 1 to phase 2, and a slight diminution at phase 3. FABP3 is also known as mammary-derived growth inhibitor, as it has been suggested a close relationship between FABP3 transcription and developmental processes in the normal bovine mammary gland[213]. The observed diminution of FABP3 in phase 3 may account for a rearrangement at the mammary gland level.

MFGE8, also known as lactadherin, is one of the major protein components associated with MFGM. Bovine MFGE8 is involved in lipid droplet secretion by binding to phospholipids[214]. Indeed, Yolken et al. showed that MFGE8 is an important milk mucin–associated defense component that inhibits enteric pathogen binding and infectivity[215-216]. MFGE8 prevents rotavirus infections and mediates engulfment of apoptotic germinal center B cells[217].

Hayanama and Nagata reported that the expression of MFGE8 in mice mammary gland is strongly up-regulated during involution. Primary epithelial cells from involuting mammary gland express MFGE8. Consistently, in MFGE8 knockout mice involution has been shown to be severely impaired[218]. MFGE8 expression in mouse mammary glands is up-regulated after parturition and increases during lactation even at a late stage[219]. A deficiency in MFGE8 causes delayed clearance of apoptotic mammary epithelial cells as well as impaired involution and inflammation of the mammary gland[213, 220-223].

Overall, FABP3 and PLIN2 proteins are hereby shown to increase during lactation. This is in contrast with previous investigations, which registered a rapid decrease in milk fat content during the first weeks after calving, reaching a minimum at about week 14 of lactation for the animals of a stable-raised cattle trial[213].

Regulation of growth, differentiation, and apoptosis appear to be mediated by tension-dependent changes in the actin cytoskeleton[224,225]. Thus, the alterations of ACTB levels observed in MFGs through the lactation process might account for a re-programming of the bovine mammary gland, likely leading to involution programs. FABP3 expression drops at phase 3, coherently with an alteration of growth of the bovine mammary gland at this stage. Involution of the mammary gland is characterized by activation of proteases that

destroy the lobular-alveolar structure of the gland and degrading the extracellular matrix and basement membrane, as well as massive loss of alveolar cells[195]. MFGE8 role in apoptotic body-engulfment might become pivotal in late stages of lactation to eliminate apoptotic mammary epithelial cells during involution[226]. Our results are in good agreement with this model.

Immunity Along with proteins involved in lipid transport/secretion, a series of proteins involved in immunity displayed either a higher concentration or a positive trend in Friesian.

Some of the proteins involved in lipid transport are also known to play a role in immune functions, such as MFGE8, as stated above. Likewise, we could detect elevated levels of proteins involved in innate immunity in Friesian MFGM. Glycoprotein 2 (zymogen granule membrane protein GP2) which is present in the pancreatic zymogen granule where it is cleaved and released into the pancreatic duct along with exocrine secretions, has been reported to expression in milk MFGM has been reported[227]. Yu and Lowe showed that GP2 binds *E. coli* expressing Type 1 fimbria[228]. In Friesian we could detect constant elevated levels of GP2 across lactation phases. Since this breed is subjected to mastitis caused by E. coli[229] it could be suggested that a greater GP2 amount could be related to selection for a resistant to infection genotype, in agreement with previous reports highlighting a correlation with and increased incidence of mastitis in Friesian breed and a possible reaction or resistance to it[229]. Moreover, this matches our results with PIGR. The polymeric immunoglobulin receptor (PIGR) is involved in the transport of immunoglobulins of the IgA and IgM class within the interstitial space underlying the mucosae[230-232]. In milk, IgAs are massively produced in mammary glands and secreted in milk as complexes with PIGR[233,234].

Higher levels of PIGR have been related to a greater amount of immunoglobulin components in milk[235]. PIGR increase in later phases of lactation has been already reported in previous studies[236]. This has been partly confirmed by our data: a relevant amount of PIGR has been observed at phase1, which significantly diminished in phase 2. Nevertheless, PIGR spot photodensity rose again at the end of lactation in both breeds. Coherently, immunoglobulin levels followed a positive trend, especially in the third lactation phase. Notably, immunoglobulin concentrations are known to increase during early mammary gland involution[237,238]. At least part of the increase in immunoglobulin may occur by a selective transport process[239]. IGJ spot intensity in Friesian increases

significantly at phase 3, in agreement with the model of late mammary gland involution proposed above, based on the observed trends for MFGE8.

Mammary gland involution Immune-related proteins follow a positive trend throughout lactation stages also in Chianina. In particular, PIGR and IGJ increase more sensibly than in Friesian. Following the model proposed above, this might be representative of an earlier involution of the mammary gland in Chianina.

Elevated levels of fibrinogen (FBG) are observed already at phase 1. A large accumulation of FBG, together with apoptotic epithelial cells, is observed in the lactating mammary alveoli and ducts of plasminogen (PLG) deficient mice, where fibrin may play a key role in the malfunction of mammary glands in the absence of PLG, possibly through blockade of mammary ducts inducing milk stasis, inhibiting milk expulsion and thereby inducing premature apoptosis and involution[240]. Mice deficient for PLG are strikingly less able to support a litter during lactation compared to wild type mice. It has been suggested that a mechanism responsible for this lactation defect could be related to plasmin activity on FBG[206.]Consistently, FBG levels in Friesian only increase at phase 3 of lactation, in agreement with trends observed for MFGE8, FABP3 and IGJ reported above.

GLYCAM1 has been found to constantly increase its concentration levels across lactation phases[241]. This protein participates in general cell-to-cell interaction mechanisms related to immunity[242] and cell development[172]. However, whether its role in milk does not seem to involve lymphocyte migration[234] its actual role is still controversial.

In a goat model, Le Provost et al. demonstrated that GLYCAM1 levels increase in mammary glands during lactation when compared against pregnancy, hinting at a possible role of this mucin-like molecule in mammary gland regulation[235]

Signalling A series of proteins involved in signaling have been found to be over-expressed in Chianina across each lactation phase.

PPIA, also known as cyclophilin A [243,244] is an ubiquitously distributed intracellular protein belonging to the immunophilin family[244]. Even if its expression is generally considered constitutive, a recent study of liver protein expression profiles states that PPIA levels change in the passage from pregnancy to lactation[245].

PPIA has a peptidylprolyl cis-trans-isomerase activity[246-249] and plays a role in the susceptibility to oxidative stress and apoptosis, as it can be secreted in response to oxidative stress[216,250-253] PPIA also plays a role in lipid droplet secretion[216] and in cell cycle regulation of various cells by influencing mitotic checkpoints[254] In particular, secreted

forms of PPIA could play a critical role in epithelial cell differentiation via catalyzing the polymerization of hensin, a protein implicated in epithelial cell differentiation[255].

YWHAB is a 14-3-3 protein, small acidic ubiquitous proteins that recognize serine/threonine-phosphorylated residues in a context-specific manner[256,257]. In mammals, seven highly homologous family members binding to many different types of proteins have been described , including cell cycle regulators, transcription factors, and proteins involved in signaling and apoptosis. 14-3-3 binding to target proteins often regulates the sub-cellular localization but is also known to induce conformational changes affecting enzymatic activity or to serve as a scaffold protein[257, 258].

YWHAB takes part in proliferative regulatory cascades involving NfKβ[216]. High levels of both PPIA and YWHAB in Chianina might explain the anatomical changes of mammary glands in comparison to Friesian. These preliminary observations should be supported by targeted investigations on the peculiar role of YWHAB and 14-3-3 proteins in bovine milk and mammary glands in general. On the other hand, it is not possible to exclude that these proteins are likely to induce proliferation and anatomical growth in the calf rather than in the mammary gland itself.

β-lactoglobulin (LGB), one of the two major whey proteins of milk, is regarded primarily as a food sourc[259]. LGB binds to several hydrophobic molecules, suggesting a role in their transport. In fact, LGB binds to membrane bilayers in different ways implying a structural role of LGB in MFG overall structure[190].

Inter-breed analysis

Most of the observed changes followed nearly overlapping trends in both breeds. Nonetheless, the initial concentrations of most of the proteins varied significantly between breeds, thus resulting in an overall different pattern. The major differences observed during the lactation process between the two breeds are the following.

A comparative model for mammary gland involution. The data previously discussed hinted at an earlier involution of mammary glands in Chianina , which is in agreement with anatomical differences between the two breeds (**Figure 12**).

A series of observations are related to the later onset of mammary involution in Friesian individual:

i) ACTB concentration at phase 3 is significantly higher in Friesian than in Chianina. This could imply that epithelium turn-over is still active in mammary glands of individuals of the former breed at phase 3;

ii) PLIN2 levels in Chianina drop in phase 2 while in Friesian, they grow across the examined phases

iii) FABP3 amount is significantly greater in Friesian than in Chianina. Our data seems to confirm the overall tendency of FABP3 synthesis to increase during lactation, and bring an insight into the differences in the fatty acid amount between the two breeds. In fact, it could be due to the fact that Friesian reaches a peak in fatty acid amounts in MFGM earlier[164]. Whereas a slight decrease in FABP3 levels is observed in Friesian individuals, this is never observed before phase 3;

iv) MFGE8 levels in Chianina are slightly higher at phase 1, while significantly lower at phase 3. As reported above, MFGE8 might be a marker of MFG secretion of mammary gland epithelium apoptosis. Significantly higher levels of MFGE8 at late lactation are consistent with the fact that Friesian glands are still functional or rather begin to involute;

v) FGB concentration is significantly higher in Chianina at phase 1, while its levels are comparable between breeds at the end of lactation stages. FGB might represent an indirect marker of mammary gland involution, thus hinting at an earlier onset of this process in non-dairy cattle;

vi) immunoglobulin concentration increase during involution of mammary glands[203,205,209,226]. Chianina seems to increase the production of IGJ earlier and more abundantly. A peak of the IGJ spot intensity for both breeds (without differences between breeds) can be noticed at the last stage of the lactation considered, hinting again at a late onset of mammary gland involution in Friesian ;

vii) PIGR and GP2 levels in Friesian individuals might account for an increased resistance to to mastitis and inflammation, in agreement with other molecular investigations reported in literature[199]. Conversely, high PPIA levels in Chianina might account for an major toleration to oxidative stress;

viii) LGB spot intensity decreases significantly in both breeds during lactation, although its prevalence in either breed differs across lactation phases. This could be related to the role of LGB as a nutrient and protein source, and thus to the different availability of protein nutrients in MFGs, as an effect of the different purpose selection of the two breeds. Structural role of LGB should not be underestimated (moreover, there is a far greater amount of LGB in the whey so the nutraceutical role in MFGM could be less relevant).

Notably, it has been reported that LGB levels, along with other major milk proteins, decrease in concentration in parallel to mammary gland involution[239] – this is consistent with the general trend in both breeds.

Further investigations are needed to define the differences in size and layer structure of MFGs between cattle breeds across lactation phases, it will be mandatory to perform qualitative and quantitative investigations on the differential expression of whey proteins among breeds with different productive attitudes, since whey constitutes the greatest protein fraction of nutrients in milk[239].

It is interesting to note that most of the relevant variations in protein levels observed in Friesian have been recorded in phase 3. To our knowledge, these observations have been never reported before and have been made hereby possible by the prolonged lactation time span covered by this study.

4. CONCLUSIONS

Our study on metabolism of Friesian and Chianina, by liver samples comparison contributes to a more detailed understanding of important biological processes which have molded the two distinct breeds. Moreover, this study provides evidence of how direct measures of gene expression, in this case protein and transcript-oriented analyses, can provide information on the global dynamic changes in the protein repertoire associated with the analysis of two distinct populations, and elucidate the important metabolic differences that have arisen upon modification of relatively few genes/proteins (or gene/protein networks), over thousand years of human breeding selection.

The analysis of swine Longissumus lumborum was aimed at detecting representative molecules which could be related to the differences in fat deposition between the Italian Casertana and the Large White breeds. Most of the differentially-expressed proteins and gene transcripts individuated account for proteins which have been proposed to play a role in meat quality [94,95].

Casertana, the endangered, semi-wild fat-type breed, showed to rely on glycolitic enzymes, in contrast with Large White, which rather appears to be oriented towards lipid mobilization and oxidation.

Considering the semi-wild rearing environment of Casertana, the expression of protein involved in fast energy production could be related to a greater need of energy compared to the more static lifestyle of Large White.

Nevertheless, glycolysis is an inefficient way to generate adenosine 5'-triphosphate (ATP), which in turn guarantees a rapid rate of biomass accumulation, resulting in fat deposition in Casertana pigs.[260]

In Large White, the presence of proteins related to mitochondrial activity, lipid mobilization, insulin resistance, and anti-oxidant proteins and transcripts are suggestive of a likely constant mitochondrial activity consuming the smaller fat mass. Large White pigs clearly showed a tendency to muscular growth. Most of the over-expressed proteins and transcripts belonged to protein groups composing the fiber and the sarcoplasmic reticulum, as well as with anti-proteolytic enzymes, as expected from a breed selected to develop lean muscular mass.

The study of MFGM milk protein fraction provided an overview of the changes of these protins across lactation, assessed in this first approach by analysing two very different cattle breeds. Our data confirm how breed selection has effects on milk production traits

at the protein level, in agreement with other studies[261]. As Chianina and Friesian cattle breeds have been selected for meat and milk production, respectively, we hereby provide further evidence that these different productive attitudes are reflected at the molecular level in the composition of MFGM milk-fraction proteins. As a result, we could postulate that variations observed at the protein level are in good agreement with a model implying an earlier involution of mammary gland in Chianina individuals, when compared with Friesian. Besides, since MFGs directly bud from cattle mammary glands, the observed differences are likely to represent an alternative non-invasive method to investigate mammary gland proteins without the need for a biopsy.

The usefulness of the 2D-IEF SDS PAGE method for the study of milk proteins should be stressed. Nevertheless, while the method holds the potential to unveil the main changes at the protein level between breeds and across phases, it is not suited to investigate how the proteins interact among each other. Further studies of MFGMs should pursuit the mapping of the native state of milk proteins and their interaction in the membrane through specific techniques, such as native gel-based approaches (blue native, for example[262]) along with quantification[193] of the least abundant protein species investigated so far. Our results suggest that comparative studies among breeds with different productive attitudes could be repeated, including whey proteins and extending the investigation to the low abundance protein fraction.

5. ACKNOWLEDGEMENTS

I wish to thank the following people who helped me in performing my research.
First and foremost my supervisor Dr. Lorraine Pariset for her constant help, support and patience.
the coordinator of my PhD course, professor Giorgio Prantera for his support.
Moreover, professor Lello Zolla and his group: Dr. Anna Maria Timperio, Dr. Gian Maria D'Amici (who teached me 2D IEF SDS PAGE), Dr. Sara Rinalducci, my wonderful colleagues: Maria Giulia Egidi, Marco Fagioni, Federica Gevi, Barbara Blasi, Angelo D'Alessandro and Valeria Pallotta.
Finally, professor Alessio Valentini, and his group: the aforementioned Dr. Pariset, Maria Gargani, Silvia Bongiorni, Federica Gabbianelli, Gianluca Prosperini, Giordano Mancini, Gabriella Porcai and Paolo Ciorba.
My PhD has been supported by the "GENZOOT" research programme, funded by the Italian Ministry of Agriculture. I would like to thank Dr. Bianca Moioli, coordinator of the project.
Finally I would like to thank Stefano Corbianco who kindly provided milk samples for the MFGM study.

References

[1] Davoli, R Braglia, S. Molecular approaches in pig breeding to improve meat quality. Brief. Funct. Genomic Prot. 2008, 6(4), 313-321.

[2] Xu, Y.J. Jin, M.L. Wang, L.J. Zhang, A. D. Zuo, B. Xu, D. Q. Ren, Z. Q. Lei, M. G. Mo, X. Y. Li, F. E. Zheng, R. Deng, C. Y. Xiong, X, Y. Differential proteome analysis of porcine skeletal muscles between Meishan and Large White. J. Anim. Sci. 2009, 87(8), 2519-2527.

[3] Bendixen E, Danielsen M, Hollung K, Gianazza E, Miller I. Farm animal proteomics - A review. J Proteomics. 2010 Nov 26. [Epub ahead of print] PubMed PMID: 21112346.

[4] Miarelli M, Signorelli F. Differential expression of liver proteins in Chianina and Friesian young bulls. J Anim Sci. 2010 Feb88(2):593-8. Epub 2009 Nov 6. PubMed PMID: 19897641

[5] Comparative proteomic profiling of 2 muscles from 5 different pure pig breeds using surface-enhanced laser desorption/ionization time-of-flight proteomics technology. J Anim Sci. 2010 Apr88(4):1522-34. Epub 2009 Dec 18. PubMed PMID: 20023129.

[6] Coffey SG. Prospects for improving the nutritional quality of dairy and meat products. Forum Nutr. 200760:183-95. Review.

[7] Davoli R, Braglia S. Molecular approaches in pig breeding to improve meat quality. Brief Funct Genomic Proteomic. 2007 Dec6(4):313-21. Epub 2008 Jan 21. Review.

[8] Bjarnadóttir SG, Hollung K, Faergestad EM, Veiseth-Kent E. Proteome changes in bovine Longissimus thoracis muscle during the first 48 h postmortem: shifts in energy status and myofibrillar stability.

[9] Picard B, Berri C, Lefaucheur L, Molette C, Sayd T, Terlouw C. Skeletal muscle proteomics in livestock production. Brief Funct Genomics. 2010 May9(3):259-78. Epub 2010 Mar 21. Review.

[10] Le Bihan-Duval E, Debut M, Berri CM, Sellier N, Santé-Lhoutellier V, Jégo Y Beaumont C. Chicken meat quality: genetic variability and relationship with growth and muscle characteristics. BMC Genet. 2008 Aug 189:53.

[11] Bendixen E, Danielsen M, Larsen K, Bendixen C. Advances in porcine genomics and proteomics--a toolbox for developing the pig as a model organism for molecular biomedical research. Brief Funct Genomics. 2010 May9(3):208-19.Review.

[12] Foxcroft GR, Dixon WT, Dyck MK, Novak S, Harding JC, Almeida FC. Prenatalprogramming of postnatal development in the pig. Soc Reprod Fertil Suppl. 200966:213-31. Review

[13] Liu J, Damon M, Guitton N, Guisle I, Ecolan P, Vincent A, Cherel P, Gondret F. Differentially-expressed genes in pig Longissimus muscles with contrasting levels of fat, as identified by combined transcriptomic, reverse transcription PCR, and proteomic analyses. J Agric Food Chem. 2009 May 1357(9):3808-17. PubMed PMID

[14] Cowan ML, Rahman TM, Krishna S. Proteomic approaches in the search forbiomarkers of liver fibrosis. Trends Mol Med. 2010 Apr16(4):171-83. Epub 2010 Mar 19. Review.

[15] C Xu YJ, Jin ML, Wang LJ, Zhang AD, Zuo B, Xu DQ, Ren ZQ, Lei MG, Mo XY, Li FE, Zheng R, Deng CY, Xiong YZ. Differential proteome analysis of porcine skeletal muscles between Meishan and Large White. J Anim Sci. 2009 Aug87(8):2519-27. Epub 2009 May 6. PubMed PMID: 19420230.

[16] D Liu J, Damon M, Guitton N, Guisle I, Ecolan P, Vincent A, Cherel P, Gondret F. Differentially-expressed genes in pig Longissimus muscles with contrasting levels of fat, as identified by combined

transcriptomic, reverse transcription PCR, and proteomic analyses. J Agric Food Chem. 2009 May 1357(9):3808-17. PubMed PMID: 19296579.

[17] Hollung K, Grove H, Færgestad EM, Sidhu MS, Berg P. Comparison of muscle proteome profiles in pure breeds of Norwegian Landrace and Duroc at threedifferent ages. Meat Sci. 2008 Oct 10. [Epub ahead of print] PubMed PMID: 20416601.

[18] Boehmer JL, Ward JL, Peters RR, Shefcheck KJ, McFarland MA, Bannerman DD. Proteomic analysis of the temporal expression of bovine milk proteins during coliform mastitis and label-free relative quantification. J Dairy Sci. 2010 Feb93(2):593-603.

[19] E Affolter M, Grass L, Vanrobaeys F, Casado B, Kussmann M. Qualitative and quantitative profiling of the bovine milk fat globule membrane proteome. J Proteomics. 2010 Apr 1873(6):1079-88. Epub 2009 Nov 26. PubMed PMID: 19944786.

[20] F: Reinhardt TA, Lippolis JD. Developmental changes in the milk fat globule membrane proteome during the transition from colostrum to milk. J Dairy Sci. 2008 Jun91(6):2307-18. PubMed PMID: 18487653.

[21] Wu WZ, Wang XQ, Wu GY, Kim SW, Chen F, Wang JJ. Differential composition of proteomes in sow colostrum and milk from anterior and posterior mammary glands. J Anim Sci. 2010 Aug88(8):2657-64. Epub 2010 Apr 23. PubMed PMID: 20418458.

[22] Hornshøj H, Bendixen E, Conley LN, Andersen PK, Hedegaard J, Panitz F, Bendixen C. Transcriptomic and proteomic profiling of two porcine tissues using high-throughput technologies. BMC Genomics. 2009 Jan 1910:30. PubMed PMID: 19152685 PubMed Central PMCID:

[23] Adessi, C., Miege, C., Albrieux, C. & Rabilloud, T. (1997) Two-dimensional electrophoresis of membrane proteins: A current challenge for immobilized pH gradients. Electrophoresis, 18, 127-135.

[24] Chevallet, M., Santoni, V., Poinas, A., Rouquie, D., Fuchs, A., Kieffer, S., Rossignol, M., Lunardi, J., Garin, J. & Rabilloud, T. (1998) New zwitterionic detergents improve the analysis of membrane proteins by two-dimensional electrophoresis. Electrophoresis, 19, 1901-1909.

[25] Galvani M., Hamdan M., Herbert B., Righetti P.G. (2001) Alkylation kinetics of proteins in preparation for two-dimensional maps: A matrix assisted laser desorption/ionization-mass spectrometry investigation. Electrophoresis, 22, 2058-2065.

[26] Galvani M., Ravotti L., Hamdan M., Herbert B., Righetti P.G. (2001) Protein alkylation in the presence/absence of thiourea in proteome analysis: A matrix assisted laser desorption/ionization-time of flight-mass spectrometry investigation. Electrophoresis, 22, 2066-2074.

[27] Görg, A., Postel, W. & Gunther, S. (1988) The current state of two-dimensional electrophoresis with immobilized pH gradients. Electrophoresis, 9, 531-546.

[28] Görg, A., Obermaier, C., Boguth, G., Harder, A., Scheibe, B., Wildgruber, R. & Weiss, W. (2000) The current state of two-dimensional electrophoresis with immobilized pH gradients. Electrophoresis, 21, 1037-1053.

[29] Herbert B., Galvani M., Hamdan M., Olivieri E., MacCarthy J., Pedersen S., Righetti P.G. (2001) Reduction and alkylation of proteins in preparation of two-dimensional map analysis: Why, when, and how? Electrophoresis, 22, 2046-2057.

[30] Herbert, B.R., Molloy, M.P., Gooley, A.A., Walsh, B.J., Bryson, W.G. & Williams, K.L. (1998) Improved protein solubility in two-dimensional electrophoresis using tributyl phosphine as reducing agent. Electrophoresis, 19, 845-851.

[31] Jefferies, J.R., Brophy, P.M. & Barrett, J. (2000) Investigation of *Fasciola hepatica*sample preparation for two-dimensional electrophoresis. Electrophoresis, 21, 3724-3729.

[32] Mastro, R. & Hall, M. (1999) Protein delipidation and precipitation by tri-n-butylphosphate, acetone, and methanol treatment for isoelectric focusing and two-dimensional electrophoresis. Analytical Biochemistry, 273, 313-315.

[33] Means, G.E. & Feeney E.f. (1971) Chemical modification of protein. Holden-Day, San Francisco, USA pp 84-89.

[34] Molloy, M.P., Herbert, B.R., Walsh, B.J., Tyler, M.I., Traini, M., Sanchez J.C., Hochstrasser D.F., Williams, K.L., Gooley, A.A. (1998) Extraction of membrane proteins by differential solubilization for separation using two-dimensional gel electrophoresis. Electrophoresis, 19, 837-844.

[35] Ramsby, M.L. & Makowski, G.S. (1999) Differential detergent fractionation of Eukaryotic cells. In, Methods in Molecular Biology: vol. 112. Ed. Link, A.J., Humana press, Totowa, USA. 53-66

[36] Rabilloud, T. (1990) Mechanisms of protein silver staining in polyacrylamide gels: A 10 year synthesis. Electrophoresis, 11, 785-794.

[37] Rabilloud, T. (1994) Silver-staining of proteins in polyacrylamide gels: A general overview. Cellular and Molecular Biology, 40 (1), 57-75.

[38] Righetti, P.G (1983) Isoelectric focusing: theory, methodology and applications. Laboratory techniques in biochemistry and molecular biology, vol. 11. Eds Work, T.S. & Burdon, R.H. Elsevier Biomedical Press, Amsterdam, Netherlands.

[39] Righetti, P.G (1990) Immobilized pH gradients: theory and methodology. Laboratory techniques in biochemistry and molecular biology, vol. 20. Eds Burdon, R.H. & van Knippenberg, P.H., Elsevier Biomedical Press, Amsterdam, Netherlands.

[40] Sabounchi-Schütt, F., Åström, J., Olsson, I., Ekland, A., Grunewald, J. & Bjellqvist, B. (2000) An immobiline DryStrip method enabling high-capacity two-dimensional gel electrophoresis. Electrophoresis, 21, 3629-3656.

[41] Storrie, B. & Madden, E.A. (1990) Isolation of subcellular organelles. In, methods in enzymology vol. 182. Ed. Deutscher M.P., Academic press 203-225

[42] Yan, J.X., Wait, R., Berkelman, T., Harry, R.A., Westbrook, J.A., Wheeler, C.H. & Dunn, M.J. (2000) A modified silver staining protocol for visualisation of proteins compatible with matrix-assisted laser desorption/ionization and electrospray ionization mass spectrometry. Electrophoresis, 21, 3666-3672.

[44] Bradford, M. M. A rapid and sensitive method for the quantitation of microgram quantities of protein utilizing the principle of protein-dye binding. *Anal. Chem.* 1976, *72*, 248–254.

[44] Roy JHB. The calf. Management of Health, 5th (Eds), vol. 1. London, England: Butterworths 1990. p. 1–117.

[45] Lewin HA. The future of cattle genome research: the beef is here, cytogen. Genome Res 2003102:10–5.

[46] D'Ambrosio C, Arena S, Talamo F, Ledda L, Renzone G, Ferrara L, et al. Comparative proteomic analysis of mammalian animal tissues and body fluids: bovine proteome database. J Chrom B 2005815:157–68.

[47] Zuo X, Speicher DW. Comprehensive analysis of complex proteomes using microscale solution isoelectrofocusing prior to narrow pH range two-dimensional electrophoresis. Proteomics 20022:58–68.

[48] Womack J, Kata SR. Bovine genome mapping: evolutionary inference and the power of comparative genomics. Curr Opin Genet Dev 19955:725–33.

[49] Fries R, Ruvinsky A. The Genetics of Cattle, vol. 13. Wallingford: CABI Publishing 1999. p. 391–410.

[50] Hochstrasser DF, Frutiger S, Wilkins MR, Hughes G, Sanchez JC. Elevation of apolipoprotein E in the CSF of cattle affected by BSE. FEBS Lett 1997416:161–3.

[51] Jobim MIM, Oberst ER, Salbego CG, Souza DO, Wald VB, Tramontina F, et al. Two-dimensional polyacrylamide gel electrophoresis of bovine seminal plasma proteins and their relation with semen freezability. Theriogenology 199861:255–66.

[52] Ricken AM, Spanel-Borowski K, Saxer Huber PR. Cytokeratin expression in bovine corpora lutea. Histochem Cell Biol 1995103:345–54.

[53] Collier RJ, Collier JL, Rhoads RP, Baumgard LH. Invited review: genes involved in the bovine heat stress response. J Dairy Sci 200891(2):445–54.

[54] Hansen PJ, Aréchiga CF. Strategies for managing reproduction in the heat-stressed dairy cow. J Animal Sci 199977:36–50.

[55] Al-Katanani YM, Paula-Lopes FF, Hansen PJ. Effect of season and exposure to heat stress on oocyte competence in Friesian cows. J Dairy Sci 200285:390–6.

[56] Shevchenko, A Wilm, M. Vorm, O. Mann, M. Mass Spectrometric Sequencing of Proteins from Silver-Stained Polyacrylamide Gels. *Anal. Chem.* 1996 *68*, 850–858 of America 2005, *102(12),* 4252-4257.

[57] Peng, X. Wood, C. Blalock, E. Chen, K. Landfield, P. Stromberg, A. Statistical implications of pooling RNA samples for microarray experiments. *BMC Bioinf.* 2003, *4(1),* 26.

[58] Kendziorski, C. Irizarry, R. A. Chen, K. S. Haag, J. D. Gould, M. N. On the utility of pooling biological samples in microarray experiments. Proceedings of the National Academy of Sciences of the United States

[59] Dobbin, K.K. Kawasaki, E.S. Peterson, D.W. Simon, R.M. Characterizing dye bias in microarray experiments. Gene expression 2005, *21(10),* 2430-2437.

[60] Naidoo, S. Denby, K.J. Berger, D.K. Microarray experiments:considerations for experimental design. *S. Afr J Sci.* 2005, *101*, 347-354.

[61] Talamo, F., C. D'Ambrosio, S. Arena, P. Del Vecchio, L. Ledda, G. Zehender, L. Ferrara, and A. Scaloni, A. 2003. Proteins from bovine tissues and biological fluids: Defining a reference electrophoresis map for liver, kidney, muscle, plasma and red blood cells. Proteomics. 3:440-460.

[62] Hernandez-Toro, J. Prieto, C. De Las Rivas, J. APID2NET: unified interactome graphic analyzer. *Bioinformatics* 2007, *23(18),* 2495-2497.

[63] Al-Shahrour, F. Minguez, P. Tárraga, J. Medina, I. Alloza, E. Montaner, D. Dopazo, J. FatiGO+: a functional profiling tool for genomic data. Integration of functional annotation, regulatory motifs and interaction data with microarray experiments. *Nucl. Acids Res.*2007,*35*, 91-96,

[64] Al-Shahrour, F. Minguez, P. Vaquerizas, J. M. Conde, L. Dopazo, J. BABELOMICS: a suite of web-tools for functional annotation and analysis of group of genes in high-throughput experiments. *Nucl. Acids Res.* 2005, *33*, 460-464.

[65] Al-Shahrour, F. Díaz-Uriarte, R. Dopazo, J. FatiGO: a web tool for finding significant associations of Gene Ontology terms with groups of genes. *Bioinformatics* 2004, *20*, 578-580[62] Hernandez-Toro, J. Prieto, C. De Las Rivas, J. APID2NET: unified interactome graphic analyzer. *Bioinformatics* 2007, *23(18),* 2495-2497.

[66] Caraux G, Pinloche S. "Permutmatrix: a graphical environment to arrange gene expression profiles in optimal linear order. Bioinformatics 200521:1280–1.

[67] Kanehisa M, Araki M, Goto S, Hattori M, Hirakawa M, Itoh M, et al. KEGG for linking genomes to life and the environment. Nucleic Acids Res 200836:D480–4.

[68] Sevi A, Rotunno T, Di Caterina R, Muscio A. Fatty acid composition of ewe milk as affected by solar radiation and high ambient temperature. J Dairy Res 200269:81–194.

[69] Xu C, Wang Z. Comparative proteomic analysis of livers from ketotic cows. Vet Res Com 200832:263–73.

[70] Bertoni G, Cappa V. Il profilo metabolico nella vacca produzione di latte. Bioch Clin 19848:131–3.

[71] Wemheuer W. Relationship between iodine requirements/ thyroid metabolism and fertility problems in dairy cows. Reprod Domest Anim 199328:385–94.

[72] Whitaker DA, Smith EJ, da Rosa GO, Kelly JM. Some effects of nutrition and management on the fertility of dairy cattle. Vet Rec 1993133:61–4.

[73] Bader N, Moeller U, Leiterer M, Franke K, Jahreis G. Pilot study: tendency of increasing iodine content in human milk and cow 's milk. Exp Clin Endocrinol 2005113:8–12.

[74] Kaufmann S, Kursa J, Kroupova V, Rambeck WA. Iodine in milk by supplementing feed: an additional strategy to erase iodine deficiency. Vet Med (Praha) 199843:173–8.

[75] Hendy GN, Bennett HPJ, Gibbs BF, Lazure C, Day R, Seidah NG. Proparathyroid hormone is preferentially cleaved to parathyroid hormone by the prohormone convertase furin. A mass spectrometric study. J Biol Chem 1995270:9517–25.

[76] Bowler RP, Nicks M, Olsen DA, Thøgersen IB, Valnickova Z, Højrup P, et al. Furin proteolytically processes the heparin-binding region of extracellular superoxide dismutase. J Biol Chem 2002277(19):16505–11.

[77] Collier RJ, Collier JL, Rhoads RP, Baumgard LH. Invited review: genes involved in the bovine heat stress response. J Dairy Sci 200891(2):445–54.

[78] Hansen PJ, Aréchiga CF. Strategies for managing reproduction in the heat-stressed dairy cow. J Animal Sci 199977:36–50.

[79] Al-Katanani YM, Paula-Lopes FF, Hansen PJ. Effect of season and exposure to heat stress on oocyte competence in Friesian cows. J Dairy Sci 200285:390–6.

[80] West J, Bondari WK, Johnson JC. Effects of bovine somatotropin on milk yield and composition, body weight, and condition score of Friesian and Jersey cows. J Dairy Sci 199073:1062–8.

[81] West JW, Mullinix BG, Johnson JC, Ash Jr KA, Taylor VN. Effects of bovine somatotropin on dry matter intake, milk yield, and body temperature in Friesian and Jersey cows during heat stress. J Dairy Sci 199073:2896–906.

[82] Elvinger F, Natzke RP, Hansen PJ. Interactions of heat stress and bovine somatotropin affecting physiology and immunology of lactating cows. J Dairy Sci 199275:449–62.

[83] Cole JA, Hansen PJ. Effect of administration of recombinant bovine somatotropin on the responses of lactating and nonlactating cows to heat stress. J Am Vet Med Assoc 1993203:113–7.

[84] Nie L, Wu G, Culley DE, Schotten JCM, Zhang W. Integrative analysis of transcriptomic and proteomic data: challenges, solutions and applications. Crit Rev Biotechnol 200727(2):63–75.

[85] Larson, G. Dobney, K. Albarella, U. Fang, M. Matisoo-Smith, E. Robins, J.Lowden, S. Finlayson, H. Brand, T. Willerslev, E. Rowley-Convy, P. Andersson, L. Cooper, A. Worldwide phylogeography of wild boar reveals multiple centers of pig domestication, Science 2005, 307, 1618–1621.

[86] Handbook to the Breeds of theWorld, Porter, V. Pigs, A. Helm Information Ltd. Near Robertsbridge, UK, 1993.

[87] Hoogland, C. Mostaguir, K. Sanchez, J-C. Hochstrasser, D. Appel, R. D. SWISS-2DPAGE, ten years later. *Proteomics* 2004, *4(8),* 2352-2356.

[88] Zullo, A. Barone, C. M. A. Colatruglio, P. Girolami, A. Matassino, D. Chemical composition of pig meat from the genetic type 'Casertana' and its crossbreeds *Meat Sci*. 2003, *63(1),* 89-100.

[89] Peng, X. Wood, C. Blalock, E. Chen, K. Landfield, P. Stromberg, A. Statistical implications of pooling RNA samples for microarray experiments. BMC Bioinf. 2003, 4(1), 26

[90] Kim, N. K. Joh, J. H. Park, H. R. Kim, O. H Park, B. Y. Lee, C. S. Differential expression profiling of the proteomes and their mRNAs in porcine white and red skeletal muscles. *Proteomics* 2004, *4(11),* 3422-3428.

[91] Wimmers, K.. Murani, E. Ngu, N. T. Schellander, K. Ponsuksili, S. Structural and functional genomics to elucidate the genetic background of microstructural and biophysical muscle properties in the pig. *J Anim. Breed. Genet*. 2007, *124(1),* 27-34.

[92] Quiroz-Rothe, E. Rivero, J. L. Coordinated expression of myosin heavy chains, metabolic enzymes, and morphological features of porcine skeletal muscle fiber types. *Microsc. Res. Tech.* 2004, *65(1-2),* 43-61.

[93] Toniolo, L. Patruno, M. Maccatrozzo, L. Pellegrino, M. A. Canepari, M. Rossi, R. D'Antona, G. Bottinelli, R. Reggiani, C:, Mascarello, F.. Fast fibres in a large animal: fibre types, contractile properties and myosin expression in pig skeletal muscles. *J Exp Biol.* 2004, *207(11),* 1875-1886.

[94] Kwasiborski, A. Sayd, T. Chambon, C. Santé-Lhoutellier, V. Rocha, D. Terlouw, C. Pig Longissimus lumborum proteome: Part I. Effects of genetic background, rearing environment and gender. *Meat Sci*. 2008, *80*, 968–981

[95] Kwasiborski, A. Sayd, T. Chambon, C. Santé-Lhoutellier, V. Rocha, D. Terlouw, C. Pig Longissimus lumborum proteome: Part II: Relationships between protein content and meat quality. *Meat Sci*. 2008, *80,* 982–996

[96] (Hornshøj, H. Bendixen, E. Conley, L. N. Andersen, P. K. Hedegaard, J. Panitz, F. Bendixen, C. Transcriptomic and proteomic profiling of two porcine tissues using high-throughput technologies. *BMC Gen.* 2009, *10*, 30.

[97] Salazar-Olivo, L. A. Castro-Muñozledo, F. Kuri-Harcuch, W. A preadipose 3T3 cell variant highly sensitive to adipogenic factors and to human growth hormone. *J Cell Sci.* 1995, *108 (5),* 2101-2107.

[98] Salvaterra, M. Agraria.org - Agrarian instruction online Italian breeds of livestock. 2000 http://eng.agraria.org/

[99] http://probes.invitrogen.com/media/pis/mp33300.pdf

[100] Fang, Y. , A. Hoyle, D. C. Hayes, A. Bashein, A. Oliver, S.G. Waddington, D. Rattray, M. A model-based analysis of microarray experimental error and normalisation. *Nucl. Acids Res.* 2003, *31(16),* e96.

[101] Megens, H. J. Crooijmans, R. P. San Cristobal, M. Hui, X. Li, N. Groenen, M. A. Biodiversity of pig breeds from China and Europe estimated from pooled DNA samples: differences in microsatellite variation between two areas of domestication. *Gen. Sel. Evol*. 2008, *40(1),* 103-128.

[102] www.ingenuity.com

[103] Shannon, P. Markiel, A. Ozier, O. Baliga, N. S. Wang, J. T. Ramage, D. Amin, N. Schwikowski, B. Ideker, T. Cytoscape: a software environment for integrated models of biomolecular interaction networks. *Gen. Res*. 2003 *13(11),* 2498-2504.

[104] Scherf, B. D. WorldWatch List for Animal Diversity, 3rd edn., FAO, 2000, Rome, Italy.

[105] Jones, G. F. Genetic aspects of domestication, common breeds and their origin, in: Ruvinsky, A. Rothschild, M. F. (Eds.), The Genetics of the Pig, CAB International, Oxon, UK, 1998, pp. 17–50.

[106] Timperio, A. M. D'Alessandro, A. Pariset, L. D'Amici, G. M. Valentini, A. Zolla, L. Comparative proteomics and transcriptomics analyses of livers from two different Bos taurus breeds: "Chianina and Friesian". *J. Proteomics* 2009, *73(2),* 309-322.

[107] Fell, D. A. Small, J. R. Fat synthesis in adipose tissue. An examination of stoichiometric constraints. *Biochem. J.* 1986, *238(3),* 781-786.

[108] Pietrolà, E. Pilla, F. Maiorano, G. Matassino, D. Morphological traits, reproductive and productive performances of Casertana pigs reared outdoors *Ital. J.Anim. Sci.* 2006, *5*, 139-146

[109] Orosz, F. Oláh, J. Ovádi, J. Triosephosphate isomerase deficiency: New insights into an enigmatic disease. *Biochim Biophys Acta.* 2009 doi:10.1016/j.bbadis.2009.09.012.

[110] Laville, E. Sayd, T. Terlouw, C. Chambon, C. Damon, M. Larzul, C. Leroy, P. Glénisson, J. Chérel, P. Comparison of sarcoplasmic proteomes between two groups of pig muscles selected for shear force of cooked meat. *J Agric. Food. Chem.* 2007, *55(14),* 5834-5841.

[111] Farrar, W. W. Deal, W. C. Jr. Purification and properties of pig liver and muscle enolases. *J. Protein. Chem.* 1995, *14(6),* 487-497.

[112] Merkulova, T. Lucas, M. Jabet, C. Lamandé, N. Rouzeau, J. D. Gros, F. Lazar, M. Keller, A. Biochemical characterization of the mouse muscle-specific enolase:developmental changes in electrophoretic variants and selective binding to other proteins. *Biochem. J.* 1997, *323 (3),* 791-800.

[113] Foucault, G. Vacher, M. Cribier, S. Arrio-Dupont, M. Interactions between beta-enolase and creatine kinase in the cytosol of skeletal muscle cells. *Biochem. J.* 2000, *346(1),* 127-131.

[114] Wallimann, T. Wyss, M. Brdiczka, D. Nicolay, K. Eppenberger, H. M. Intracellular compartmentation, structure and function of creatine kinase isoenzymes in tissues with high and fluctuating energy demands: the 'phosphocreatine circuit' for cellular energy homeostasis. *Biochem. J.* 1992, *281 (1),* 21-40.

[115] Ventura-Clapier, R. Kaasik, A. Veksler, V. Structural and functional adaptations of striated muscles to CK deficiency *Mol. Cell. Biochem.* 2004, *257*, 29–41.

[116] McComb, J. M. McMaster, E. A. MacKenzie, G. Adgey, A. A. Myoglobin and creatine kinase in acute myocardial infarction. *Br. Heart J.* 1984, *51(2),* 189-194.

[117] Ordway, G. A. Garry, D. Myoglobin: an essential hemoprotein in striated muscle *J. Exp. Biol*. 2004, *207*, 3441-3446

[118] Mueller, E. Drori, S. Aiyer, A. Yie, J. Sarraf, P. Chen, H., Hauser, S. Rosen, E. D. Ge, K. Roeder, R. G. Spiegelman, B. M. Genetic analysis of adipogenesis through peroxisome proliferator-activated receptor γ isoforms. *J. Bio.l Chem.* 2002, 277(44),41925-41930.

[119] Takemasa, T. Sugimoto, K. Miyazaki, M. Machida, M. Ikeda, S. Hitomi, Y. Kizaki, T. Ohno, H, Yamashita, K. Haga, S. Simple method for the identification of oxidative fibers in skeletal muscle. *Eur. J. Appl. Physiol.* 2004, *91(2-3),* 357-359.

[120] Cummins, C. L. Volle, D. H. Zhang, Y. McDonald, J. G. Sion, B. Lefrançois-Martinez, A. M. Caira, F. Veyssière, G. Mangelsdorf, D. J. Lobaccaro, J. M. Liver X receptors regulate adrenal cholesterol balance. *J. Clin. Invest.* 2006, 116(7), 1902-1912.

[121] Xu, C. Li, C. Y. Kong, A. N. Induction of phase I, II and III drug metabolism/transport by xenobiotics. *Arch. Pharm. Res.* 2005, *28(3),* 249-268.

[122] Reusch, J. E. Colton, L. A. Klemm, D. J. CREB activation induces adipogenesis in 3T3-L1 cells. *Mol. Cell. Biol.* 2000, *20(3),* 1008-1020.

[123] Vankoningsloo, S. De Pauw, A. Houbion, A. Tejerina, S. Demazy, C. de Longueville, F. Bertholet, V. Renard P, Remacle J, Holvoet P, Raes M, Arnould T. CREB activation induced by mitochondrial dysfunction triggers triglyceride accumulation in 3T3-L1 preadipocytes. *J. Cell. Sci.* 2006, *119(7),* 1266-1282.

[124] Bujalska, I. J. Gathercole, L. L. Tomlinson, J. W. Darimont, C. Ermolieff, J. Fanjul, A. N. Rejto, P. A. Stewart, P. M. A novel selective 11beta-hydroxysteroid dehydrogenase type 1 inhibitor prevents human adipogenesis. *J. Endocrinol*. 2008, *197(2),* 297-307.

[125] Song, L. Alcalai, R. Arad, M. Wolf, C. M. Toka, O. Conner, D. A. Berul, C. I. Eldar, M. Seidman, C. E. Seidman, J. G. Calsequestrin 2 (CASQ2) mutations increase expression of calreticulin and ryanodine receptors, causing catecholaminergic polymorphic ventricular tachycardia. *J. Clin. Invest.* 2007, 117(7), 1814-1823.

[126] Szabo, E. Qiu, Y. Baksh, S. Michalak, M. Opas, M. Calreticulin inhibits commitment to adipocyte differentiation. *J. Cell. Biol*. 2008, 182(1), 103-116.

[127] Ringseis, R. Piwek, N. Eder, K. Oxidized fat induces oxidative stress but has no effect on NF-kappaB-mediated proinflammatory gene transcription in porcine intestinal epithelial cells. *Inflamm. Res.* 2007, 56(3), 118-125.

[128] Galili, O. Versari, D. Sattler, K. J. Olson, M. L. Mannheim, D. McConnell, J. P. Chade, A. R. Lerman, L. O. Lerman, A. Early experimental obesity is associated with coronary endothelial dysfunction and oxidative stress. *Am. J. Physiol. Heart. Circ. Physiol*. 2007*292(2),* H904-911.

[129] Suzawa, M. Takada, I. Yanagisawa, J. Ohtake, F. Ogawa, S. Yamauchi, T. Kadowaki, T. Takeuchi, Y. Shibuya, H. Gotoh, Y. Matsumoto, K. Kato, S. Cytokines suppress adipogenesis and PPAR-gamma function through the TAK1/TAB1/NIK cascade. *Nat. Cell. Biol.* 2003, *Mar5(3),* 224-230.

[130] Huxford, T. Ghosh, G. Inhibition of transcription factor NF-kappaB activation by kappaB-Ras. *Met. Enzymol.* 2006, *407*, 527-534.

[131] Maine, G. N. Burstein, E. COMMD proteins: COMMing to the scene. *Cell. Mol. Life Sci.* 2007, 64(15), 1997-2005.

[132] Dragsted, L. O. Biomarkers of exposure to vitamins A, C, and E and their relation to lipid and protein oxidation markers. *Eur. J. Nutr.* 2008, *47(2),* 3-18.

[133] Voss, P. Engels, M. Strosova, M. Grune, T. Horakova, L. Protective effect of antioxidants against sarcoplasmic reticulum (SR) oxidation by Fenton reaction, however without prevention of Ca-pump activity. *Toxicol. In Vitro.* 2008, *22(7),* 1726-1733.

[134] Fernandez-Robredo, P. Moya, D. Rodriguez, J. A. Garcia-Layana, A. Vitamins C and e reduce retinal oxidative stress and nitric oxide metabolites and prevent ultrastructural alterations in porcine hypercholesterolemia. *Invest. Ophthalmol. Vis. Sci.* 2005, *46(4),* 1140-1146.

[135] May, J. M. Morrow, J. D. Burk RF. Thioredoxin reductase reduces lipid hydroperoxides and spares alpha-tocopherol. Biochem Biophys Res Commun. 2002, *292(1),* 45-49.

[136] Kumar, S. Holmgren, A. Induction of thioredoxin, thioredoxin reductase and glutaredoxin activity in mouse skin by TPA, a calcium ionophore and other tumor promoters. *Carcinogenesis.* 1999, *20(9),* 1761-1767.

[137] Marumoto, M. Suzuki, S. Hosono, A. Arakawa, K. Shibata, K. Fuku, M. Goto, C. Tokudome, Y. Hoshino, H. Imaeda, N. Kobayashi, M. Yodoi, J. Tokudome, S. Changes in thioredoxin concentrations: an observation in an ultra-marathon race. *Environ. Health Prev. Med*. 2009 DOI 10.1007/s12199-009-0119-4

[138] Metzger, J. M. Moss, R. L. Myosin light chain 2 modulates calcium-sensitive cross-bridge transitions in vertebrate skeletal muscle. *Biophys. J.* 1992, *63(2),* 460-468.

[139] Strehler, E. E. Periasamy, M. Strehler-Page, M. A. Nadal-Ginard, B. Myosin light-chain 1 and 3 gene has two structurally distinct and differentially regulated promoters evolving at different rates. *Mol. Cell. Biol.* 1985, *5(11),* 3168-3182.

[140] Moss, R. L. Diffee, G. M. Greaser, M. L. Contractile properties of skeletal muscle fibers in relation to myofibrillar protein isoforms. *Rev. Physiol. Biochem. Pharmacol*. 1995, *126*, 1–63.

[141] Bicer, S. Reiser, P. J. Myosin light chain isoform expression among single mammalian skeletal muscle fibers: species variations *J. Musc. Res. Cell. Mot*. 2004, *25*, 623–633.

[142] Yoshioka, M. Tanaka, H. Shono, N. Snyder, E.E. Shindo, M. St-Amand, J. Serial analysis of gene expression in the skeletal muscle of endurance athletes compared to sedentary men. *FASEB J.* 2003, *17(13),* 1812-1819.

[143] Barany, K. Barany, M. Gillis, J. M. and Kushmerick, M. J. Phosphorylation-dephosphorylation of the 18,000-dalton light chain of myosin during the contraction-relaxation cycle of frog muscle. *J. Biol. Chem.* 1979, *254*, 3617–3623.

[144] Helferich, W, Jump, D. B. Anderson, D. B. Skjaerlund, D. M. Merkel, R. A. Bergen, W. G. Skeletal muscle alpha-actin synthesis is increased pretranslationally in pigs fed the phenethanolamine ractopamine. Endocrinology. 1990, *126(6),* 3096-3100.

[145] Juliano, R. L. Signal transduction by cell adhesion receptors and the cytoskeleton: functions of integrins, cadherins, selectins, and immunoglobulin-superfamily members. *Ann. Rev. Pharmacol. Toxicol*. 2002, *42*, 283-323.

[146] Akaaboune, M. Verdière-Sahuqué, M. Lachkar, S. Festoff, B. W. Hantaï, D. Serine proteinase inhibitors in human skeletal muscle: expression of beta-amyloid protein precursor and alpha 1-antichymotrypsin in vivo and during myogenesis in vitro. *J. Cell. Physiol*. 1995, *165(3),* 503-511.

[147] Zenke, F. T. Krendel, M. DerMardirossian, C. King, C. C. Bohl, B. P. Bokoch, G. M. p21-activated kinase 1 phosphorylates and regulates 14-3-3 binding to GEF-H1, a microtubule-localized Rho exchange factor. *J. Biol. Chem.* 2004, *279(18),* 18392-18400.

[148] Fu, H. Subramanian RR, Masters SC. 14-3-3 proteins: structure, function, and regulation. *Annu. Rev. Pharmacol. Toxicol.* 2000, *40*, 617-647.

[149] Lametsch, R. Kristensen, L. Larsen, M. R. Therkildsen, M. Oksbjerg, N. Ertbjerg, P. Changes in the muscle proteome after compensatory growth in pigs. *J. Anim. Sci*. 2006, *84(4),* 918-924.

[150] Brajenovic, M. Joberty, G. Küster, B. Bouwmeester ,T, Drewes G. Comprehensive proteomic analysis of human par protein complexes reveals an interconnected protein network. *J. Biol. Chem*. 2004, *279(13),* 12804-12811.

[151] Trinczek, B. Brajenovic, M. Ebneth, A. Drewes G. MARK4 Is a Novel Microtubule-associated Proteins/Microtubule Affinity-regulating Kinase That Binds to the Cellular Microtubule Network and to Centrosomes. *J. Biol. Chem.* 2004, *279(7),* 5915-5923.

[152] McCright, B. Virshup, D. M. Identification of a new family of protein phosphatase 2A regulatory subunits. *J. Biol. Chem.* 1995, *270(44),* 26123-26128.

[153] Heximer, S. P. Blumer, K. J. RGS proteins: Swiss army knives in seven-transmembrane domain receptor signaling networks. *Sci STKE* 2007, *370,* pe2.

[154] Wu, C. Zeng, Q. Blumer, K. J. Muslin, A. J. RGS proteins inhibit Xwnt-8 signaling in Xenopus embryonic development. *Development.* 2000, *127(13),* 2773-2784.

[155] Kang, S. W. Chae, H. Z. Seo, M. S. Kim, K. Baines I. C. Rhee S. G. Mammalian peroxiredoxin isoforms can reduce hydrogen peroxide generated in response to growth factors and tumor necrosis factor-alpha. *J. Biol. Chem*. 1998, *273(11),* 6297-6302.

[156] Yonggang, L. A novel porcine gene, MAPKAPK3, is differentially expressed in the pituitary gland from mini-type Diannan small-ear pigs and large-type Diannan small-ear pigs. *Mol. Biol. Rep*. 2009, doi: 10.1007/s11033-009-9921-8

[157] Gaestel, M. MAPKAP kinases - MKs - two's company, three's a crowd. *Nat. Rev. Mol. Cell. Biol*. 2006 ,7(2), 120-130.

[158] Adida, A. Spener, F. Intracellular lipid binding proteins and nuclear receptors involved in branched-chain fatty acid signaling. *Prost. Leukot Essent. Fatty Acids.* 2002, *67(2-3),*91-98.

[159] Wolf, G. Retinoic acid as cause of cell proliferation or cell growth inhibition depending on activation of one of two different nuclear receptors. *Nutr. Rev.* 2008, *66(1),* 55-59.

[160] Wu, Z. Puigserver, P. Andersson, U. Zhang, C. Adelmant, G. Mootha, V. Troy, A. Cinti, S. Lowell, B. Scarpulla, R. C. Spiegelman, B. M. Mechanisms controlling mitochondrial biogenesis and respiration through the thermogenic coactivator PGC-1. *Cell* 1999, *98(1),* 115-124.

[161] Yoon, J. C. Puigserver, P. Chen, G. Donovan, J. Wu, Z. Rhee, J. Adelmant, G. Stafford, J. Kahn, CR, Granner DK, Newgard CB, Spiegelman BM. Control of hepatic gluconeogenesis through the transcriptional coactivator PGC-1. Nature. 2001413(6852):131-8.

[162] Mootha, V. K. Handschin, C. Arlow, D. Xie, X. St Pierre, J. Sihag, S. Yang, W. Altshuler, D. Puigserver, P. Patterson, N. Willy, P. J. Schulman, I. G. Heyman, R. A. Lander, E. S. Spiegelman, B. M. Erralpha and Gabpa/b specify PGC-1alpha-dependent oxidative phosphorylation gene expression that is altered in diabetic muscle. *Proc. Natl. Acad. Sci U.S.A.* 2004, *101(17),* 6570-6575.

[163] Huss, J. M. Torra, I. P. Staels, B. Giguère, V. Kelly, D. P. Estrogen-related receptor alpha directs peroxisome proliferator-activated receptor alpha signaling in the transcriptional control of energy metabolism in cardiac and skeletal muscle. *Mol. Cell Biol.* 2004, *24(20),* 9079-9091.

[164] Luo, J. Sladek, R. Carrier, J. Bader, J. A. Richard, D. Giguère, V. Reduced fat mass in mice lacking orphan nuclear receptor estrogen-related receptor alpha. *Mol. Cell. Biol*. 2003, *23(22),* 7947-7956.

[165] Chapman, M. J. Le Goff, W. Guerin, M. Kontush, A. Cholesteryl ester transfer protein: at the heart of the action of lipid-modulating therapy with statins, fibrates, niacin, and cholesteryl ester transfer protein inhibitors. *Eur. Heart J.* 2009, doi:10.1093/eurheartj/ehp399

[166] Han, R. Lai, R. Ding, Q. Wang, Z. Luo, X. Zhang, Y. Cui, G. He, J. Liu, W. Chen, Y. Apolipoprotein A-I stimulates AMP-activated protein kinase and improves glucose metabolism *Diabetol*. 2007, *50*, 1960–196

[167] Berthon, P. M. Howlett, R. A. Heigenhauser, G. J. Spriet, L. L. Human skeletal muscle carnitine palmitoyltransferase I activity determined in isolated intact mitochondria. *J. Appl. Physiol.* 1998, *85(1),* 148-153.

[168] Gibala, M. J. Young, M. E. Taegtmeyer, H. Anaplerosis of the citric acid cycle: role in energy metabolism of heart and skeletal muscle. *Acta Physiol. Scand.* 2000, *168(4),* 657-665.

[169] Chuanxi, C. S. Weisleder, N. Ko, J. K. Komazaki, S. Sunada, Y. Nishi, M. Takeshima, H. Ma, J. Membrane Repair Defects in Muscular Dystrophy Are Linked to Altered Interaction between MG53, Caveolin-3, and Dysferlin. *J. Biol. Chem.* 2009, *284(23),* 15894–15902.

[170] Lemay, D. G., D. J. Lynn, W. F. Martin, M. C. Neville, T. M Casey,.G. Rincon, E. V. Kriventseva,.W. C. Barris, A. S. Hinrichs, A. J. Molenaar, K. S. Pollard, N. J. Maqbool, K. Singh, R. Murney, E.M. Zdobnov, R. L. Tellam, J. F. Medrano, J. B. German and M. Rijnkels. 2009. The Bovine lactation genome: insights into the evolution of the mammalian milk. Genome Biol. 10:43.

[171] Szyda, J., and J. Komisarek. 2006. Statistical Modeling of Candidate Gene Effects on Milk Production Traits in Dairy Cattle. J. Dairy Sci. 90:2971-2979.

[172] D'Alessandro, A., L. Zolla, and A. Scaloni. 2010b. The bovine milk proteome: cherishing, nourishing and fostering molecular complexity. An interactomics and functional overview. Mol. Biosys. doi: 10.1039/C0MB00027B.

[173] Keenan, T.W., D. P. Dylewski, D. Ghosal, and B. H. Keon. 1992. Milk lipid globule membrane precursor release from endoplasmic reticulum in a cell-free system, Eur. J. Cell Biol. 57:21–29.

[174] Wu, C. C., K. E. Howell, M. C. Neville, J. R. Yates, and J. L. McManaman. Proteomics reveal a link between the endoplasmic reticulum and lipid secretory mechanisms in mammary epithelial cells. Electrophoresis. 21:3470-3482.

[175] Mather, I. H., and T. W. Keenan. 1998. Origin and secretion of milk lipids. J. Mammary Gland Biol. *Neoplasia*. 3: 259-273.

[176] Davies, C.R., V. Morris, V. Griffiths, V. Page, A. Pitt, T. Stein, and B. A. Gusterson. 2002. Proteomic analysis of the mouse mammary gland is a powerful tool to identify novel proteins that are differentially expressed during mammary development. Proteomics.6:5694-5704.

[177] Reinhardt, T.A., and J. D. Lippolis. 2006a. Developmental changes in the milk fat globule membrane proteome during the transition from colostrum to milk. J. Dairy Sci. 91:2307–2318.

[178] Peterson, J.A., M. Hamosh, C. D. Scallan, R. L. Ceriani, T. R. Henderson, N. Mehta, R. Armand, and P. Hamosh. 1998. Milk fat globule glycoproteins in human milk and in gastric aspirates of mother's milk-fed preterm infants. Pediatr. Res. 44:499-450.

[179] Gauthier, S.F., Y. Pouliot, and J. L. Maubois. 2006. Growth factors from bovine milk and colostrum: composition, extraction and biological activities. Lait. 86: 99-125.

[180] Fong, B.Y., and C. S. Norris. 2009. Quantification of milk fat globule membrane proteins using selected reaction monitoring mass spectrometry. J. Agric. Food Chem. 57:6021-6028

[181] McPherson, A.V. Kitchen, B.J. Reviews of the progress dairy science: the bovine milk fat globule membrane— its formation, composition, structure and behaviour in milk and dairy products. *J. Dairy Res.* 1983, *50*, 107-133.

[182] Mather, I.H. Proteins of the milk-fat-globule membrane as markers of mammary epithelial cells and apical plasma membrane. In *The Mammary Gland: Development, Regulation and Function* Neville, M.C., Daniel, C.W., Eds. Plenum Publ. Corp.: New York, NY, USA, 1987 pp. 217-267

[183]Keenan, T.W. Mather, I.H. Dylewski, D.P. Physical equilibria: lipid phase. In *Fundamentals of Dairy Chemistry*, 3rd ed. Wong, N.P., Ed. Van Nostrand Reinhold Co.: New York, NY, USA, 1987 pp. 511-582.

[184] Mather, I.H. A review and proposed nomenclature for major proteins of the milk-fat globule membrane, *J. Dairy Sci.* 2000, *83*, 203-247.

[185] Quaranta, S., M. G. Giuffrida, M. Cavaletto, C. Giunta, J. Godovac- Zimmermann, B. Canas, C. Fabris, E. Bertino, M. Mombro, and A. Conti. 2001. Human proteome enhancement: High-recovery method and improved two-dimensional map of colostral fat globule membrane proteins. Electrophoresis. 22:1810-1818.

[186] Wessel, D., and U. I. Flügge. 1984. A method for the quantitative recovery of protein in dilute solution in the presence of detergents and lipids. Anal. Biochem. 138:141-143.

[187] Neuhoff V, Arold N, Taube D, Ehrhardt W. Improved staining of proteins in polyacrylamide gels including isoelectric focusing gels with clear background at nanogram sensitivity using Coomassie Brilliant Blue G-250 and R.250. Electrophoresis 19889:255–62.

[188] Beresini, M. H. Sugarman, B. J. Shepard, H.M. Epstein, L. B. Synergistic induction of polypeptides by tumor necrosis factor and interferon-γ in cells sensitive or resistant to tumor necrosis factor: Assessment by computer based analysis of two-dimensional gels using the PDQUEST system. *Electrophoresis* 1990, *11*, 232–241.

[189] Talamo, F., C. D'Ambrosio, S. Arena, P. Del Vecchio, L. Ledda, G. Zehender, L. Ferrara, and A. Scaloni, A. 2003. Proteins from bovine tissues and biological fluids: Defining a reference electrophoresis map for liver, kidney, muscle, plasma and red blood cells. Proteomics. 3:440-460.

[190] Lefevre, T., and M. Subirade. 2000. Interaction of b-lactoglobulin with phospholipid bilayers: a molecular level elucidation as revealed by infrared spectroscopy. Int. J. Biol. Macromol. 28:59–67.

[191] Timperio, A. M., A. D'Alessandro, L. Pariset, G. M. D'Amici, A. Valentini, and L. Zolla. 2009. Comparative proteomics and transcriptomics analyses of livers from two different Bos Taurus breeds: “Chianina and Friesian”. J. Proteomics. 73:309-322.

[192] Peterson, J.A., M. Hamosh, C. D. Scallan, R. L. Ceriani, T. R. Henderson, N. Mehta, R. Armand, and P. Hamosh. 1998. Milk fat globule glycoproteins in human milk and in gastric aspirates of mother’s milk-fed preterm infants. Pediatr. Res. 44:499-450.

[193] Andersen, H., O. N. Jensen, and E. F. Eriksen. 2003. A proteome study of secreted prostatic factors affecting osteoblastic activity: identification and characterisation of cyclophilin A. Eur. J. Cancer. 39:989–995.

[194] Gauthier, S.F., Y. Pouliot, and J. L. Maubois. 2006. Growth factors from bovine milk and colostrum: composition, extraction and biological activities. Lait. 86: 99-125.

[195] Aoki, N. 2006. Regulation and Functional Relevance of Milk Fat Globules and Their Components in the Mammary Gland. Biosci. Biotechnol. Biochem. 70:2019–2027.

[196] Closel, M. J., A.R. Howlett, and C. D. Roskelley. 1997. Lactoferrin expression in mammary epithelial cells is mediated by changes in cell shape and actin cytoskeleton. J. Cell. Sci. 110:2861-2871.

[197] Robenek, H.O., I. Hofnagel, S. Buers, M. Lorkowski, M. Schnoor, and J. Robenek. 2006. Butyrophilin controls milk fat globule secretion. Proc. Nat. Acad. Sci. U.S.A. 103:10385-10390.

[198] Heid, H. H., M. Schnolzer, and T. W. Keenan. 1996. Adipocyte differentiation-related protein is secreted into milk as a constituent of milk lipid globule membrane. Biochem. J. 320:1025-1030.

[199] Elkins, D. A., D. M. Spurlock. 2009. Phosphorylation of perilipin is associated with indicators of lipolysis in Friesian cows. Horm. Metab. Res.41:736–740.

[200] Jiang, H. P., and G. Serrero, 1992. Isolation and characterization of a full-length cDNA coding for an adipose differentiation-related protein. Proc. Natl. Acad. Sci. U.S.A. 89:7856-7860.

[201] Eisinger, D. P. and G. Serrero. 1993. Structure of the gene encoding mouse adipose differentiation-related protein (ADRP). Genomics. 16:638-644.

[202] Heid, H. H., M. Schnolzer, and T. W. Keenan. 1996. Adipocyte differentiation-related protein is secreted into milk as a constituent of milk lipid globule membrane. Biochem. J. 320:1025-1030.

[203] Freudenstein, C., T. W. Keenan, W. N. Eigel, M. Sasaki, J. Stadler, and W. Franke. 1979. Butyrophilin of milk lipid globule membrane contains *N*-linked carbohydrates and cross-links with xanthine oxidase Exp. Cell. Res. 118:277-294.

[204] Franke, W. W., H. W. Heid, , C. Grund, S. Winter, C. Freudenstein, C. E. Schmid, E. D. Jarasch, and T. W. Keenan. 1981. Antibodies to the Major Insoluble Milk Fat Globule Membrane-associated Protein: Specific Location in Apical Regions of Lactating Epithelial Cells J. Cell Biol. 89:485-494.

[205] Jarasch, E.-D., C. Grund, G. Bruder, H. W. Heid, T. W. Keenan and W. W. Franke. 1981. Localization of xanthine oxidase in mammary-gland epithelium and capillary endothelium. Cell. 25: 67-82.

[206] Jeong, J. A. U., J. Rao, S. L. Xu, Y. Ogg, C. Hathout, C. Fenselau, and I. H. Mather. 2009. The PRY/SPRY/B30.2 domain of butyrophilin 1A1 (BTN1A1) binds to xanthine oxidoreductase: implications for the function of BTN1A1 in the mammary gland and other tissues. J. Biol. Chem. 284:22444-22456..

[207] Bruder, G., H. Heid, E. D. Jarasch, T. W. Keenan, and I. H. Mather. 1992. Characteristics of membrane-bound and soluble forms of xanthine oxidase from milk and endothelial cells of capillaries. Biochim. Biophys. Acta. 701: 357–369.

[208] Ishii, T., N. Aoki, A. Noda, T. Adachi, R. Nakamura, and T. Matsuda. 1995. Carboxy-terminal cytoplasmic domain of mouse butyrophilin specifically associates with a 150- kDa protein of mammary epithelial cells and milk fat globule membrane. Biochim. Biophys. Acta. 1245:285– 292.

[209]Arnett, H. A., S. S. Escobara, and S. L. Viney. 2009. Regulation of costimulation in the era of butyrophilins. Cytokine 46:370–375.

[210] Briely, M. S., and R. Eisenthal. 1974. Association of xanthine oxidase with the bovine milk-fat-globule membrane. Catalytic properties of the free and membrane-bound enzyme. Biochem. J. 143:149–157.

[211]Silanikove, N., and F. Shapiro. Distribution of xanthine oxidase and xanthine dehydrogenase activity in bovine milk: Physiological and technological implications. Int. Dairy J. 17:1188–1194

[212] D'Alessandro, A., A. Scaloni, and L. Zolla, 2010a. Human milk proteins: an interactomics and updated functional overview. J. Prot. Res. 9:3339-3373.

[213] Bionaz, M., and J. J. Loor. 2008. ACSL1, AGPAT6, FABP3, LPIN1, and SLC27A6 are the most abundant isoforms in bovine mammary tissue and their expression is affected by stage of lactation 1–3. J. Nutr., 138:1019-1024.

[214] Affolter, M., L. Grass, F. Vanrobaeys, B. Casado, and M. Kussmann. 2010. Qualitative and quantitative profiling of the bovine milk fat globule membrane proteome. J. Proteomics. 73:1079-1088.

[215] Yolken, R.H., J. A. Peterson, S. L. Vonderfecht, E. T. Fouts, K. Midthun, and D. S. Newburg. 1992.Human milk mucin inhibits rotavirus replication and prevents experimental gastroenteritis. J.Clin. Invest. 90:1984-1991.

[216] Andersen, M. H., H. Graversen, S. N. Fedosov, T. E. Petersen, and J. T. Rasmussen. 2000. Functional analyses of two cellular binding domains of bovine lactadherin. Biochemistry. 39:6200-6206.

[217] Kranich, J., N. J. Krautler, E. Heinen, M. Polymenidou, C. Bridel, A Schildknecht, C Huber, M. H. Kosco-Vilbois, R. Zinkernagel, G. Miele, and A. Aguzzi. 2008. Follicular dendritic cells control engulfment of apoptotic bodies by secreting Mfge8. J. Exp. Med. 205:1293–1302.

[218] Clarkson, R. W., M. T. Wayland, J. Lee, T. Freeman, and C. J. Watson. 2004. Gene expression profiling of mammary gland development reveals putative roles for death receptors and immune mediators in post-lactational regression. Breast Cancer Res. 6:92-109.

[219] Hanayama, R., M. Tanaka, K. Miwa, A. Shinohara, A. Iwamatsu, and S. Nagata. 2002. Identification of a factor that links apoptotic cells to phagocytes. Nature. 417:182-187.

[220] Hanayama, R., M. Tanaka, K. Miyasaka, K. Aozasa, M. Koike, Y. Uchiyama, and S. Nagata. 2004. Autoimmune disease and impaired uptake of apoptotic cells in MFGE8- deficient mice. Science. 304:1147-1150.

[221] Atabai, K., R. Fernandez, X. Huang, I. Ueki, A. Kline, Y. Li, S. Sadatmansoori, C. Smith- Steinhart, W. Zhu, R. Pytela, Z. Werb, and D. Sheppard. 2005. Mfge8 is critical for mammary gland remodeling during involution. Mol. Biol. Cell. 16:5528-5537.

[222] Nakatani, H., N. Aoki, Y. Nakagawa, S. Jin-No, K. Aoyama, K. Oshima, S. Ohira, C. Sato, D. Nadano, and T. Matsuda. Weaning-induced expression of a milk-fat globule protein, MFG-E8, in mouse mammary glands as demonstrated by the analyses of its mRNA, protein and phosphatidylserine-binding activity. Biochem. J. 395:21-30.

[223] Craninx, M., A. Steen, H. Van Laar, T. Van Nespen, J. Martìn-Tereso, B. De Baets, and V. Fievez. 2008. Effect of Lactation Stage on the Odd- and Branched-Chain Milk Fatty Acids of Dairy Cattle Under Grazing and Indoor Conditions J. Dairy Sci. 91:2662–2677.

[224] Ingber, D. E. 2003. Tensegrity II. How structural networks influence cellular information processing networks. J. Cell Sci. 116:1397–1408.

[225] Neville, M.C., T. B. McFadden, and I. Forsyth. 2002. Hormonal regulation of mammary differentiation and milk secretion. J. Mammary Gland Biol. Neoplasia. 7:49-66.

[227] Hood, L., M. Kronemberg, T. T. Hunkapiller. 1985. Cell antigen receptors and the immunoglobulin gene family. Cell. 40: 225-229.

[228] Yu, S., and A. W. Lowe. 2009. The pancreatic zymogen granule membrane protein, GP2, binds Escherichia coli type 1. Gastroenterology. 9:58.

[229] Ismail, Z.A., and C. Dickinson. 2010. Alterations in coagulation parameters in dairy cows affected with acute mastitis caused by E. coli and S. aureus pathogens. Vet. Res. Comm. 34: 533-539.

[230] Childers, N.K., M.G. Bruce and J. R. McGhee. 1989. Molecular mechanisms of immunoglobulin A defense. Annual Review of Microbiology, 43:503–536.

[231] Kraehenbuhl, J. P., and M. R. Neutra. 1992. Molecular and cellular basis of immune protection of mucosal surfaces. Phys. Rev. 72:853–879.

[232] Wheeler, T. T., A. J. Hodgkinson, C. G. Prosser, and S. R. Davis. 2007. Immune components of colostrums and milk – a historical perspective. J. Mammary Gland Biol. Neoplasia. 12:237–247.

[233] De Groot, N., P. Van Kuik-Romeijn, S. H. Lee, and A. H. de Boer. 1999. Over-expression of the murine polymeric immunoglobulin receptor gene in the mammary gland of transgenic mice. Transgenic Res. 8:125–135.

[234] Nishimura, T. 2003. Expression of potential lymphocyte trafficking mediator molecules in the mammary gland. Vet. Res. 34(1):3-10.

[235] Mostov, K. E. 1994. Transepithelial transport of immunoglobulins. Annu. Rev. Immunol. 12:63–84.

[236] Van der Felz, M. J. M, N. de Groot, J. P. Barley, S. H. Lee, M. P. Verbert, and H. A. De Boer. 2001. Lymphocyte homing and Ig Secretion in the Murine Mammary Gland. J. Immunol. 54:292-300.

[237] Singh, K., S. R. Davis, J. M. Dobson, A. J. Molenaar, T. T. Wheeler, C. G. Prosser, V. C. Farr, K. Oden K. M. Swanson, C. V. Phyn, D. L. Hyndman, T. Wilson, H. V. Henderson, and K. Stelwagen. 2008. cDNA microarray analysis reveals that antioxidant and immune genes are upregulated during involution of the bovine mammary gland. J. Dairy Sci. 91:2236-2246.

[238] Faustini, M., C. Colombani, D. Vigo, R. Communod, V. Russo, and T. Chlapanidas. 2010. Dimensional analysis of milk fat globules in sowmilk: effects of the lactation stage and fat content and comparison with vaccine milk. Vet. Res. Comm. 34:29-32.

[239] Hurley, W. L. 1989. Mammary Gland Function During Involution. J. Dairy Sci. 72:1637-1646.

[240] Green, K. A., F. J. Nielsen, J. Castellino, L. Rømer, and L. R. Lund. 2006. Lack of plasminogen leads to milk stasis and premature mammary gland involution during lactation. Dev. Biol. 299:164-175.

[241] Le Provost, F., S. Cassy, H. Hayes, and P. Martin. 2003. Structure and expression of goat GLYCAM1 gene: lactogenic-dependent expression in ruminant mammary gland and interspecies conservation of the proximal promoter. Gene. 313: 83-89.

[242] Liu, J. F. K. 1993. 506 and cyclosporin, molecular probes for studying intracellular signal transduction. Immunol. Today. 14:290.

[243] Liu, J. F. K. 1993. 506 and cyclosporin, molecular probes for studying intracellular signal transduction. Immunol. Today. 14:290.

[244] Fruman, D. A., S. J. Burakoff, and B. E. Bierer. 1994. Immunophilins in protein folding and immunosuppression. FASEB. J. 8: 391.

[245] Galat, A. 1993. Peptidylproline cis-trans-isomerases: Immunophilins. Eu. J. Biochem. 216:689.

[246] Bergsma, D. J., C. Eder, M. Gross, H. Kersten, D. Sylvester, E. Appelbaum,D Cusimano, G. Livi, M. M. McLaughlin, and K. Kasyan. 1991. The cyclophilin multigene family of peptidylprolyl isomerases. Characterization of three separate human isoforms. J. Biol. Chem. 266:23204.

[247] Kofron, J. L., P. Kuzmic, V. Kishore, E. Colon-Bonilla, and D. H. Rich. 1991. Determination of kinetic constants for peptidyl prolyl cis-trans isomerases by an improved spectrophotometric assay. Biochemistry. 30:6127.

[248] Rhoads, R.P. 2003. The Housekeeping Genes GAPDH and Cyclophilin Are Regulated by Metabolic State in the Liver of Dairy Cows. J. Dairy Sci. 86:3423–3429.

[249] Sherry, B., N. Yarlett, A. Strupp, and A. Cerami. 1992. Identification of cyclophilin as a proinfl ammatory secretory product of lipopolysaccharide-activated. Proc. Nat. Acad. Sci. U. S. A. 89:3511-3515.

[250] Crompton, M. 2000. Mitochondrial intermembrane junctional complexes and their role in cell death. J. Physiol. 529:11.

[251] Hailstrap, A. P., E. Doran, J. P. Gillespie and A. O'Toole. 2000. Mitochondria and cell death. Biochem. Soc.Trans. 28:170.

[252] Jin, Z. G., M. G. Melaragno, D. F. Liao. 2000. Cyclophilin A is a secreted growth factor induced by oxidative stress. Circ. Res. 87:789–796.

[253] Obchoei, S., S. Wongkhan, C. Wongkham, M. Li, Q. Yao, and C. Chen. 2009. Cyclophilin A: potential functions and therapeutic target for human cancer. Med. Sci. Monit. 15:221-232.

[254] Lu, K. P., S. D. Hanes, and T. Hunter. 1996. A human peptidyl-prolyl isomerase essential for regulation of mitosis. Nature. 380:544–547.

[255] Peng, H., S. Vijayakumar, and C. Schiene-Fischer. 2009. Secreted Cyclophilin A, a Peptidylprolyl cis-trans Isomerase, Mediates Matrix Assembly of Hensin, a Protein Implicated in Epithelial Differentiation. J. Biol. Chem. 284:6465-6475.

[256] Muslin, A. J., J. W. Tanner, P. M. Allen, and A. S. Shaw. 1996. Interaction of 14-3-3 with signaling proteins is mediated by the recognition of phosphoserine. Cell. 84:889–897

[257] Yaffe, M.B., K. Rittinger, S. Volinia, P. R. Caron, A. Aitken, H. Leffers, S. J: Gamblin, S. J. Smerdon., and L. C. Cantley. 1997. The structural basis for 14-3-3:phosphopeptide binding specificity. Cell. 91:961–971.

[258] Fu, H., R. R. Subramanian, and S. C. Masters. 2000. He structural basis for 14-3-3: phosphopeptide binding specificity. Annu. Rev. Pharmacol. Tossicol. 40:617–647.

[259] Jost, R. 1993. Functional characteristics of dairy proteins. Trends Food Sci Technol. 4:283–288.

[260] Dowbenko, D., A. Kikuta, C. Fennie, N. Gillett, L. A. Lasky. 1993. Glycosylation-dependent cell adhesion molecule 1 (GlyCAM 1) mucin is expressed by lactating mammary gland epithelial cells and is present in milk. J. Clin. Invest. 92: 952-960.

[261] Glantz, M., H. L. Mansson, H. Stålhammar, L. O. Bårström, M. Fröjelin, A. Knutsson, C. Teluk, and M. Paulsson. 2009. Effects of animal selection on milk composition and processability. J. Dairy Sci. 92:4589-4603.

[262] Schagger, H., and G von Jagow. 1991. Blue native electrophoresis for isolation of membrane protein complexes in enzymatically active form. Anal. Biochem. 199:223-231.